Deutsches Geodätisches Forschungsinstitut
Ingenieurfakultät Bau Geo Umwelt
Technische Universität München

Annual Report 2015

Deutsches Geodätisches Forschungsinstitut der Technischen Universität München (DGFI-TUM)

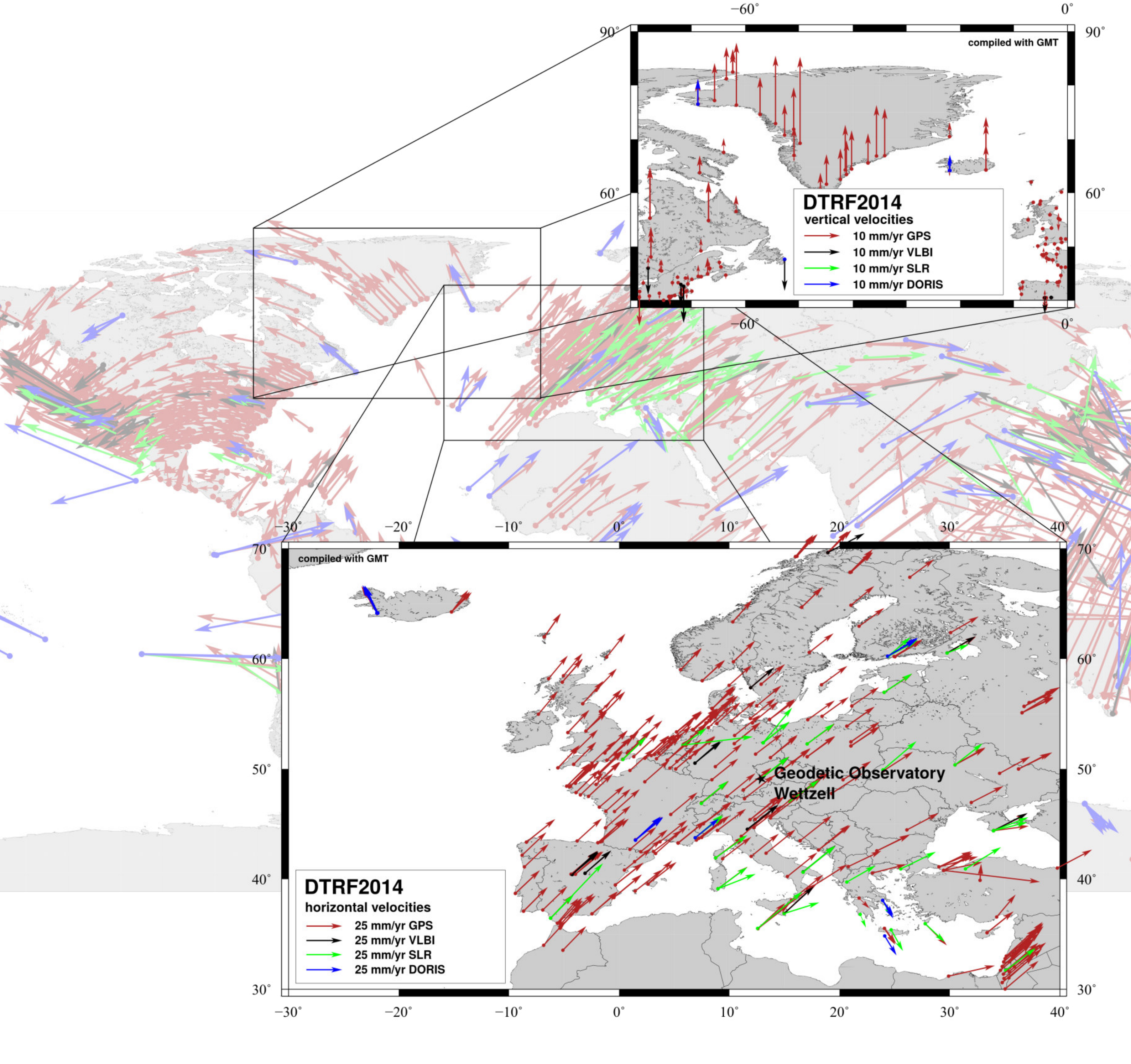

Front cover:
The image shows the DTRF2014, DGFI-TUM's realization of the fundamental Earth-fixed coordinate system *International Terrestrial Reference System (ITRS)*. The plot in the background displays the global distribution of geodetic observatories (colors indicate different observation techniques) and the corresponding horizontal velocity field related to plate tectonics. The lower box shows an enlarged view for Europe and the location of the Geodetic Observatory Wettzell that is jointly operated by the TUM and the Federal Agency for Cartography and Geodesy (BKG). The upper plot shows a detail of vertical movements of stations in Greenland that are caused by postglacial uplift.

Technische Universität München
Ingenieurfakultät Bau Geo Umwelt
Deutsches Geodätisches Forschungsinstitut (DGFI-TUM)

Arcisstr. 21
D - 80333 München

www.dgfi.tum.de

Contents

Preface

Integration of the Deutsches Geodätisches Forschungsinstitut into the Technical University of Munich

After a period of more than 62 years as an autonomous research institute at the Bavarian Academy of Sciences and Humanities (BAdW) the Deutsches Geodätisches Forschungsinstitut (DGFI) has been integrated into the Technical University of Munich (TUM) with effect from January 1, 2015. It is now part of the Chair of Geodetic Geodynamics within TUM's Faculty of Civil, Geo and Environmental Engineering (BGU) and will resume its internationally recognized geodetic basic research under its new official name *Deutsches Geodätisches Forschungsinstitut der Technischen Universität München (DGFI-TUM)*.

The DGFI has a history of more than six decades as the largest purely geodetic research institution in Germany. Originally, the institute was established in 1952 as an independent research facility at the BAdW in Munich, and it was affiliated with BAdW's German Geodetic Commission (DGK).

The institute has continuously been involved in various national and international research activities. In the first decades after the foundation of the DGFI, outstanding results were achieved particularly in the fields of geodetic-astronomical observations and electro-optical distance measurements for the determination of the German and European triangulation as well as in gravimetric surveys for gravity networks. The DGFI was involved in the first global network of satellite triangulation and played an important role in the development of dynamical methods of satellite geodesy for precise orbit determination, point positioning and gravity field modelling. A key aspect of DGFI's research has always been the realization of global and regional horizontal and vertical terrestrial reference systems and in the past decade also of the celestial reference system.

National and international involvement

Today, the DGFI-TUM is strongly linked to other institutions around the world. Intensive collaborations exist in particular within the framework of the international scientific organizations IUGG (International Union of Geodesy and Geophysics), IAU (International Astronomical Union) and IAG (International Association of Geodesy). In particular, the scientists of the DGFI-TUM have been taking leading positions and supporting functions in IAG's commissions, services, projects, working and study groups, and in IAG's Global Geodetic Observing System (GGOS). The institute operates - mostly by long-term commitments - data centres, analysis centres, and research centres.

The collaboration at key positions within the international organizations enables the DGFI-TUM to crucially contribute to shaping the future direction of international geodetic research. DGFI-TUM's research activities and its co-operations in the international organizations are closely coupled: the most recent globally collected observation data are made available for the institute's research, and the newest scientific findings enter directly into the computation of geodetic products of highest quality. The international organizations coordinate the generation of these products under predefined standards and conventions. In this context, DGFI-TUM has a position of particular importance by chairing IAG's *GGOS Bureau of Products and Standards*. Furthermore, DGFI-TUM staff is prominently involved in the management of the international scientific unions IAU and EGU (European Geosciences Union) by acting as vice-president of IAU Commission A2 (*Rotation of the Earth*) and president of the EGU Division *Geodesy*.

The DGFI-TUM also participates in research programmes and bodies of the European Union (EU) and the European Space Agency (ESA), and it cooperates in activities of the United Nations (UN). In this context, the DGFI-TUM is currently involved in the implementation of a UN resolution for a Global Geodetic Reference Frame (GGRF) that recognizes the importance of geodesy for many societal and economic benefit areas, including navigation and transport, construction and monitoring of infrastructure, process control, surveying and mapping, and the growing demand for precisely observing our planet's changes in space and time. The resolution stresses the significance of the global reference frame for accomplishing these tasks, for natural disaster management, and to provide reliable information for decision-makers. The United Nations Global Geospatial Information Management (UN-GGIM) Working Group on the GGRF has the task to draft a roadmap for the enhancement of the GGRF under UN mandate. Based on its competence in the realization of reference frames, the DGFI-TUM is involved in this activity by contributing to the compilation of a policy paper in the frame of the IAG. The main purpose of this paper is to provide a common understanding for the definition of the GGRF and the scientific basis for the preparation of the roadmap to be accomplished by the UN-GGIM Working Group on the GGRF.

On the national level, the DGFI has been a member of the Forschungsgruppe Satellitengeodäsie (FGS) since 1984. The FGS is a follow-on cooperation of the former DFG-Sonderforschungsbereich SFB 78, closely affiliated with the Geodetic Observatory Wettzell in the Bavarian Forest. In the framework of the FGS, the DGFI-TUM is cooperating with other units of the TUM (Chair of Astronomical and Physical Geodesy, Research Facility Satellite Geodesy), the Federal Agency for Cartography and Geodesy (Bundesamt für Kartographie und Geodäsie, BKG) and the Institute of Geodesy and Geoinformation of the University of Bonn (IGG).

Geodetic basic research for Earth system science at the DGFI-TUM

The scientific activities of DGFI-TUM are oriented toward geodetic basic research, guided by the vision that geodesy can provide a high-precision, consistent and long-term valid metric for Earth system sciences. Through new technological achievements in Earth observation systems, in particular in satellite technology and in the field of scientific computing, geodesy has developed toward an important discipline for Earth system research. In the context of global change, geosciences are facing new challenges. Large-scale changes in the Earth system come along with implications on environment and living conditions, and catastrophic consequences of natural disasters become more frequent. Research of processes and interactions in the system Earth is of increasing importance. This fundamentally requires reliable observations of changes on various spatial scales over long time spans.

By strong international and interdisciplinary collaboration, the DGFI-TUM aims at the determination and provision of accurate and consistent geometrical and physical parameters related to the Earth's geometry, gravity field and rotation. In this context, the DGFI-TUM processes, analyzes and combines observations from various space geodetic observation systems and complementary data sources and publicly provides the results through various data portals. The institute operates several globally distributed geodetic observing stations and contributes to the operation and scientific data processing of the Geodetic Observatories Wettzell (Germany) and AGGO (Argentina) in the frame of the FGS. A large part of DGFI-TUM's research activities is financed through third-party funds from various sources (for details see Section 5).

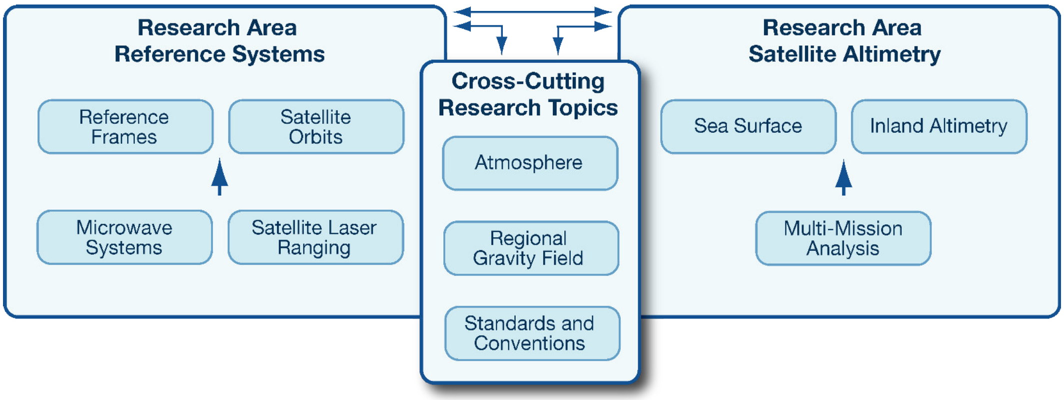

Fig. 1: *Research Areas of the DGFI-TUM*

The research at the DGFI-TUM is structured into the two research areas Reference Systems and Satellite Altimetry, each subdivided into several research topics, and the three cross-cutting research topics Atmosphere, Regional Gravity Field, and Standards and Conventions (Fig. 1).

The institute takes a leading position in the realization of global and regional horizontal and vertical terrestrial reference systems and of the celestial reference system from a combined analysis of various geometrical space geodetic observing systems. As an ITRS Combination Centre the DGFI-TUM regularly computes solutions for the highly precise International Terrestrial Reference Frame (ITRF). The ITRF is the fundamental backbone for referencing all observations and, thus, for enabling a reliable monitoring and interpretation of changes over long time spans. Furthermore, it is the prerequisite for the use of global navigation and positioning systems and for surveying. For its realization the IAG requires an accuracy of 1 mm for the positions of globally distributed observing stations and 0.1 mm per year for their linear velocities (cover picture). This enormous accuracy and utmost long-term stability is necessary in order to detect very small changes in the Earth system (e.g., the global mean sea level rise of about 3 mm per year) reliably over a long period of time. The newest version of DGFI-TUM's realization of the ITRF is the DTRF2014.

In the field of satellite altimetry, the DGFI-TUM maintains complete data holdings of all altimeter missions since 1991 (radar and laser) and provides an open altimetry database (OpenADB) for the distribution of satellite altimeter data and derived high-level products to the scientific community and users free of charge. All altimeter missions are carefully harmonized and cross-calibrated. The derived global multi-mission dataset is used for various ocean and inland applications, among them the determination of global and regional sea level changes, ocean currents and the monitoring of inland water bodies, such as lakes, reservoirs, rivers, and wetlands.

The research areas are complemented by the three cross-cutting research topics Atmosphere (with a strong focus on ionosphere research), Regional Gravity Field, and Standards and Conventions. The latter topic is closely related to the above-mentioned GGOS Bureau of Products and Standards that is chaired by the DGFI-TUM and operated in the frame of the FGS.

In the frame of its integration into the TUM, the institute has taken over additional teaching responsibilities. Scientists of the DGFI-TUM contribute with 30 weekly hours primarily to the education in the master programmes Geodesy and Geoinformation, Earth Oriented Space Science and Technology (ESPACE), and Environmental Engineering. Several dissertations and master's theses were prepared at the institute and supervised by DGFI-TUM staff (for details see Section 6).

1 Research Area Reference Systems

The work in the research area "Reference Systems" relies on the space geodetic observation techniques Very Long Baseline Interferometry (VLBI), Satellite and Lunar Laser Ranging (SLR/LLR), Global Navigation Satellite Systems (GNSS), and Doppler Orbitography and Radiopositioning Integrated by Satellite (DORIS). The geometric techniques allow a high-precision and continuous determination of the figure of the Earth and provide valuable information to identify and quantify even the smallest geometric variations in space and time, e.g., as indicators for global change or for near real-time warning systems. A fundamental requirement are highly accurate, consistent and long-term stable geodetic reference frames with highest reliability.

This research area is primarily concerned with the analysis of space-geodetic observations and the determination and interpretation of parameters describing the shape and orientation of the Earth. As part of the Forschungsgruppe Satellitengeodäsie (FGS), DGFI-TUM contributes to the complete processing chain from the operation of observing stations, data acquisition and provision, development of procedures and theoretical models, data analysis and combination, and parameter determination. Among the institute's core products are highly accurate regional and global realizations of three-dimensional geodetic reference systems that are determined from the combination of the above-mentioned space geodetic observation techniques.

The activities are divided into four research topics:

- *1.1 Analysis of space-based microwave observations*
- *1.2 Analysis of satellite laser ranging observations*
- *1.3 Computation of satellite orbits*
- *1.4 Determination of reference frames*

DGFI-TUM's engagement in the international scientific services of the International Association of Geodesy (IAG) provides a fundamental basis for this research area (see Section 4). It ensures the direct access to the original data of the space geodetic techniques and to the products generated by the scientific services. This is, on the one hand, of great benefit for the research activities at DGFI-TUM (such as the computation of geodetic reference frames) that rely on the newest and most accurate observation data. On the other hand, the basic research performed at the institute ensures a high quality of the geodetic products distributed over these services to the science community and users. Mostly by virtue of long-term commitments, DGFI-TUM operates data centres, analysis centres, and research centres within the IAG. Table 1.1 summarizes the activities that are closely related to this research area. These responsibilities require an operational analysis of SLR, VLBI and GNSS data and a timely generation of geodetic products. The specific software packages (DOGS-OC for SLR and OCCAM/DOGS-RI for VLBI) and the DGFI-TUM combination software DOGS-CS need to be updated regularly according to the latest versions of conventions, models and processing standards.

1.1 Analysis of Space-Based Microwave Observations

VLBI data analysis and combination

As one of the operational analysis centers of the IVS, DGFI-TUM regularly submits constraint-free normal equations of 24-hour VLBI sessions for the IVS rapid and quarterly products (Schmid et al. 2015a). Besides, a reprocessing was started in 2013 to include the estimation

Table 1.1: *Long-term commitments of DGFI-TUM in IAG Services. Besides the activities listed below, DGFI-TUM scientists also contribute to several Working Groups and have taken over various responsibilities and functions within the IAG (see Section 4.2)*

IAG Service	Responsibility of DGFI-TUM
International Earth Rotation and Reference Systems Service (IERS)	ITRS Combination Centre
International GNSS Service (IGS)	Regional Network Associate Analysis Centre for SIRGAS (RNAAC-SIR), Tide Gauge Monitoring Working Group (TIGA)
International Laser Ranging Service (ILRS)	Global Data and Operation Centre (EDC), Analysis Centre
International VLBI Service for Geodesy and Astrometry (IVS)	Analysis Centre, Combination Centre (jointly with BKG)

of source positions. Table 1.2 shows all 666 sessions that were analyzed in 2015. Considering previous years, 1567 consistently analyzed sessions for the time span from September 2004 to November 2015 were available at the end of 2015.

All routine VLBI analyses are still performed with OCCAM. Besides, the development of a new software called DOGS-RI (DGFI Orbit and Geodetic Parameter Estimation Software - Radio Interferometry) that strictly follows IERS 2010 Conventions is in progress. In 2015, intensive comparisons between DOGS-RI and OCCAM were carried out to debug the new software. Progress could also be made within the framework of the “VLBI Analysis Software Comparison Campaign 2015” organized by the Chalmers University of Technology.

Together with the Federal Agency for Cartography and Geodesy (BKG), DGFI-TUM also operates an IVS Combination Center. In this connection, DGFI-TUM is in charge of developing combination procedures and maintaining the combination software DOGS-CS.

Table 1.2: *VLBI sessions analyzed in 2015 using OCCAM.*

Session type	2004	2005	2006	2007	2008	2009	2013	2014	2015	Total
AOV	–	–	–	–	–	–	–	–	2	2
APSG	2	2	2	2	–	–	–	–	1	9
AUS	–	–	–	–	–	–	–	–	1	1
CONT05	–	15	–	–	–	–	–	–	–	15
EUROPE	1	3	6	6	–	–	–	1	4	21
IVS-CRF	–	2	1	2	–	–	–	–	–	5
IVS-E3	1	4	1	–	–	–	–	–	–	6
IVS-OHIG	1	3	6	7	3	–	–	6	3	29
IVS-R1	17	49	52	51	15	–	–	3	46	233
IVS-R4	18	50	51	52	15	1	–	7	43	237
IVS-R&D	1	10	10	9	3	–	1	6	4	44
IVS-T2	4	6	6	4	2	–	–	1	1	24
QUAKE	–	–	1	–	–	–	–	–	–	1
VLBA	3	13	8	7	2	–	–	1	5	39
Total	48	157	144	140	40	1	1	25	110	666

Monitoring of tide gauges with GNSS

DGFI-TUM operates several continuously tracking GNSS stations (four along the Bavarian Alps, three in Bolivia, three in Chile, and two in Peru). The operation of these stations is supported by local partner institutions which take care of the appropriate functioning of the equipment and the data delivery to DGFI-TUM where the data are archived and distributed to the processing centres. DGFI-TUM regularly processes these data within the scope of several projects like modelling of regional deformations, computation of the regional reference frame SIRGAS, GNSS monitoring of tide gauges, and vertical datum unification in South America. These stations also contribute to the IGS Tide Gauge Benchmark Working Group (TIGA), the IGS Multi-GNSS Experiment (MGEX), and the regional densification of the ITRF in Latin America.

In the case of TIGA (Schöne et al. 2015), DGFI-TUM processes a global network with about 450 continuously operating GNSS stations, including IGS reference stations as fiducial points and tide gauges with a homogeneous global distribution (Fig. 1.1). The main objective is to generate precise station position time series to be combined with tide gauge registrations and satellite altimetry observations at selected sites; in particular, at those tide gauges realizing the local vertical datums. The station position time series shall be computed for the period from January 1997 to December 2014 following the IERS Conventions 2010 and the GNSS-specific guidelines defined by the IGS for the second reprocessing of its global network (http://acc.igs.org/reprocess2.html). At present, daily and weekly solutions from January 2007 to December 2012 were reprocessed.

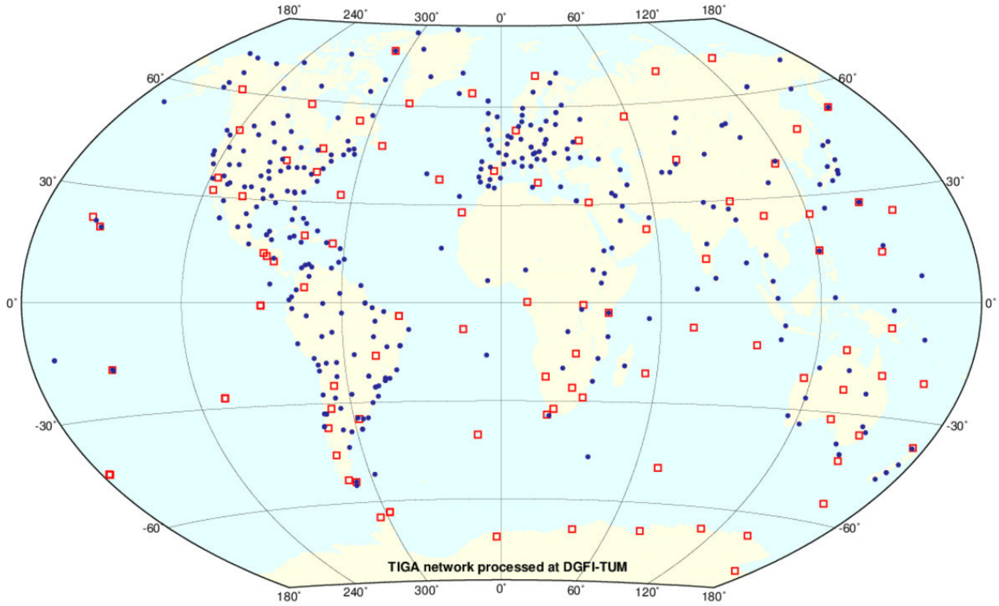

Fig. 1.1: *Network processed by DGFI-TUM for the monitoring of tide gauges using GNSS (TIGA). Red squares represent IGS reference stations.*

Monitoring of regional deformations with GNSS

Strong earthquakes cause large changes in the station positions and velocities of the geodetic reference stations, i.e., the global ITRF and its regional densifications like SIRGAS (Sistema de Referencia Geocéntrico para Las Américas) in Latin America and the Caribbean. To ensure the long-term stability of the geodetic reference frames, the transformation of station positions between different epochs requires the computation of reliable continuous surface deformation (or velocity) models. DGFI-TUM computed a new crustal deformation model for Latin America and the Caribbean inferred from GNSS (GPS+GLONASS) measurements registered after the strong earthquakes in Chile and Mexico in 2010. It is based on a multi-year velocity solution for a network of 456 continuously operating GNSS stations and covers a five year period from March 14, 2010 to April 11, 2015. This new deformation model called VEMOS2015 (Velocity model for SIRGAS 2015) was computed using the least squares collocation (LSC) approach with empirically determined covariance functions. The results, displayed in terms of velocity (Fig. 1.2) and strain field (Fig. 1.3), make evident that the tectonic structure in South America has to be redefined: The area from 35°S to 40°S latitude was usually considered as a stable part of the South American plate; now it is obvious that there is a large and extended crustal deformation zone. Comparisons with reference frame solutions based on measurements before the 2010 earthquakes (like the ITRF2008 or former SIRGAS solutions) and with the previous model VEMOS2009 show the strong deformation caused by these earthquakes and highlight the necessity of updating reference frames and deformation models in the affected region.

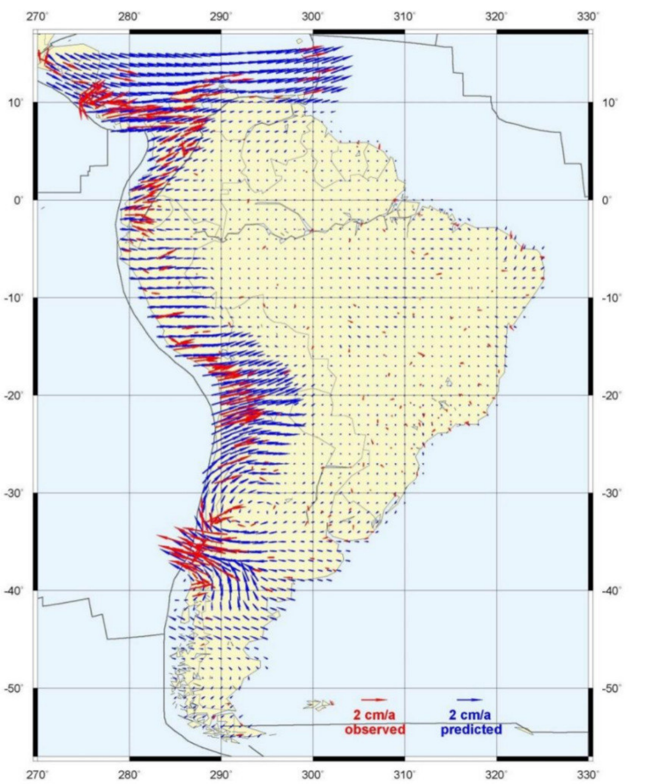

Fig. 1.2: Deformation model VEMOS2015 relative to the South American plate.

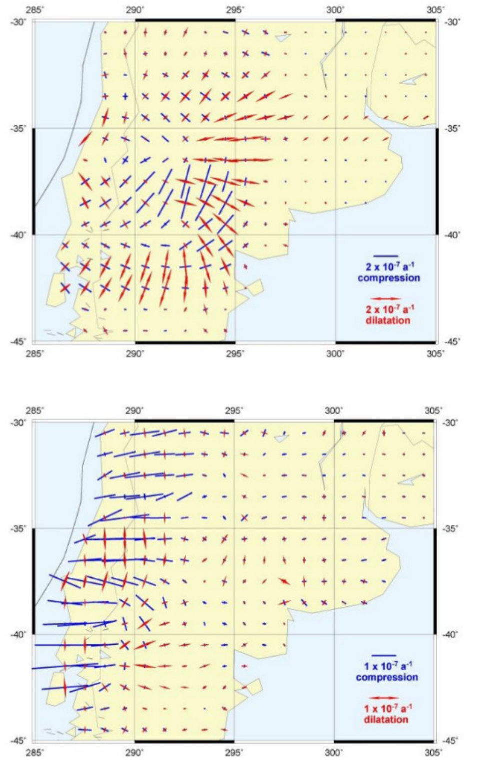

Fig. 1.3: Strain field after (2010-2015, top) and before (2000-2008, bottom) the Maule 2010 earthquake.

1.2 Analysis of Satellite Laser Ranging Observations

SLR data management

Since the foundation of the International Laser Ranging Service (ILRS) in 1998, the EUROLAS Data Centre (EDC) acts as one of two global ILRS data centres: the EDC at DGFI-TUM and the Crustal Dynamics Data Information System (CDDIS) at NASA. The EDC, as ILRS Operation Center (OC) and ILRS Data Center (DC) has to ensure the quality of submitted data sets by checking their format (Schwatke 2015). Furthermore, a daily and hourly data exchange with the NASA OC and CDDIS is performed. All data sets and products are publicly available for the ILRS community via ftp (ftp://edc.dgfi.tum.de) and website (edc.dgfi.tum.de).

EDC is running several mail lists for the exchange of information, data and results. The Consolidated Prediction Format (CPF) files (47358 in 2015) of 87 satellites are sent automatically to the SLR stations and stored at the ftp server. Mailing lists such as SLR-Mail (57 in 2015), SLR-Report (1079 in 2015), Urgent and Rapid-Service-Mail (22 in 2015) are maintained by EDC.

In 2015, 40 SLR stations observed 91 satellites. There were eight new satellite missions tracked by SLR stations, namely Compass-IS1, Compass-IS2, Compass-MS1, Compass-MS2, Galileo-205, Galileo-206, IRNSS-1D, and LightSail-1. Figure 1.4 shows the ILRS station network in 2015.

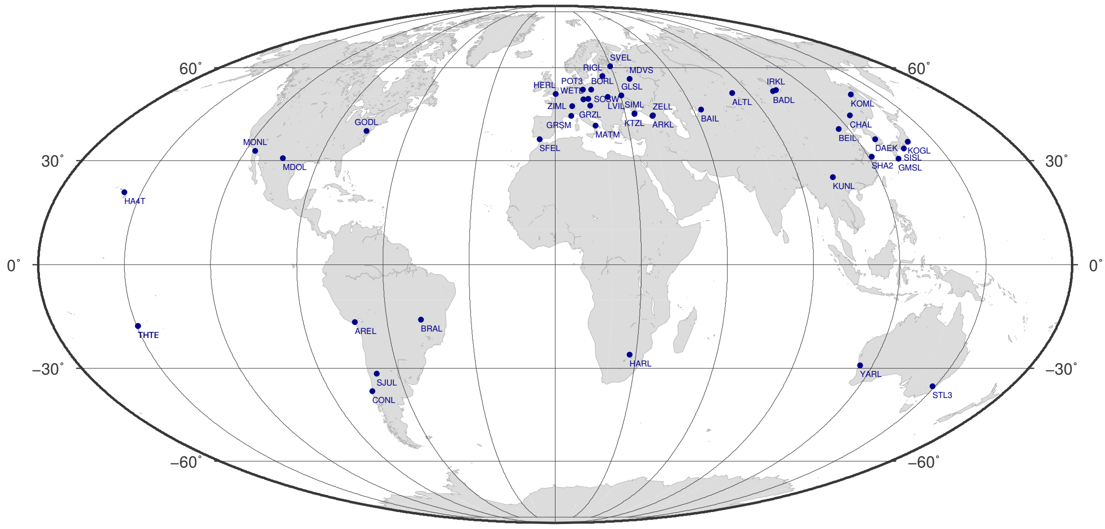

Fig. 1.4: *The ILRS station network in 2015*

SLR quality control

Within the "ILRS Quality Control Standing Committee (Q/C SC), DGFI-TUM performs the daily processing of station biases on a pass-by-pass basis for most of the relevant geodetic satellites. To ensure comparable results of the Q/C centres, the use of the same set of station coordinates is mandatory. The computation of preliminary coordinates for new stations is done by DGFI-TUM as responsible centre. Stations with long data outages (> 60 days) or major upgrades are automatically put under quarantine. The validation of quarantined sites is also part of the Q/C SC responsibility.

On the DGFI-TUM website (ilrs.dgfi.tum.de/quality/weekly_biases/), a daily report on the computed biases is published. In case of bias anomalies the station is contacted via the ILRS Rapid Service Mail. In 2015, 24 bias alerts were issued by the Q/C centres.

SLR data analysis

As one of the analysis centres of the ILRS Analysis Standing Committee (ILRS/ASC), formerly known as the ILRS Analysis Working Group (ILRS/AWG), DGFI-TUM is involved in various activities. It delivers daily and weekly products including station coordinates and Earth orientation parameters on the basis of weekly arcs. Additionally, DGFI-TUM contributes to all pilot projects of the ILRS/ASC and delivers input for the ITRF computations. In preparation of future pilot projects, DGFI-TUM computes orbits for all geodetic satellites.

So far, SLR analysts assumed that core sites were generally free from range or time biases. Only for certain periods fixed biases computed from long-term analyses have to be applied to these stations. On the DGFI-TUM website (ilrs.dgfi.tum.de/data_handling/ILRS_Data_Handling_File.snx), a table with these corrections is maintained.

In the meantime, the ILRS/ASC intends a pilot project assuming that no station is free from systematic errors. Therefore, biases for all stations and all satellites will be solved. In this framework, DGFI-TUM has performed various test computations to figure out whether biases were constant with range and whether biases were correlated with the orbit and through the orbit with biases from other stations. Therefore, two different solution types were computed to solve the biases for eleven geodetic satellites:

- solve for only one bias per station per run, all other biases fixed
- solve for individual biases for all stations in one common adjustment

The results showed that the correlation between biases is negligible and that it is not necessary to solve for each bias separately. There is also no large impact if a bias is solved for each station separately or if all biases are solved together. A dependence of a bias on the distance of the satellite (a so-called range-dependent bias) could not be detected, since the bias estimation for low Earth orbiters (LEOs) is not stable enough and needs further investigation. Figure 1.5 shows that even stable core stations with a long history of SLR observations cannot be assumed bias-free.

Since SLR is important for the realization of the scale of the terrestrial reference frame, we studied the impact of the bias estimation on the SLR scale by comparing different SLR solutions. One solution was the standard ILRS solution assuming no biases for the core stations. In a second solution, we solved for range biases of the core network, applied these biases to the stations and simultaneously solved for station coordinates and biases. Results show that the bias handling has a small impact on the scale estimation but needs further investigation.

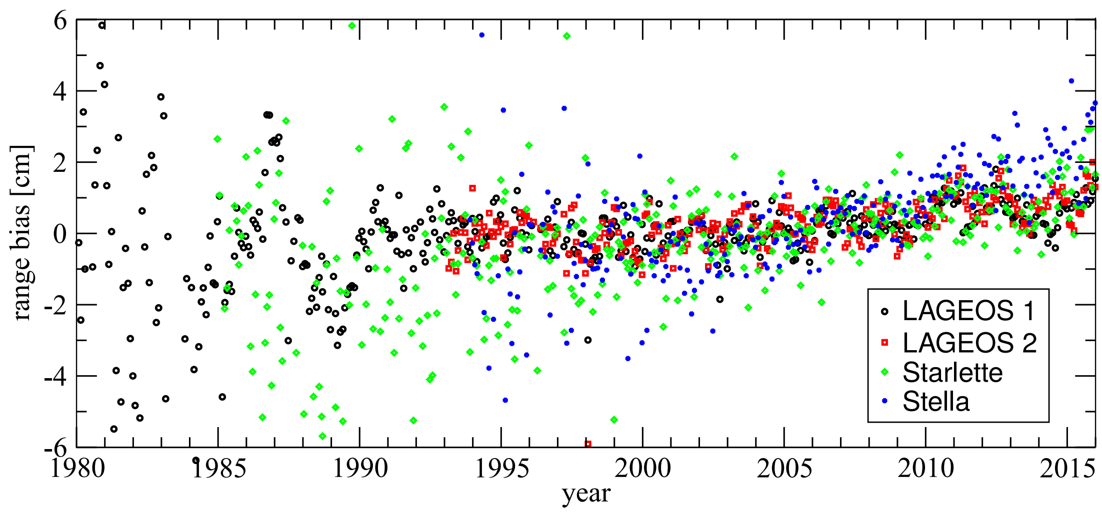

Fig. 1.5: *Station-dependent range bias from 1980 to 2015 for Yarragadee (Australia, 7090), using four geodetic satellites.*

1.3 Computation of Satellite Orbits

SLR multi-satellite analysis

Within the DFG Research Unit (FOR1503) on “Space-time reference systems for monitoring global change and for precise navigation in space”, DGFI-TUM is working on the realization of “Consistent dynamic satellite reference frames and terrestrial geodetic datum parameters‘”. Since SLR observations are already used for the definition of the origin and the scale of the International Terrestrial Reference Frame, it has to be investigated to which extent the SLR observations could also be used for the definition of the TRF orientation. Therefore, SLR observations to LEOs with a non-spherical shape are analyzed since low satellite orbits are much more sensitive to the Earth’s gravitational field. Potentially, this information might be used to connect the TRF orientation with the gravity field of the Earth.

For these investigations, DOGS-OC (DOGS library for orbit computation) had to be upgraded with the modeling of non-gravitational perturbations (e.g., solar radiation pressure, Earth IR radiation, Earth albedo, thermospheric drag) for satellites of various shapes. For validation, several tests using the non-spherical satellite Jason-2, launched in 2008 and still in orbit, were carried out, since this satellite is extensively observed by the global tracking network of the ILRS. The time series of Jason-2 SLR observations from July 2008 to February 2015 (about 6.5 years) was processed with DOGS-OC using 3.5-day arcs (except for arcs containing orbital maneuvers which were truncated at the beginning of the maneuver and restarted afterwards).

In Figure 1.6, the dynamical and the observation model adopted for the Jason-2 precise orbit determination (POD) are specified together with a list of the estimated parameters. The final SLR RMS values of the processed Jason-2 arcs are shown in Fig. 1.7 with an average value of 1.18 cm. In Fig. 1.8, the differences between the DOGS orbit and a dynamic ESOC orbit (SLR-only) are shown for a 3.5-day arc with most values below 10.0 cm. Jason-2 was then combined with up to 10 spherical satellites to perform an SLR multi-satellite solution with up to

Dynamical model	Description
Earth gravity field	EIGEN-6S2 (Rudenko et al., 2014) up to degree/order 120
Solid Earth tides	IERS2010 Conventions (anelastic Earth, conventional permanent tide)
Ocean tides	EOT11a (Bosch and Savcenko, 2011) up to degree/order 50 (18 main + 63 secondary waves)
Ocean loading tides	EOT11a (Bosch and Savcenko, 2011) (11 main + 342 secondary waves)
Atmospheric tides	IERS2010 Conventions (S1/S2 incorporated in EOT11a)
Atmospheric loading tides	IERS2010 Conventions (Ray and Ponte, 2003)
Pole tides	IERS2010 Conventions
Lunar gravity field (static)	(Ferrari, 1977) up to degree/order 4
General relativistic correction	IERS2010 Conventions (Schwarzschild, deSitter, Lense-Thirring)
Third body effect	DE-421: Mercury, Venus, Mars, Jupiter, Saturn, Sun and Moon (Folkner et al., 2008)
Non-tidal gravity perturbation	None
Empirical accelerations	sine/cosine terms; along- and cross-track directions
Solar radiation pressure	CNES macro-model (Cerri and Ferrage, 2014) for box-wing satellite model
Earth radiation pressure	albedo and IR (Knocke et al.,1988)
Atmospheric drag	atmospheric density model JB2008 (Bowman et al., 2008) + external geomagnetic storm and solar flux indices

Observation model	Description
Elevation cut-off angle	5 deg
Laser retro-reflector array (LRA) optical center[1]	X = +1.1940 m, Y = +0.5980 m, Z = +0.6840 m
LRA phase center offset	4.9 cm subtracted from the computed range
Initial mass	505.9 kg (mass history file)
Initial center of mass (CoM)[1]	X = +0.9768 m, Y = +0.0001 m, Z = +0.0011 m (CoM history file)
Tropospheric correction	(Mendes and Pavlis, 2004)

[1] *in the satellite reference frame*

Estimated parameters	Temporal resolution
In POD process:	
Keplerian elements	One set per arc (initial epoch)
Solar radiation pressure coefficient	One per arc
Albedo coefficient	One per arc
Empirical coefficients (CPRs)	One set per arc (sine/cosine terms; along- and cross-track)
Drag coefficients	Two per day
Added in geodetic parameter estimation process:	
Earth orientation parameters (EOPs)	One set per day (terrestrial pole coordinates, UT1-UTC) → piece-wise linear polygons at midnight epochs
Station coordinates	One set per arc
Stokes gravity coefficients	One set per arc (up to degree/order 60)

Fig. 1.6: *Dynamical model, observation model and list of estimated parameters for the processing of Jason-2 SLR observations.*

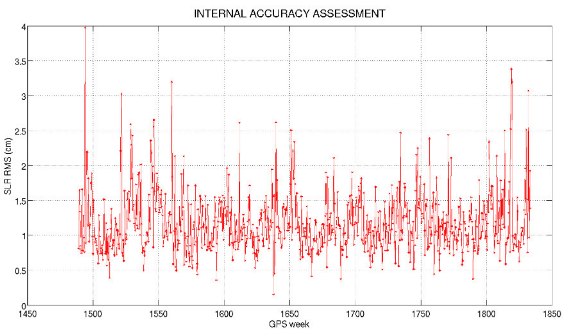

Fig. 1.7: SLR RMS values of Jason-2 POD (July 2008 – February 2015).

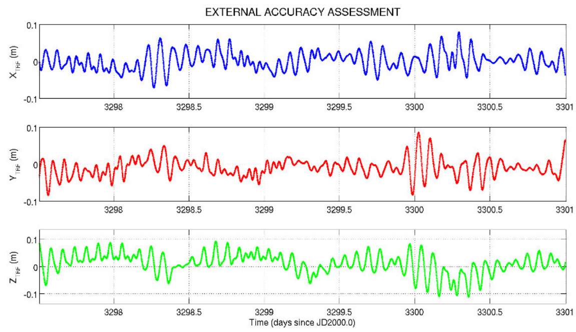

Fig. 1.8: Differences between the DOGS and the ESOC Jason-2 orbit for a 3.5-day arc in 2009.

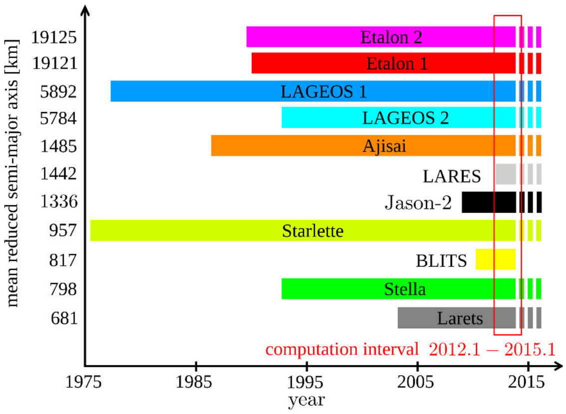

Fig. 1.9: Satellites within the computation interval from 2012.1 to 2015.1 used for the SLR multi-satellite solution.

11 satellites altogether (Fig. 1.9). The geodetic parameters shown in Fig. 1.6 were computed for a period of 3 years. First of all, datum-free (constraint-free) normal equations (NEQs) for each satellite arc were computed with DOGS-OC. Those NEQs were combined on a weekly basis and solved with DOGS-CS (combination and solution package). Therefore, the NEQs have to pass through several pre-processing steps, and various constraints to remove rank deficiencies have to be added (Bloßfeld et al. 2015a). The initial datum-free NEQs include the following parameters: Keplerian elements, Stokes coefficients up to degree/order 60 to describe the Earth's gravitational field, Earth orientation parameters (terrestrial pole coordinates and UT1-UTC), station coordinates, scaling coefficients for solar radiation pressure, Earth albedo and thermospheric drag (only for satellites at altitudes below 2000 km) as well as empirical accelerations such as along-track accelerations (for satellites above 2000 km) and amplitudes of cycle-per-revolution (CPR) coefficients. The procedure is illustrated in Fig. 1.10.

The 11-satellite solution including Jason-2 was then compared with a 10-satellite solution to assess the contribution of Jason-2 to the estimated geodetic parameters. Fig. 1.11 and 1.12 show the spectra of translation and scale offsets w.r.t. SLRF2008 for the combination of 10 and 11 satellites. In the 11-satellite solution, the 117-day draconitic period of Jason-2 is visible in the z-translation, while the 23.5-day period (5th harmonic of the draconitic period of Jason-2) appears in the scale. Both periods are probably due to deficiencies in the Jason-2 solar radiation pressure modeling.

Fig. 1.13 illustrates the differences between the standard deviations (STDs) of the Stokes coefficients resulting from an 11- and a 10-satellite solution. The consideration of Jason-2 for the SLR multi-satellite solution yields a reduction of the STDs of about 10 % for the tesseral and sectorial harmonics up to degree 20. In contrast, the zonal harmonics of degree 2 cannot benefit, because Jason-2 has an inclination of about 66° and, as a consequence, is less sensitive to the zonal harmonics.

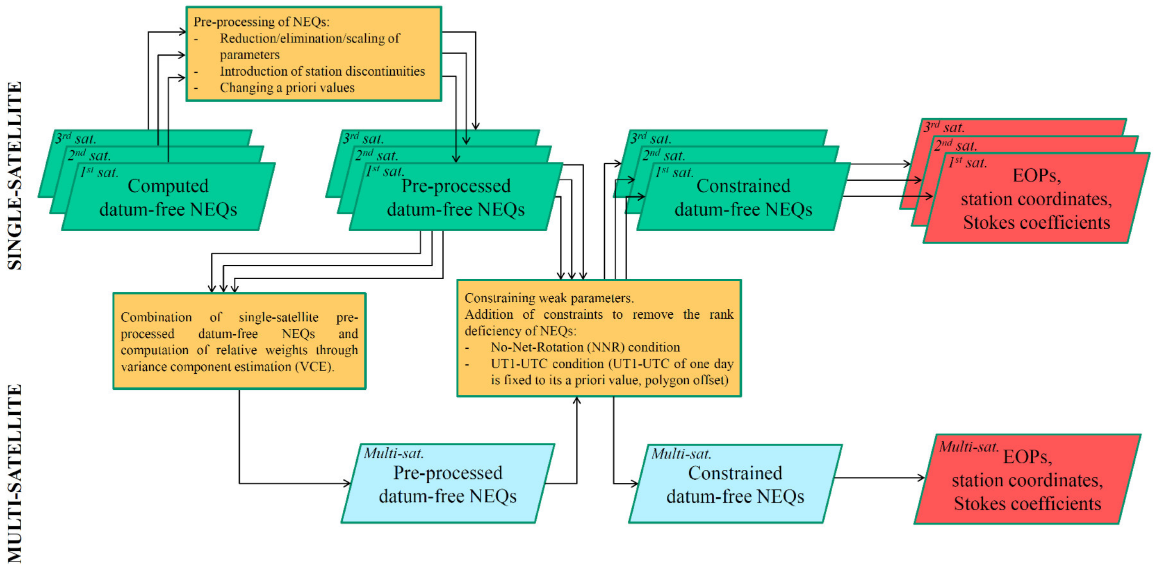

Fig. 1.10: *Flowchart of the parameter estimation procedure for the single-satellite and the multi-satellite SLR solution. Both solutions are based on identical input data.*

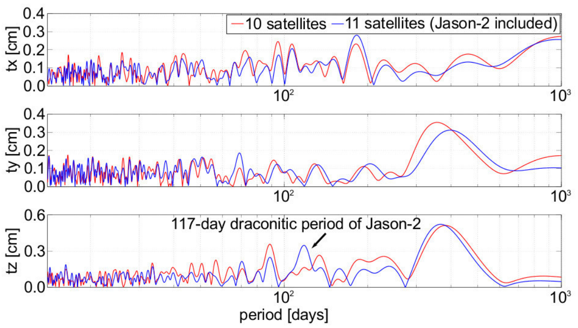

Fig. 1.11: *Spectra of the translation offsets w.r.t. SLRF-2008 for a 10- (red) and 11-satellite solution (blue).*

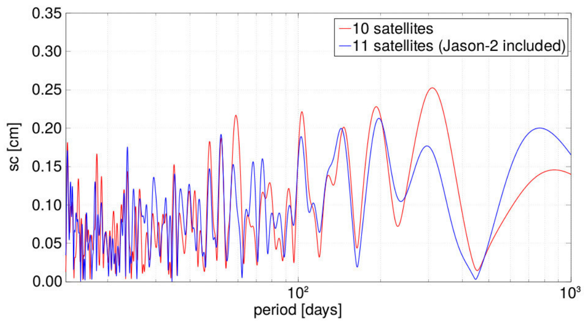

Fig. 1.12: *Spectrum of the scale offset w.r.t. SLRF2008 for a 10- (red) and 11-satellite solution (blue).*

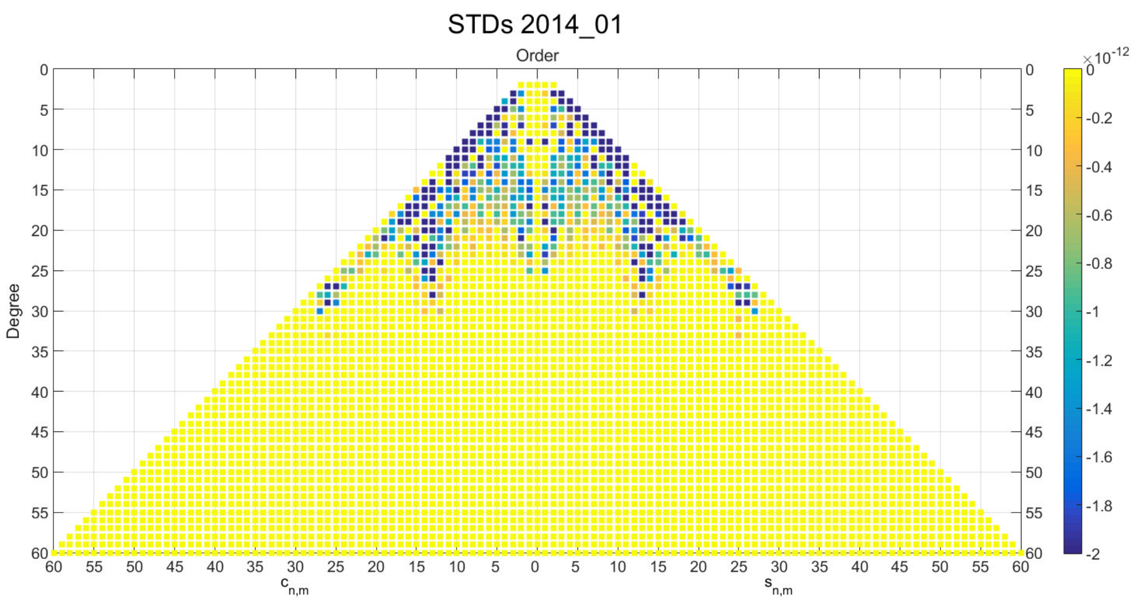

Fig. 1.13: *Difference between the STDs of the Stokes coefficients resulting from an 11- and a 10-satellite SLR solution.*

1.4 Determination of Reference Frames

DTRF2014, the new DGFI-TUM realization of the ITRS

Three ITRS Combination Centers of the IERS (DGFI-TUM, IGN, and JPL) are in charge of the computation of the new realization of the International Terrestrial Reference System (ITRS), the ITRF2014 (Seitz et al. 2015, Bloßfeld et al. 2015b). The solution computed by DGFI-TUM is called DTRF2014. The ITRS realization is based on the combination of the observation data of four space geodetic techniques: VLBI, SLR, GNSS, and DORIS. Observations are included from the respective start of the techniques until the end of 2014 (see Table 1.3). The DTRF2014 contains station positions and velocities as well as consistently estimated Earth orientation parameters. Additionally, for the first time, non-tidal atmospheric and hydrological loading is considered. This new realization includes six more years of data as the previous realization, the DTRF2008, and new observing stations as well as improved models are considered.

Table 1.3: *Input data sets for the ITRF2014 (NEQ: constraint-free normal equation). In addition, local tie information provided by the ITRS Centre is used as input as well as non-tidal atmospheric and hydrological loading data provided by the GGFC of the IERS.*

Technique	Service	Data	Time period
GNSS	IGS	daily solutions	1994.0 – 2015.2
VLBI	IVS	24 h session NEQ	1980.3 – 2015.0
SLR	ILRS	15/7 day solutions	1982.9 – 2015.0
DORIS	IDS	weekly solutions	1993.0 – 2015.0

The general concept of the combination strategy used at DGFI-TUM is based on the combination of constraint-free normal equation systems resulting from the observation time series of the space geodetic techniques. The combination procedure consists of two main steps:

- the generation of multi-year normal equation systems comprising all available data of a single technique (accumulation of time series)
- the combination of the single-technique multi-year normal equation systems to one common solution (inter-technique combination)

Figure 1.14 shows a simplified scheme of the DTRF2014 combination procedure. Some statistics of the DTRF2014 computation are displayed in Fig. 1.15. The horizontal station velocities of the DTRF2014 solution are shown in Fig. 1.16.

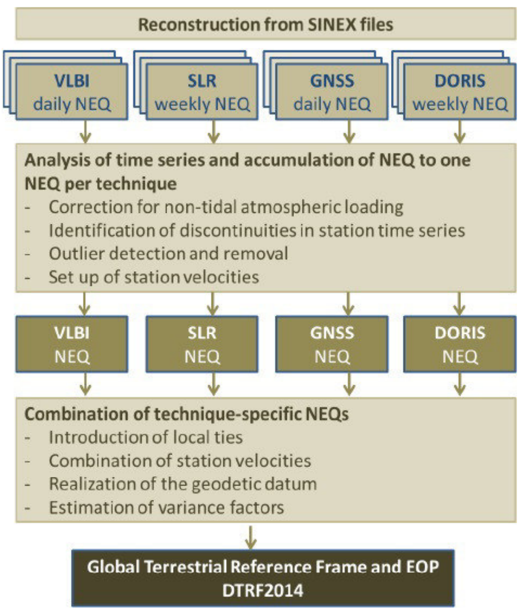

Fig. 1.14: *Simplified processing scheme for the DTRF2014 computation at DGFI-TUM.*

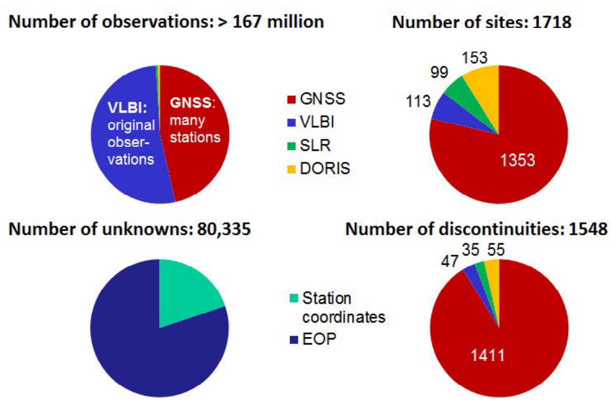

Fig. 1.15: *DTRF2014 solution statistics. The size of the DTRF2014 normal equation matrix is 49.2 GB.*

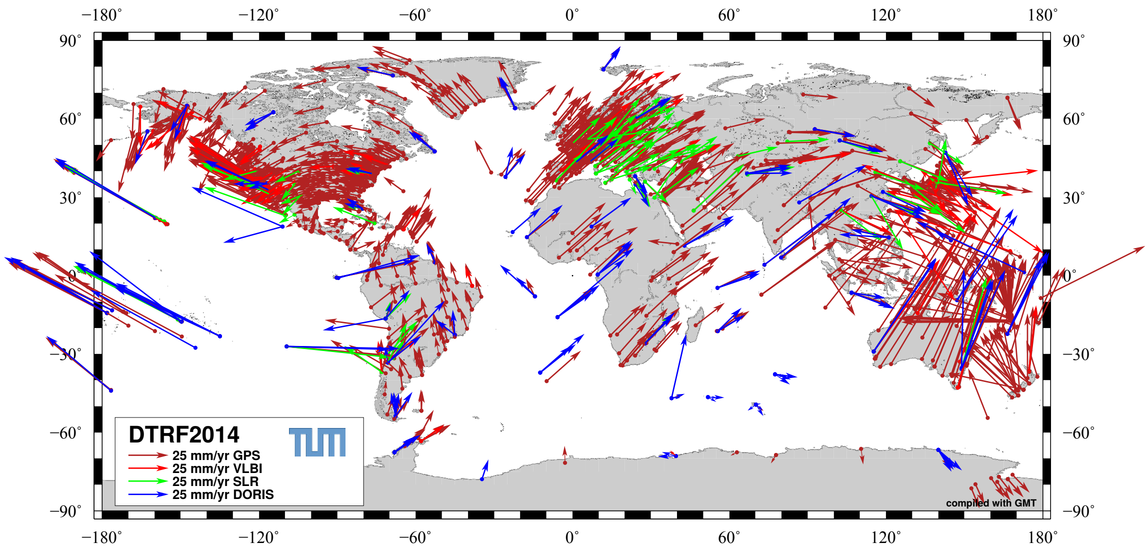

Fig. 1.16: *Horizontal station velocities of the DTRF2014 solution.*

To evaluate the internal accuracy of the DTRF2014 solution we performed 14-parameter similarity transformations between the single-technique solutions and the combined DTRF2014 solution. These transformations were carried out separately for each technique by using globally distributed core stations. As a result, two quality estimates are obtained for each technique-specific network:

- the transformation parameters between the single-technique solutions and the DTRF2014 as a measure for the accuracy of the datum definition (see Table 1.4)
- the RMS for station positions and velocities as a measure for the accuracy of the network geometry (see Fig. 1.17)

Table 1.4: *Results of 14-parameter Helmert transformations between single-technique solutions and the DTRF2014. Values are given for the origin (realized by SLR) and the scale (realized by a weighted mean of SLR and VLBI).*

Technique		Tx	Ty	Tz	Sc
SLR	offset (mm)	0.1 ± 0.21	0.6 ± 0.21	0.9 ± 0.21	0.2 ± 0.21
	rate (mm/yr)	0.0 ± 0.04	0.0 ± 0.04	-0.1 ± 0.04	0.0 ± 0.04
VLBI	offset (mm)				0.4 ± 0.09
	rate (mm/yr)				0.1 ± 0.01

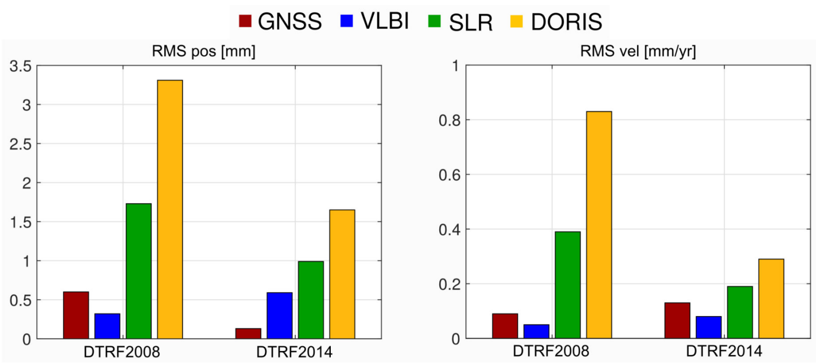

Fig. 1.17: *RMS station position and velocity results of Helmert transformations between the single-technique solutions and the DTRF2014 compared to the results for the DTRF2008.*

Although the ITRF2014 was not released by the ITRS Centre before 2016, first comparisons between the DTRF2014 and the ITRF2014 solution generated by IGN (France) were made at DGFI-TUM in 2015. Technique-specific similarity transformations should demonstrate the level of agreement for the datum parameters as well as for station positions and velocities. The results of this external comparison are shown in Fig. 1.18. As regards the terrestrial scale, there is a significant discrepancy. As shown in Table 1.4, the SLR and VLBI scales agree well in the DTRF2014 solution, whereas the two techniques differ by more than 1 ppb in the IGN solution. This scale issue is subject to further investigation.

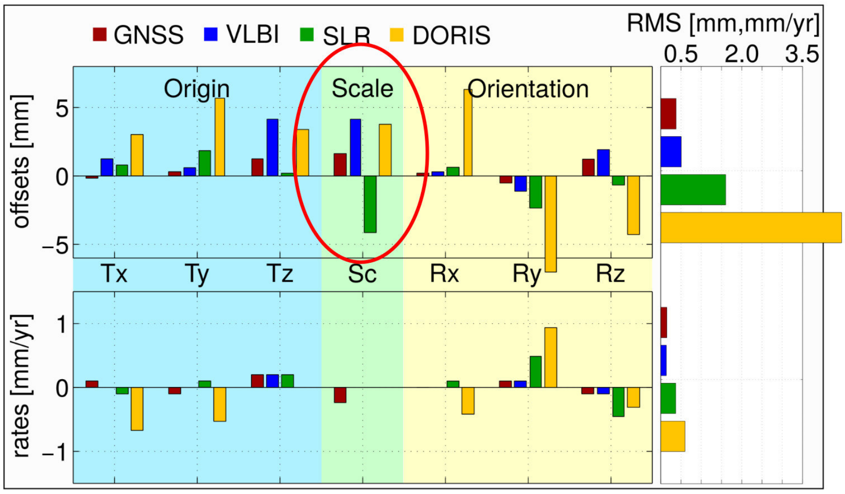

***Fig. 1.18:** Results of technique-specific 14-parameter Helmert transformations between DTRF2014 and ITRF2014.*

Regional terrestrial reference frame in Latin America (SIRGAS)

The SIRGAS reference frame is currently composed of 389 continuously operating GNSS stations and comprises two hierarchy levels: a core network (SIRGAS-C) providing the primary link to the global ITRF, and national reference networks (SIRGAS-N) improving the geographical density of the reference stations and ensuring the accessibility of the global reference frame at national and local levels (Sánchez et al. 2015a). The SIRGAS reference stations are processed by 10 SIRGAS Processing Centres (CEPGE Ecuador, CNPDG-UNA Costa Rica, CPAGS-LUZ Venezuela, DGFI-TUM Germany, IBGE Brazil, IGAC Colombia, IGN Argentina, IGM Chile, INEGI Mexico, SGM Uruguay) which generate loosely constrained weekly solutions to be integrated in a unified solution for the entire network. The individual solutions are combined by two SIRGAS Combination Centres: DGFI-TUM and IBGE. In charge of the IGS Regional Network Associate Analysis Centre for SIRGAS (IGS RNAAC SIRGAS), DGFI-TUM processed the entire SIRGAS network from June 1996 until August 2008. Currently, DGFI-TUM supports SIRGAS by

- processing the SIRGAS-C core network
- combining the core network with the national reference networks
- ensuring that the SIRGAS processing strategy meets the IERS standards and IGS guidelines
- developing strategies to guarantee the reliability of the reference frame over time; this

includes (i) the estimation of the reference frame kinematics (Fig. 1.19), (ii) the evaluation of the seismic impacts on the reference frame, and (iii) the modeling of crustal deformation in the SIRGAS region

- making available the SIRGAS products via www.sirgas.org and ftp.sirgas.org

Fig. 1.19: *Multi-year solution SIR15P01. It covers the time span from 2010.2 to 2015.2, includes 303 stations and refers to IGb08 (epoch 2013.0). Its accuracy is estimated to be ±1.8 mm in the horizontal position, ±3.5 mm in the vertical position, ±1.0 mm/a in the horizontal velocities and ±1.2 mm/a in the vertical velocities. This solution was the input for the computation of the deformation model VEMOS2015 (see Section 1.1).*

Geocentric regional epoch reference frame for Latin America

In the frame of the DFG-funded project DIGERATI (Direct geocentric realization of the South American reference frame by combination of geodetic observation techniques) DGFI-TUM aims at realizing a regional epoch reference frame (ERF) for SIRGAS that is geocentric, epoch-wise for short periods (up to several weeks) and has a stable datum (origin, orientation, and scale). The regional ERF is going to be realized directly by combining SLR (origin, scale), VLBI (scale) and GNSS (orientation; non-deforming no-net-rotation condition using IGS stations as fiducial points) at the normal equation level.

SLR is the only technique that allows the determination of the geocentre with high accuracy and contributes to the realization of the scale of a conventional reference frame. In addition, due to the high sensitivity of the SLR-tracked satellites on the Earth's gravitational field, SLR is a crucial technique for the determination of geometric parameters (e.g., station coordinates and Earth orientation parameters) together with low-degree spherical harmonics of the Earth's gravitational field.

The DOGS-OC software contains a simulation tool for SLR observations. Existing routines were extended or adapted. So far, the global distribution of SLR stations is quite inhomogeneous, and only few stations in the SIRGAS region are operational. In the framework of DIGERATI, SLR observations for virtual stations and/or satellites were simulated to evaluate the influence of future changes in the SLR network geometry on SLR-derived reference frames (Fig. 1.20). When simulating the observations to a predefined satellite, the software allows to set the observation rate, the mass centre correction, and a minimum elevation angle as global parameters for all stations. Additionally, performance (percentage of observed passes), measurement accuracy, coordinate changes or range and time biases can be defined for each station individually. Instead of setting the observation rate and performance parameters, given simulation epochs for each station can be imported. Further studies on variations of the observation strategy will be performed, e.g., by limiting the observations of each station to a small set at the beginning, mid and end of a pass.

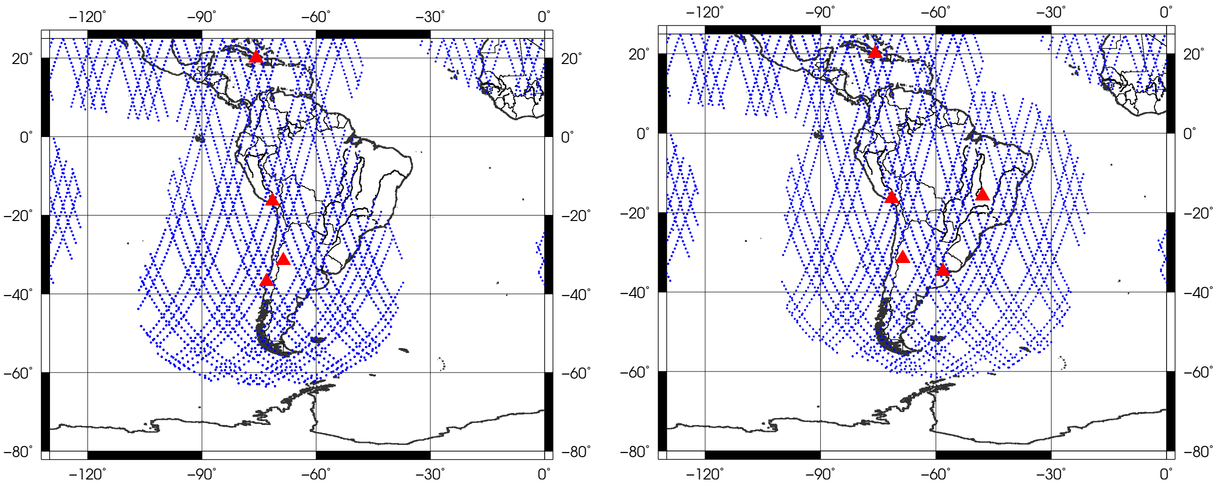

Fig. 1.20: Comparison of the pre-2014 (left) and post-2016 (right) SLR network in South America (red). LARES orbits visible from the stations (blue), simulated for GPS week 1833.

Consistent realization of terrestrial and celestial reference systems

In 2015, the DFG Research Unit (FOR 1503) on "Space-time reference systems for monitoring global change and for precise navigation in space" entered its second funding phase (2015–2018). Within the framework of project PN5 (only funded until 2017), DGFI-TUM aims at "Consistent celestial and terrestrial reference frames by improved modeling and combination".

With Resolution 3 adopted by the General Assembly in 2011, the IUGG urged "that highest consistency between the ICRF, the ITRF, and the EOP as observed and realized by the IAG and its components such as the IERS should be a primary goal in all future realizations of the ICRS". So far, the highest consistency could not be achieved, as three independent IERS product centers are in charge of computing the terrestrial and celestial reference frame as well as the connecting EOP. DGFI-TUM has the goal to demonstrate the benefit from estimating all three components in a common adjustment.

As routine DGFI-TUM analyses of VLBI data did not consider the estimation of source coordinates in the past, a reprocessing of all available 24-hour sessions was initiated in 2013. At the end of 2015, consistent solutions were available back to September 2004 (see Section 1.1). By stacking normal equations of more than 1400 24-hour sessions, an initial VLBI-only solution comprising more than 50 stations and more than 1800 radio sources could be generated.

Figure 1.21 shows the differences in declination and right ascension of the estimated source positions with respect to their ICRF2 a priori coordinates. The corrections for non-defining sources can amount to several mas, as lots of them were observed in only few sessions. The corrections for the so-called defining sources are considerably smaller. Significant differences are obtained mainly for sources in the southern hemisphere. They might be caused by the observations of several new Australian telescopes that were not available for the generation of the ICRF2.

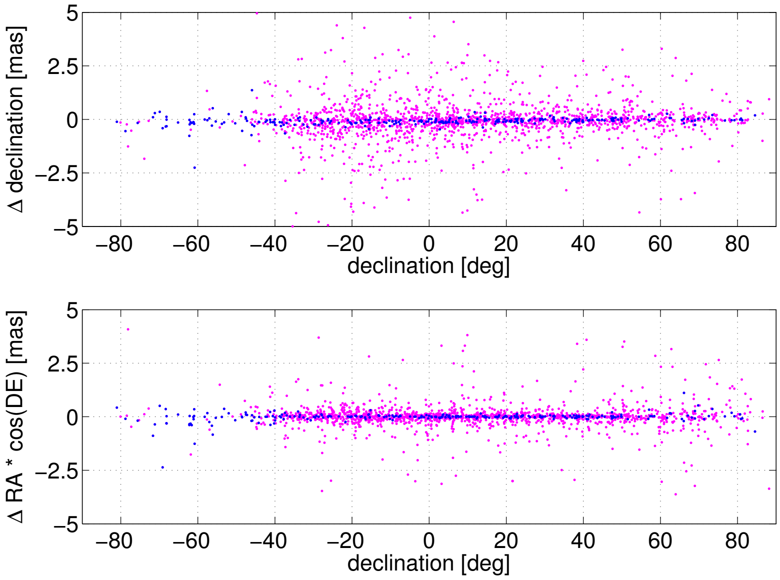

Fig. 1.21: *Differences in declination (top) and right ascension (bottom) between source positions resulting from a VLBI-only solution (based on data from 2005–2015) and ICRF2 a priori values for defining (blue) and other sources (magenta).*

Vertical reference systems – a conventional value for the geoid reference potential W_0

The Global Geodetic Observing System (GGOS) promotes, within the scope of its Focus Area 1 (Unified Height System), the definition and realization of a global vertical reference system with homogeneous consistency and long-term stability. DGFI-TUM supported this initiative by coordinating (for the term 2011–2015) the Working Group on “Vertical Datum Standardisation” (Sánchez et al. 2015b, whs.dgfi.tum.de) which directly depends on GGOS Focus Area 1 and which is supported by the IAG Commissions 1 (Reference Frames) and 2 (Gravity Field) as well as by the International Gravity Field Service (IGFS). The main purpose of this working group is to provide a geopotential value W_0 to be introduced as the conventional reference level for the realization of the global height system.

Since the most accepted definition of the geoid is understood to be the equipotential surface that coincides with the mean ocean surface, a usual approximation of W_0 is the averaged potential value W_S at the mean sea surface. Hence, the value of W_0 not only depends on the Earth’s gravity field model, but also on the conventions to define the mean sea surface. W_0 computations performed since 2005 demonstrated that recent estimations differed by up to 2.6 m^2s^{-2} (corresponding to a level difference of about 27 cm) which could be caused by the differences in the treatment of the input data. Therefore, DGFI-TUM concentrated on a new W_0 estimation relying on the newest gravity field and sea surface models and applying standardized data and procedures. The following aspects were analyzed: (1) sensitivity of the W_0 estimation to the Earth’s gravity field model (especially omission and commission errors and time-dependent Earth’s gravity field changes); (2) sensitivity of the W_0 estimation to the mean sea surface model (e.g., geographical coverage, time-dependent sea surface variations, accuracy of the mean sea surface heights); (3) dependence of the W_0 empirical estimation on the tide system; and (4) weighted computation of the W_0 value based on the input data quality.

The results indicate that the satellite-only component (n = 200) of a static (quasi-stationary) global gravity model is sufficient for the computation of W_0. This model should, however, be based on a combination of at least SLR, GRACE and GOCE data. The mean sea surface modeling should be based on mean sea surface heights referring to a certain epoch and derived from a standardized multi-mission cross-calibration of several satellite altimeters. Uncertainties caused by geographically correlated errors, including shallow waters in coastal areas and sea water ice content at polar regions, should be considered in the computation of W_0 by means of a weighted adjustment using the inverse of the input data variances as a weighting factor.

As a reference parameter, W_0 should be time-independent (i.e., quasi-stationary) and it should remain fixed for a long-term period (e.g., 20 years). However, it should have a clear relationship with the mean sea surface level, as this is the convention for the realization of the geoid. According to this, a suitable recommendation is to adopt a potential value obtained for a certain epoch as the reference value W_0 and to monitor the changes of the mean potential value at the sea surface W_S. As soon as large differences appear between W_0 and W_S (e.g., > 2 m^2s^{-2}), the adopted W_0 may be replaced by an updated (best estimate) value. The potential value obtained for the epoch 2010.0 (62 636 853.4 m^2s^{-2}) was recommended as the present best estimate for W_0. This value was officially adopted by the IAG as the conventional W_0 at the General Assembly in Prague, 2015.

Related publications

Bloßfeld M., Müller H., Gerstl M., Stefka V., Bouman J., Göttl F., Horwath M.: Second-degree Stokes coefficients from multi-satellite SLR. Journal of Geodesy 89(9): 857–871, doi: 10.1007/s00190-015-0819-z, 2015a

Bloßfeld M., Seitz M., Angermann D., Moreaux G.: Quality assessment of IDS contribution to ITRF2014 performed by DGFI-TUM. Advances in Space Research, doi:10.1016/j.asr.2015.12.016, 2015b

Sánchez L., Drewes H., Brunini C., Mackern M.V., Martínez-Díaz W.: SIRGAS core network stability. IAG Symposia 143, doi:10.1007/1345_2015_143, 2015a

Sánchez L., Dayoub N., Cunderlík R., Minarechová Z., Mikula K., Vatrt V., Vojtísková M., Síma Z.: Report of Joint Working Group 0.1.1: Vertical Datum Standardization (JWG 0.1.1). Travaux de l'AIG IAG Reports 2011–2015 Vol. 39, url: iag.dgfi.tum.de/index.php?id=329, 2015b (Open Access)

Schmid R., Gerstl M., Seitz M., Angermann D.: DGFI Analysis Center Annual Report 2014. In: Baver K.D., Behrend D., Armstrong K.L. (Eds.) International VLBI Service for Geodesy and Astrometry 2014 Annual Report, 210–212, NASA/TP-2015-217532, 2015a

Schöne T., Bingley R., Deng Z., Griffiths J., Habrich H., Hunegnaw A., Jia M., King M., Merrifield M., Mitchum G., Neilan R., Noll C., Prouteau E., Sánchez L., Teferle N., Thaller D., Tregoning P., Williams S., Wöppelmann G., Woodworth P.: Tide Gauge Benchmark Monitoring Working Group Technical Report 2014. In: Jean Y., Dach R. (Eds.) International GNSS Service Technical Report 2014, 187-202, IGS Central Bureau, 2015

Schwatke C.: Historical development of the SLR data holding at EDC between 1976 and 2014. Proceedings of 19th International Laser Ranging Workshop, Annapolis, USA, 2015

Seitz M., Angermann D., Bloßfeld M., Gerstl M., Müller H.: ITRS Combination Centres: Deutsches Geodätisches Forschungsinstitut (DGFI). In: Dick W.R., Thaller D. (Eds.) IERS Annual Report 2014, Verlag des Bundesamts für Kartographie und Geodäsie, pp 120–123, 2015

2 Research Area Satellite Altimetry

Measuring sea surface height variations is essential for climate change monitoring. About two thirds of the Earth surface are covered by water. Satellite altimetry is the only technique that is able to provide absolute and precise sea surface height measurements globally and with homogeneous data distribution. The heights are given with respect to a geometric reference frame (i.e., ITRF) implicitly defined by the orbits of the altimeter satellites. The observations are equally distributed in time and space and provide consistent information on sea level change on different spatial and temporal scales for a time period of about 25 years.

DGFI-TUM maintains complete data holdings of all altimeter missions since 1991 (radar and laser) and manages and provides an open database for satellite altimeter data and derived high-level products (OpenADB). All altimeter missions are carefully harmonized and cross-calibrated on a regular basis (Section 2.1). The derived global multi-mission dataset is used for various ocean applications (Section 2.2) but also for water level monitoring of inland waters, such as lakes, reservoirs, rivers, and wetlands (Section 2.3).

2.1 Multi-Mission Altimetry

Open altimeter database

In order to ensure a long-term altimeter dataset with optimal temporal and spatial resolution, a joint analysis of data from all available altimeter missions is mandatory. For this purpose, comprehensive, consistent and up-to-date altimeter data and corrections are required. This necessitates a continuous update of DGFI's open altimeter database. In 2015, different geophysical correction models and external products (e.g., MSS CLS11, MDT CNES-CLS13) have been integrated in the database together with newly reprocessed data from ERS (REAPER project) and Jason-1 (GDR-E dataset).

Prior to using the new data versions for multi-mission applications, a cross-calibration with respect to other missions was performed. The first three years (2002–2005) of GDR-E data of Jason-1 reveal a significant reduction of the range bias from 10.7 to 4.4 cm relative to TOPEX (see Fig. 2.1). Moreover, the geographically correlated errors are slightly reduced compared to the old GDR-C dataset with GDR-D orbit. Still no systematic drifts w.r.t. TOPEX are detectable.

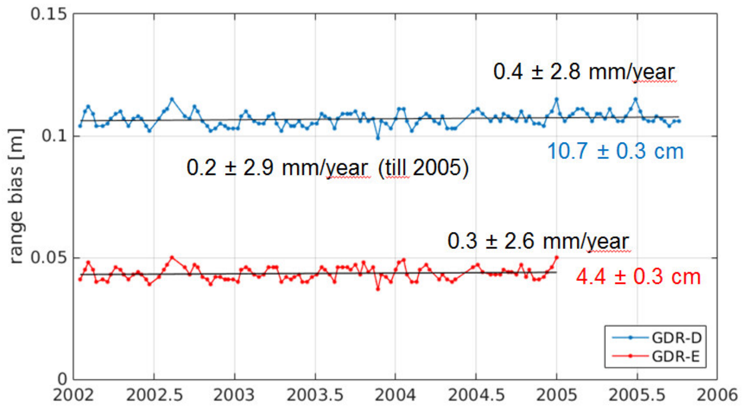

Fig. 2.1: *Relative range bias of Jason-1 with respect to TOPEX.*

Also for the ERS REAPER products a change of the range bias is visible. For ERS-1, the mean range bias changed from 43.9 cm to 65.9 cm and for ERS-2 from 7.1 cm to 65.2 cm. Even though the offsets with respect to TOPEX became larger for both missions, the inter-mission bias is now close to zero. For ERS-2, a systematic effect in the geographically correlated errors is visible in the REAPER product which was not part of the old OPR dataset (see Fig. 2.2). It is caused by the radiometer correction and is responsible for a systematic offset in the C20 term difference with respect to TOPEX. This effect can be reduced by using model corrections for the wet troposphere delay. Further investigations are necessary to understand this effect.

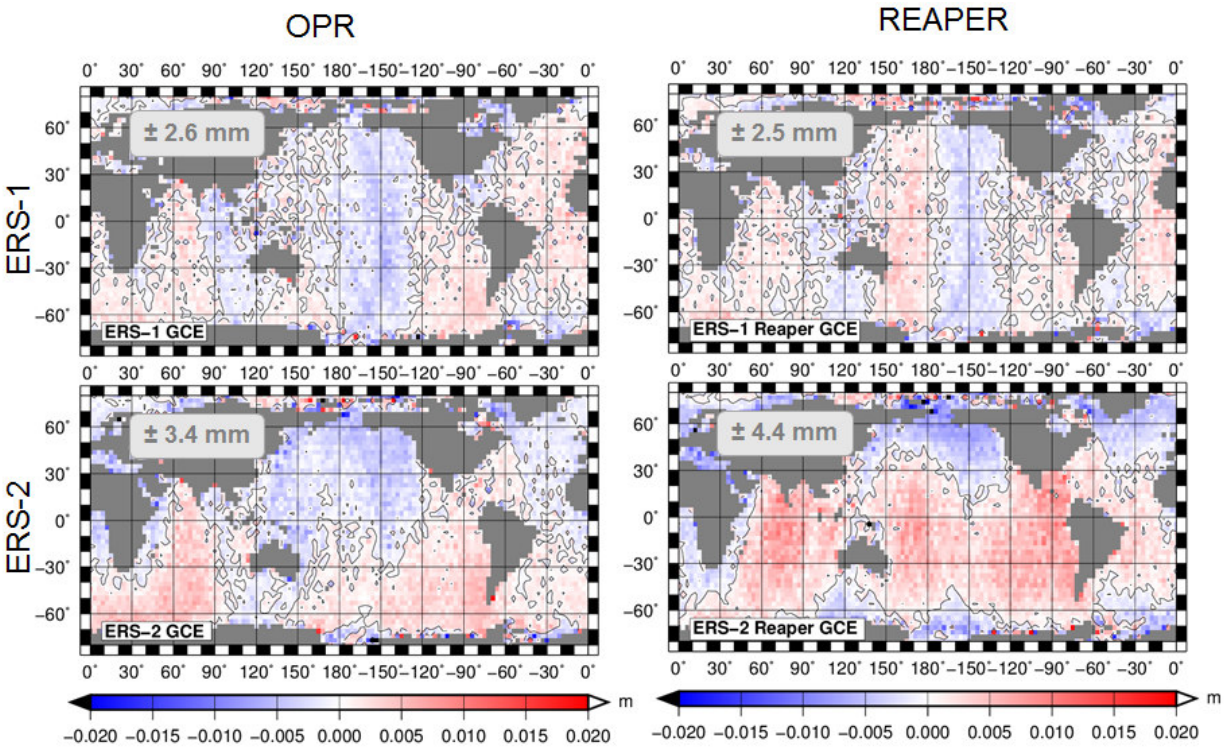

Fig. 2.2: Geographically correlated mean errors of ERS-1 (top) and ERS-2 (bottom) for old OPR dataset (left) and new REAPER product (right).

CryoSat-2 SAR stack data

In contrast to all other active and past altimeter systems, CryoSat-2 can be operated in the so-called SAR (synthetic aperture radar) mode and is the first of the new generation of Delay-Doppler altimeters. This technique is also part of Sentinel-3 launched in February 2016.

By exploiting the Doppler effect, Delay-Doppler altimeters are able to perform multi-looked acquisitions, i.e. to associate to one resolution cell a certain number of looks (variable; depending on the processing settings) acquired at different incidence angles as the satellite flies over the imaged area. Using processing techniques inherited from the classical SAR processing, such as range compression and range migration correction, all the returns corresponding to the resolution cell are aligned in a stack diagram (Fig. 2.3A). The CryoSat-2 multi-looked radar waveforms, such as the example in Fig. 2.3C, are obtained by summing all single echoes in the stack in the along-track dimension. These waveforms correspond to the classical waveforms of pulse-limited altimetry but have slightly different shapes. By summing up the returns in cross-track dimension (Fig. 2.3B), a so-called 'stack waveform' can be generated. It contains information concerning the backscattering properties of the illuminated surface, but it also reveals details of the distribution of the scatterers as the satellite spans different incidence angles passing over the nadir position.

Analyzing the stack waveforms of CryoSat-2 can provide additional information on the surface properties within the altimeter footprint and might help to classify the altimeter returns. Generally speaking, when the satellite flies over a very smooth surface, as in the case of small lakes or leads (small open water areas in sea ice regions), the signal will be specularly reflected back and the stack waveform will be peaky. In contrast, when flying over areas containing scatterers with different orientation (e.g., wavy seas or ice) the backscattered power will rather be normally distributed.

Preliminary studies have been performed at DGFI to exploit the stack waveform for classification purposes over small inland waters and sea ice regions. More information on this is provided in Sections 2.2 and 2.3.

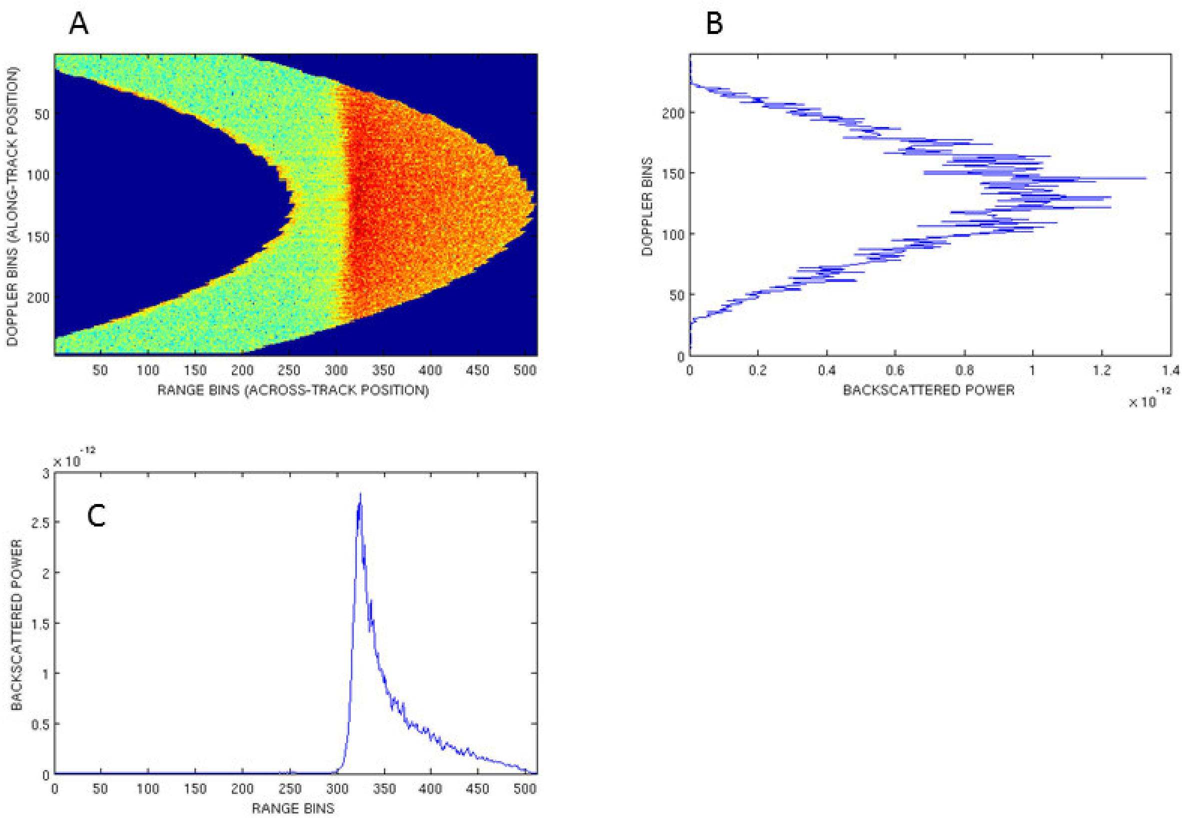

Fig. 2.3: Example of a stack diagram (A), a stack waveform (B) and a multi-looked waveform (C) acquired by CryoSat-2 over sea ice.

2.2 Sea Surface

Ocean tides and sea surface variability

For the composition of an astronomy exhibition in the Abraj Al-Bait Towers in Mecca, DGFI-TUM was commissioned to create a spatially and temporally highly resolved record of ocean surface variability due to the tidal influence of Sun and Moon. These data were used to create an animation to be shown in the new museum. The film mainly visualizes ocean tidal effects using the EOT11a (Empirical Ocean Tide) model developed by DGFI some years ago. Figure 2.4 shows a snapshot of the animation.

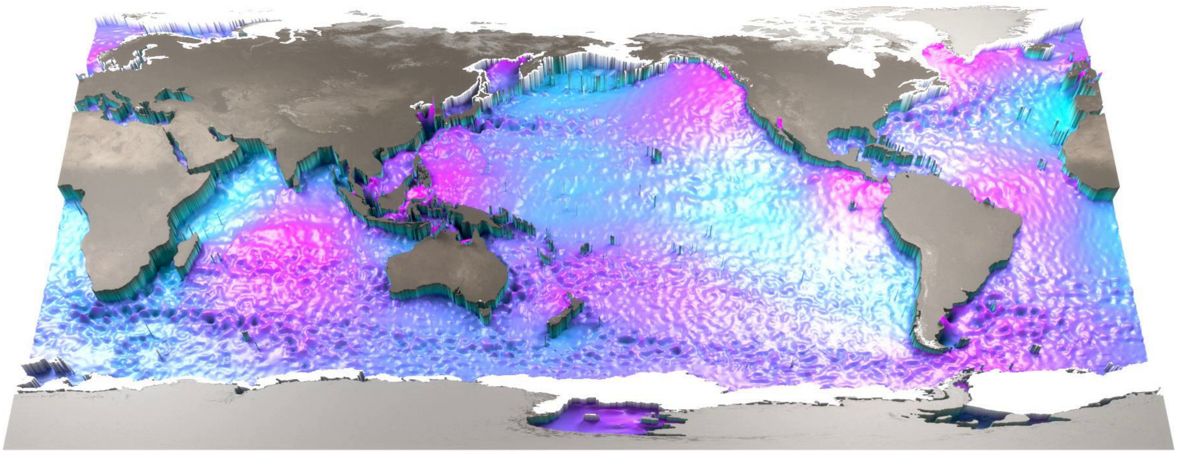

Fig. 2.4: *Sea surface heights with respect to a mean sea surface (CLS01). Tides from EOT11a are included.*

One can see the deviations of the sea level from a mean sea surface (long-term average of more than 20 years). The largest effects are due to ocean tides superimposed by smaller effects from currents and eddies. Clearly visible are different tidal heights in the Atlantic and Indian Ocean (many m) compared to closed seas like the Mediterranean or the Baltic Sea (few dm). Even regional peculiarities show up in the animation, e.g., in the Red Sea, the English Channel, or the Persian Gulf. The sea surface heights were created on a regular 0.1 degree spatial grid based on data from the radar altimetry missions Jason-1, Jason-2, and Envisat in combination with the EOT11a model. The dataset is available globally and can be used to visualize different ocean regions.

Instantaneous Dynamic Ocean Topography (iDOT)

Within the last years, an approach for estimating instantaneous dynamic ocean topography (iDOT) profiles on individual ground tracks of altimeter satellites has been developed at DGFI. An updated iDOT version has recently been computed. It is based on a new global GRACE/ GOCE geoid (GOCO05S[1]), improved and extended altimeter datasets as well as a new outlier detection. In contrast to long-term averaged mean dynamic topography fields (MDT), the DGFI iDOTs represent temporal variations within the ocean topography and allow for deriving gridded time series of DOT states representing seasonal (monthly or even 10-day) variations. For a validation of iDOTs, a comparison with in-situ measurements of surface currents by drifters and ARGO floats is straightforward. For this purpose, the iDOT heights (i.e., their gradients) are used to estimate ocean surface velocities applying the geostrophic assumption. In addition to a comparison of gridded products (1 degree spatial resolution for both altimetry and in-situ observations), a point-wise comparison is performed in order to avoid any unnecessary smoothing of the datasets.

For the comparison the geodetic multi-mission DOT heights are used to estimate geostrophic velocity components (u and v) directly at individual observation points of ARGO floats and surface drifters. This is done by fitting a plane to each point of comparison. The slope of this plane directly provides the geostrophic velocity components. These are compared to surface currents observed by the in-situ systems that are corrected for wind and Ekman drift. These differences

[1]Mayer-Gürr et al. (2015): The combined satellite gravity field model GOCO05s. Presentation at EGU 2015, Vienna

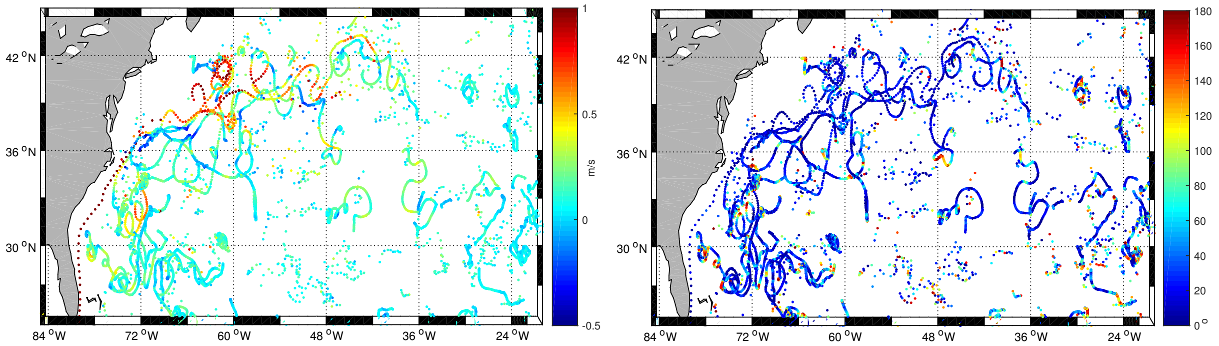

Fig. 2.5: *Geostrophic velocity differences in the Gulf Stream (in-situ minus iDOT) for July–September 2009. The left plot shows the differences in amplitude (speed) and the right plot the differences in phase (direction) of the velocities.*

are formed for different ocean regions, mainly for areas with strong western boundary currents. Figure 2.5 shows the velocity differences (in-situ minus iDOT) for a time period of three months in the region of the Gulf Stream. The differences between in-situ and iDOT-derived geostrophic velocities are very small with standard deviations of about 0.2 m/s (depending on the region). The u-components are slightly more accurate than the v-components. The iDOT-derived velocities show smaller differences with respect to in-situ measurements than mean fields (e.g., MDT CNES-CLS13), especially in the Gulf Stream region and for the Agulhas Current.

Due to the spatio-temporal sampling of altimetry with repeat orbits a smoothing of DOT-derived geo- strophic velocities is unavoidable and manifests itself by a scaling factor with respect to in-situ measurements. Even with optimized estimation parameters (interpolation radius and maximum temporal spacing) a factor of about 1.4 remains in the differences (see Fig. 2.6). This is related to the altimeter data distribution in space and time and depicts the limiting factor for such a comparison.

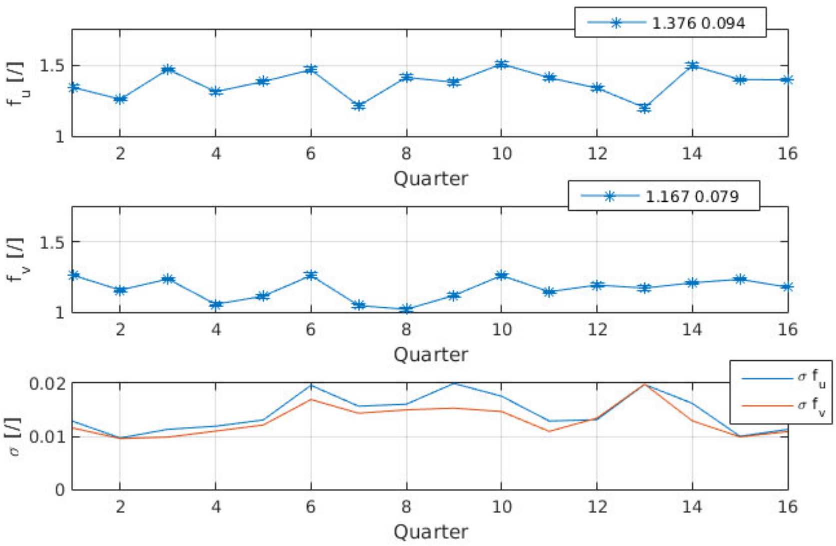

Fig. 2.6: *Estimated scaling factors (iDOT divided by in-situ) for u- and v-components, as a function of time (number of 3-month period starting from January 2007) and their formal errors (bottom plot).*

Classification of open water returns in sea ice regions

During the last two decades the contribution of the mass loss from the Greenland ice sheet to the global sea level rise doubled. Additionally, the mass loss of Greenland's marine-based outlet glaciers might have an impact on the surface circulation and the coastal currents in the North Atlantic Ocean. In 2015, DGFI started to work on the DFG-funded project NEG-OCEAN dealing with 'Variations in ocean currents, sea ice concentration, and sea surface temperature along the north-east coast of Greenland'. The project aims at providing important information on the future development of ocean conditions and its interplay with atmosphere parameters and land ice melting.

In order to estimate ocean currents in the semi-enclosed Greenland Sea from satellite altimetry data, it is necessary to get proper range observations without a 'contamination' by sea ice. For this purpose, in a first step, we have to separate open water regions (i.e., open ocean as well as leads and polynyas) from ice returns. This is a challenging task within this region due to the fast changing conditions in a mostly ice-covered ocean. We aim to use the original altimetry measurements and perform a classification based on the shape of the returning altimeter pulse.

The shape of the returning pulse is strongly affected by the reflecting surface. Smooth surfaces like areas with very calm water (i.e., leads) produce specular reflections and the resulting waveforms show peaky shapes. In contrast, measurements over waves, ice or topography appear noisier and can have several peaks. Furthermore, different mission features, e.g., sensor and orbit characteristics, influence the size of the footprint and the repetition frequency of the measurements and, thus, the waveform shapes.

Concerning the classification of the pulse-limited altimetry waveforms we employ –as a first approach– a threshold-based method by using statistically derived waveform parameters describing, e.g., the kurtosis, skewness, and peakiness of a waveform. A similar approach can be applied for inland water applications (see Section 2.3). For the sea ice classification we use four different classes (3 surfaces and 1 undefined) and three waveform features. At first, all single-peak waveforms are selected by using the pulse peakiness criterion to identify leads and polynyas. In a second step, the waveforms are clustered in ocean-like and ice returns by analyzing the returned energy. In the last step, waveforms with a low backscatter coefficient (less than 10 dB) are assigned to the ice class. All remaining waveforms are classified as undefined. Figure 2.7 shows an example for one SARAL/Altika track with color-coded classification results based on empirically determined thresholds.

In order to validate the classification results, remote sensing data from optical (MODIS, Landsat 5–8) and imaging SAR missions with different wave bands and polarizations (ALOS and Sentinel-1) have been geolocated in areas where an altimeter pass close in time was available. This validation is a challenging task, especially in the Arctic Ocean, as only a few remote sensing missions provide georeferenced images with an appropriate spatial and temporal resolution. Moreover, as the high northern latitudes are often very cloudy and hazy, it is difficult to find cloudless optical images. Additionally, a close acquisition time interval between the satellite image and the altimeter crossing is required since the ice floes move rapidly due to wind and ocean currents.

Figure 2.7 shows the waveform classification results together with a MODIS image. The time lag between both measurement types is around 4 h. One can see a meaningful detection of unbroken ice surfaces and a reliable classification of major open water areas. However, uncertainties and wrong classifications especially in areas with floes and small open water areas can also be detected. One of the major difficulties and disadvantages of the threshold-based classification is the manual definition of the thresholds which have to be adapted regularly due to fast changing ice and scatter conditions and different satellite mission characteristics.

Recently, DGFI has started developing a classification approach that clusters and classifies the pulse-limited data in an unsupervised manner and without any training data. Besides the classical pulse-limited data, we use altimetry observations from Delay-Doppler altimeters, i.e. CryoSat-2 (see Section 2.1). This new measurement mode provides additional observation types and allows for an improved open water detection. A methodology is under study that fits a modeled waveform to the stack returns and classifies the returns to determine the kind of surface the satellite illuminates. In the sea ice domain, this could be highly beneficial in order to isolate water returns where the sea surface height can be estimated. By relating the values of width and amplitude of the fitted stack curve to the characteristics of the imaged area, it is possible to set thresholds and automate the surface type classification.

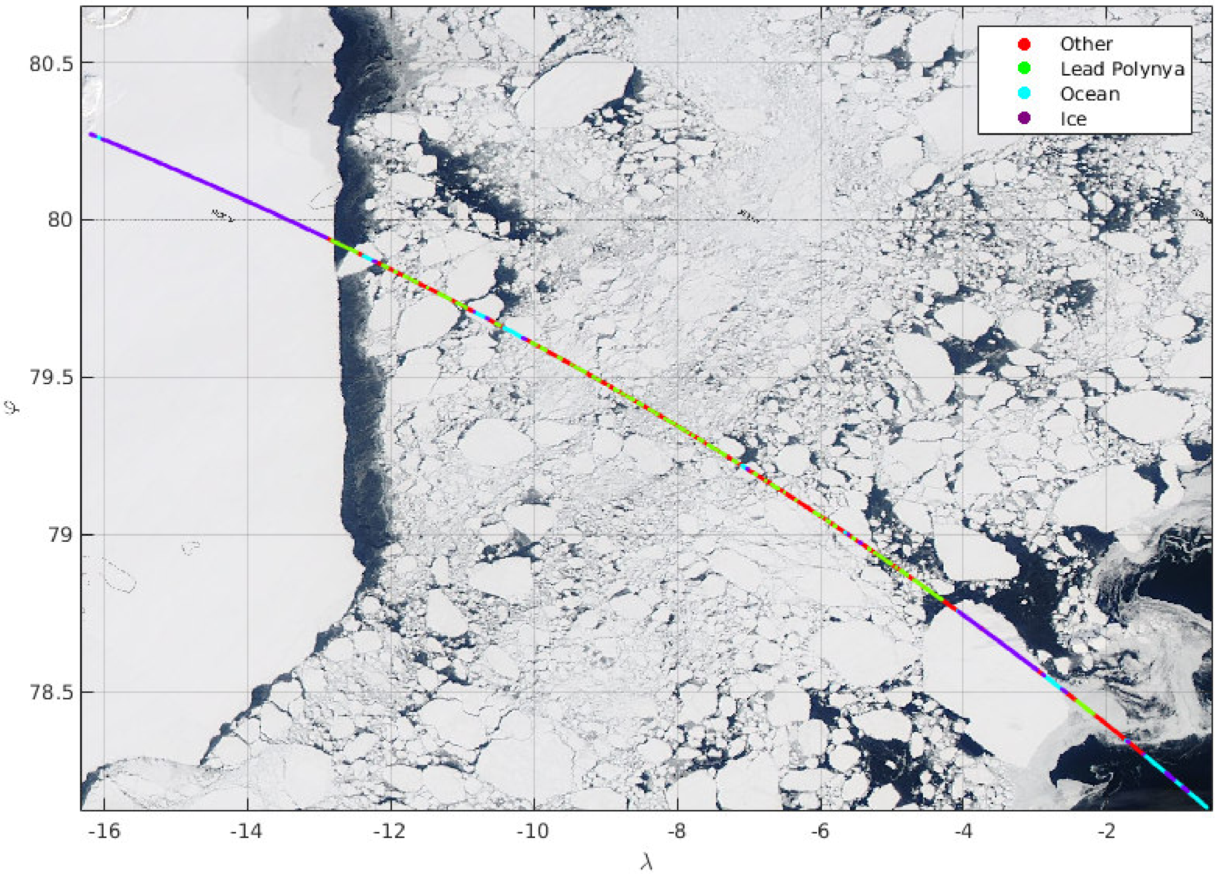

Fig. 2.7: *Corrected MODIS Aqua surface reflectance (true color) image recorded on May 8th, 2014 7:20 UTC overlaid with SARAL/Altika altimeter track (cycle 12, pass 999; May 8th, 2014 3:05 UTC) showing an example of open water classification based on empirically chosen thresholds (pulse peakiness, returning energy, and backscatter). In green, returns from calm water (leads, polynyas) are shown, open ocean returns are plotted in cyan and ice returns in purple. Undefined returns are given in red.*

2.3 Inland Altimetry

Database for Hydrological Time Series of Inland Waters (DAHITI)

In the last decade, satellite altimetry has become more and more important for continental hydrology. The fact that altimetry - originally designed for open ocean applications - can also provide reliable results over inland waters makes it a very useful tool for continental hydrology, as it helps to understand the water cycle of the Earth system.

The 'Database for Hydrological Time Series of Inland Waters' (DAHITI) has been developed by DGFI-TUM since 2013. Meanwhile, it provides about 350 water level time series of inland waters such as rivers, lakes, reservoirs, and wetlands. Compared to 2014, this is close to a duplication. All datasets are freely available, but provided without guarantee. In 2015, we updated the DAHITI web site with completely new design, improved features, and additional time series at dahiti.dgfi.tum.de.

The general processing strategy for the estimation of water level time series is based on a Kalman filter approach and an extended outlier detection. The methodology is described in detail by Schwatke et al. (2015). This paper also performs a comprehensive validation with in-situ data. Furthermore, DAHITI results are compared with external alimeter-based water level time series from Hydroweb (LEGOS), River & Lake (ESA), and GRLM (USDA). Table 2.1 shows the results of the validation for selected rivers and lakes. It demonstrates the performance of the DAHITI approach compared to other altimetric datasets.

In 2015, a classification approach for pulse-limited altimeter waveforms has been added to

Table 2.1: *Water level time series of selected lakes and rivers from DAHITI, Hydroweb, River & Lake and GRLM compared with in-situ data. For each comparison of water level time series from altimetry with in-situ data an RMS difference and squared correlation is computed. Minimum and maximum RMS values are highlighted (bold/italic).*

Target name – Station name (DAHITI ID)	DAHITI *RMS* [cm]	DAHITI R^2	Hydroweb *RMS* [cm]	Hydroweb R^2	River & Lake *RMS* [cm]	River & Lake R^2	GRLM *RMS* [cm]	GRLM R^2
Superior, Lake – Grand Marais[1] (3)	**4.4**	0.95	5.2	0.95	8.5	0.80	*11.8*	0.75
Huron, Lake – Harbor Beach[1] (33)	**5.2**	0.98	*7.7*	0.97	6.4	0.89	6.8	0.96
Michigan, Lake – Kewaunee[1] (11)	5.4	0.92	6.7	0.86	**5.0**	0.94	*8.7*	0.80
Erie, Lake – Fairport[1] (6)	**5.2**	0.95	8.6	0.93	12.6	0.74	*13.5*	0.79
Ontario, Lake – Olcott[1] (35)	**4.5**	0.97	6.1	0.96	4.9	0.96	*11.0*	0.85
Athabasca, Lake – Crackingstone Point[2] (100)	**15.1**	0.90	32.1	0.79	*80.5*	0.30	55.7	0.27
Great Slave, Lake – Hay River[2] (99)	**13.3**	0.68	*31.2*	0.37	–	–	–	–
Claire, Lake – Prairie Point[2] (578)	**19.6**	0.37	–	–	*37.9*	0.25	–	–
Winnipeg, Lake – George Island[2] (101)	**11.8**	0.87	28.6	0.66	*41.9*	0.49	33.0	0.59
Winnipegosis, Lake – Winnipegosis[2] (281)	**16.5**	0.91	*36.7*	0.63	34.2	0.61	36.2	0.53
Argentino, Lake – Calafate[3] (182)	**14.6**	0.97	*21.9*	0.93	–	–	–	–
Buenos Aires, Lake – Los Antiguos[3] (139)	**19.0**	0.73	*29.4*	0.70	–	–	–	–
Solimões, River – Tabatinga[4] (406)	**17.4**	1.00	–	–	*119.9*	0.88		
Solimões, River – Tefé[4] (389)	**12.3**	1.00	–	–	*14.8*	1.00		
Solimões, River – Itapéua[4] (384)	**33.9**	0.99	*110.9*	0.91	–	–	–	–
Purus, River – Aruma-Jusante[4] (583)	**20.0**	1.00	24.1	1.00	*318.9*	0.61	–	–
Japurá, River – Vila Bittencourt[4] (580)	**41.0**	0.98	61.3	0.93	*115.1*	0.80	–	–
Madeira, River – Humaitá[4] (371)	**19.4**	1.00	45.1	0.99	*53.2*	0.99	–	–
Negro, River – Porto de Manaus[4] (161)	**7.6**	1.00	25.2	1.00	*72.0*	0.96	–	–
Negro, River – Moura[4] (346)	**43.6**	0.98	*46.3*	0.97	44.1	0.98	–	–
Paraguay, River – Sao Francisco[4] (1095)	**22.5**	0.96	–	–	–	–	–	–

Source of in-situ data: [1]NOAA Tides and Currents, [2]Canada Wateroffice, [3]Ministerio de Planificación Federal, República Argentina, [4]Agência Nacional de Águas (ANA)

DAHITI. It enables an improved estimation of water level time series of inland waters. The waveform shapes vary between Brown-like shapes in the center of larger lakes and quasi-specular waveforms for rivers. There is a steady and uniform transition of the shape of the waveforms at the water edges. An identification of disturbed altimeter observations can be used to reject these measurements or to apply a class-dependent handling such as the usage of special retracking algorithms in order to achieve more realistic ranges and, finally, an improved water level time series of the investigated inland water body.

The methodology of classifying altimeter waveforms is based on the application of selected thresholds on waveform-related statistical parameters such as skewness, kurtosis, peakiness, maximum power of altimeter waveforms, and signal-to-noise ratio. The classification divides the altimeter returns into four major classes: ‘corrupted’, ‘single peak’, ‘ocean-like’, and ‘peaky + noisy’ (shown in Fig. 2.8 on the right). Each major class is subdivided in further sub-classes. The class ‘corrupted’ includes damaged waveforms that should not be used for further investigations. The class ‘single peak’ contains pure quasi-specular waveforms which become more degenerated (e.g., single peak with noise) with increasing class number. The class ‘ocean-like’ includes typical Brown-like waveforms which occur mostly over the ocean.

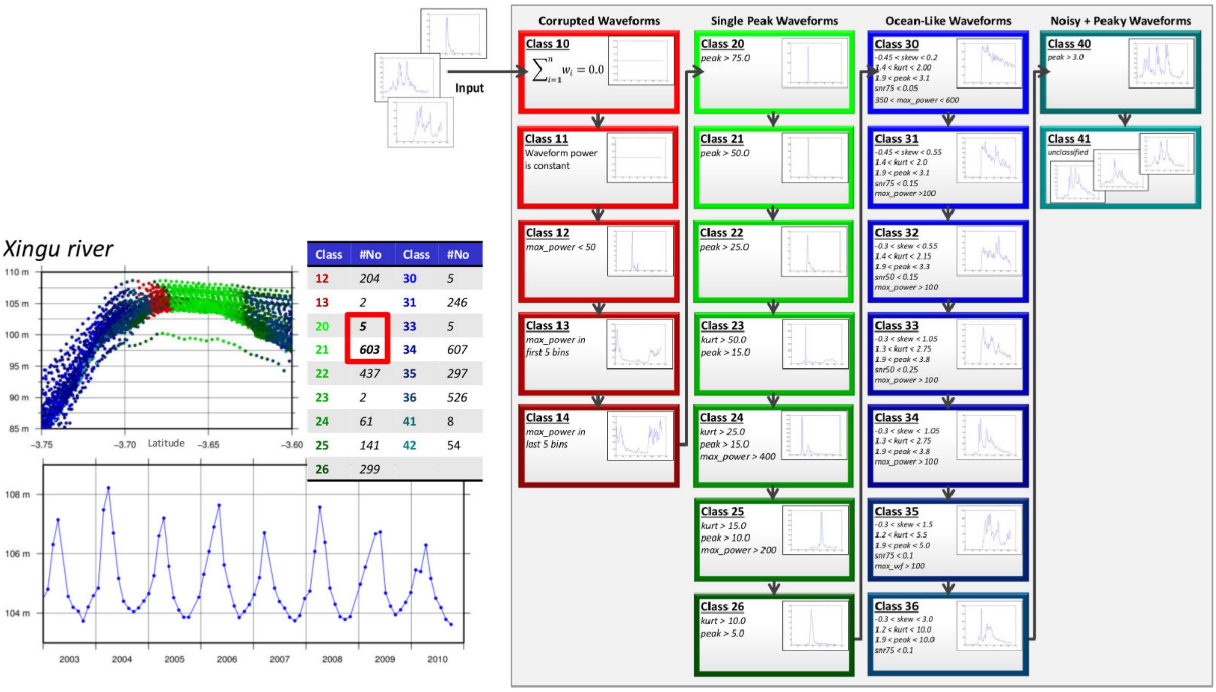

Class	#No	Class	#No
12	204	30	5
13	2	31	246
20	5	33	5
21	603	34	607
22	437	35	297
23	2	36	526
24	61	41	8
25	141	42	54
26	299		

Fig. 2.8: *Methodology of classifying altimeter waveforms based on different thresholds (right) and results of the classification over the Xingu river (left).*

Figure 2.8 (left) shows an example of the classification using an Envisat track that crosses the Xingu river (Brazil, South America). The table shows the distribution of the classified waveforms into the different groups. For each river crossing all available water levels of all cycles are plotted (top) and color-coded depending on the assigned class. The attached table shows the distribution of the measurements into the different classes. Additionally, a water level time series using water levels (based on the Ice-1 product of Envisat) of the classes 20 and 21 are computed and plotted (bottom) for the investigated river crossing. Thereby, a median was computed from the remaining water levels for each cycle to achieve a final water level time series. The resulting water level time series show clear seasonal variations and are hardly affected by outliers. This classification enables to estimate more reliable water level time series for small rivers with a width of about 100 to 200 m.

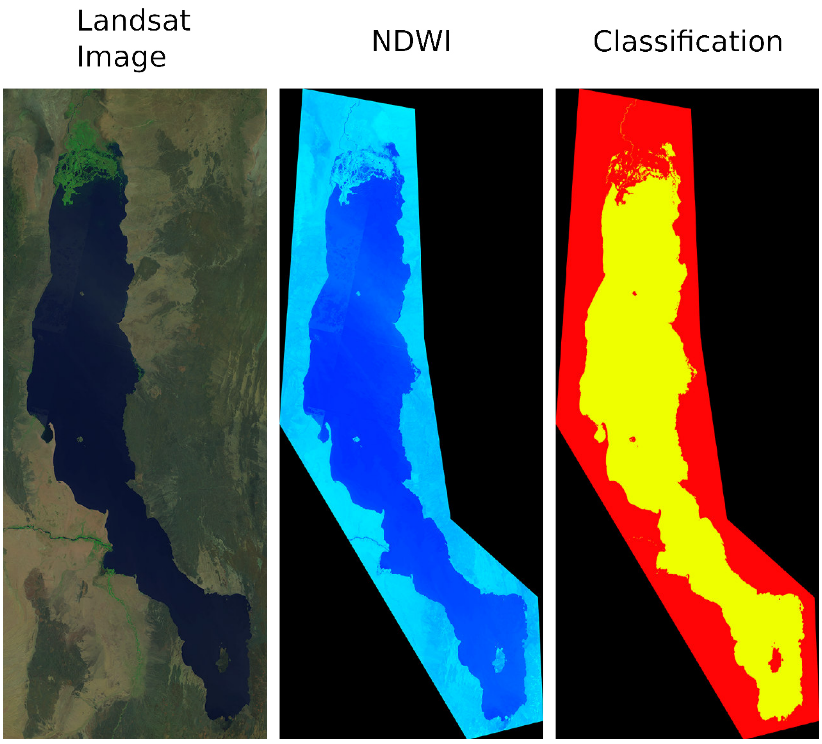

Fig. 2.9: *Visualization of steps to compute the surface extent of Lake Turkana.*

Estimation of lake volume changes

Satellite altimetry provides water levels and their temporal variations. The approach used in DAHITI (see above) is able to estimate highly accurate lake level variations based on multi-mission datasets. However, for hydrological purposes the change of water volume is more important than the water level. In the DFG project WLDYN ("Assessing the spatio-temporal dynamics of water volumes in large wetlands and lakes by combining remote sensing with macro-scale hydrological modeling") DGFI works together with hydrologists from the GFZ and the University of Frankfurt on the characterization and quantification of water storage dynamics of six large lakes and wetlands by combining altimetry and remote sensing information with global scale hydrological modeling. In order to derive volume changes from water level changes, it is necessary to know the temporal variation of the surface area of the water body.

One of the lakes under investigation is Lake Turkana located in the eastern part of central Africa (Kenya and Ethiopia). Due to its position in an arid surrounding the cloud cover over the lake is sparse and, therefore, optical satellite sensors can be used for water surface extraction (see Fig. 2.9 left). We derive Normalized Difference Water Index (NDWI) grids from monthly composites of Landsat satellite imagery (see Fig. 2.9 middle). The NDWI grids are filtered and split into land and water classes to compute the monthly surface extent (see Fig. 2.9 right). For lakes in humid areas with frequent cloud cover, three or six month composites must be used.

From the time series of surface extent and altimetric water levels, time series of water volume change can be retrieved. For Lake Turkana, a very high correlation between the water levels and the water surface area can be detected (see Fig. 2.10). Therefore, the water surface area change can be approximated by a linear relationship with the altimetry time series. For Lake Turkana, the time series of water volume change were calculated from both methods and compared. The differences are considerably smaller than the amplitude of volume change (differences are not visible in the bottom plot of Fig. 2.10).

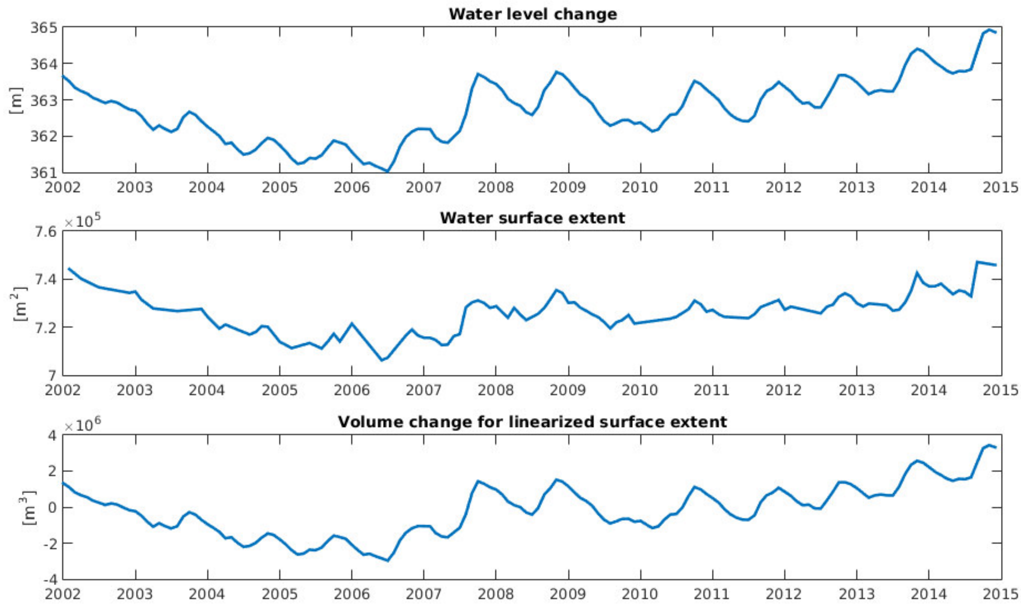

Fig. 2.10: *Water level change (top), surface extent (middle), and volume change (bottom) for Lake Turkana.*

CyroSat-2 SAR data over inland waters

The CryoSat-2 mission differs from the classical radar altimeter missions in two main points. First, it exhibits a long repeat orbit of more than one year and, thus, provides a good cross-track spatial resolution, but only a sparse temporal resolution. Secondly, the SAR Interferometer Radar Altimeter (SIRAL) onboard CryoSat-2 operates in three different measurement modes, one of them is the SAR or Delay-Doppler mode (see Section 2.1). This mode allows for an improved spatial along-track resolution and is very promising for inland water applications. DGFI-TUM investigates the potential of CryoSat-2 SAR data for monitoring water levels of small lakes and rivers.

The estimation of lake level variations from satellite altimetry data is a challenging task as the majority of altimeter waveforms of smaller lakes is contaminated by land. The smaller the surface footprint size of the altimeter, the smaller the corruption of the altimeter waveforms. For the SAR mode, the SIRAL onboard CryoSat-2 has a footprint size of about 0.3 km along-track and 1.7 km cross-track, remarkably smaller than the Envisat RA-2 or SARAL/AltiKa altimeter (up to 10 km or 8 km), respectively. We investigated the performance of the CryoSat-2 SAR mode altimetry over smaller lakes such as the Lake Okeechobee in Florida. This was done based on ESA Baseline B Level 1b datasets, i.e. classical multi-looked waveforms (c.f. Section 2.1). In a first step we classified the waveforms into three classes: land, lake margin and water by applying thresholds on waveform statistical parameters such as the maximum power of the waveform (Pmax), waveform center of gravity (COG) and width of the waveform (W). In Fig. 2.11 the results of the classification are shown together with the threshold levels and the typical waveform shapes for the three classes. The waveforms over land are characterized by a much higher power than the waveforms over lakes. Furthermore, the waveforms over land show a sharp peak whereas the waveforms over lake margins show two main peaks and the waveforms over water have the typical Brown-like shape. Therefore, different retracking methods are used for the waveform classes 'lake margins' and 'water'. The waveforms over the lake margins are retracked with the Narrow Primary Peak Threshold (NPPT) retracker (Jain et al., 2015[2]) with a threshold of 50% in order to identify the first peak that is supposed to

[2]Jain M., Andersen O.B., Dall J., Stenseng L.: Sea surface height determination in the Arctic using

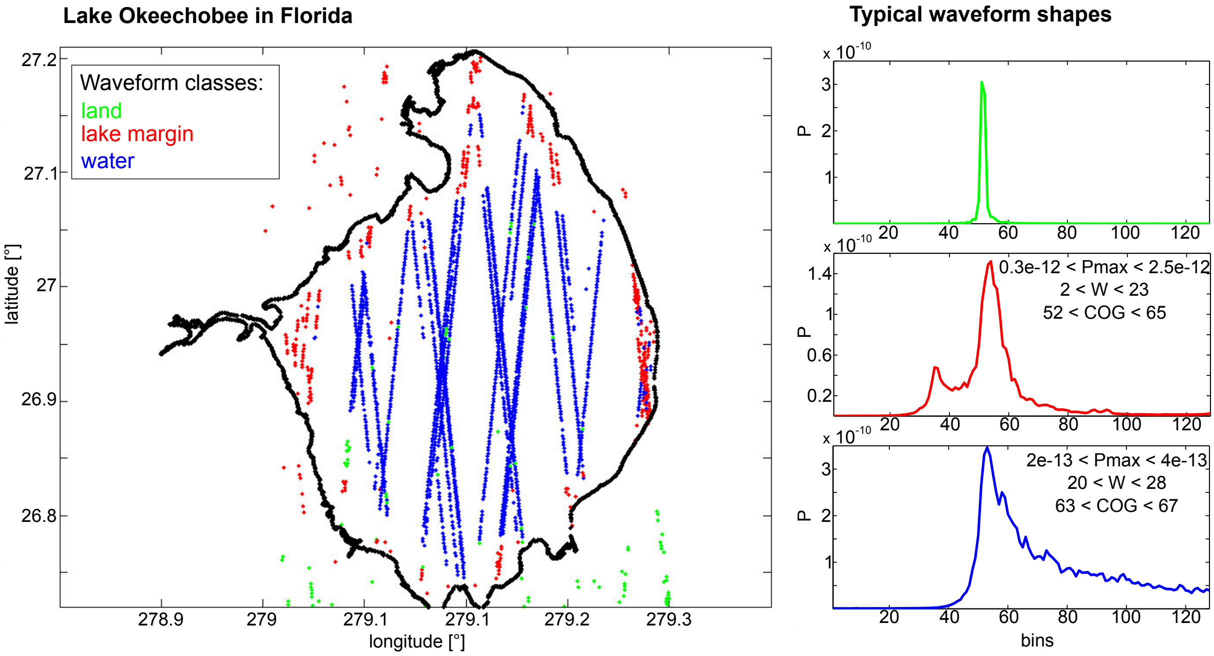

Fig. 2.11: *The map of the Lake Okeechobee shows the results of the waveform classification. In order to reduce the figure size, waveforms classified as land are mainly not displayed. On the right hand side the typical waveform shapes for the three classes are shown together with the threshold levels.*

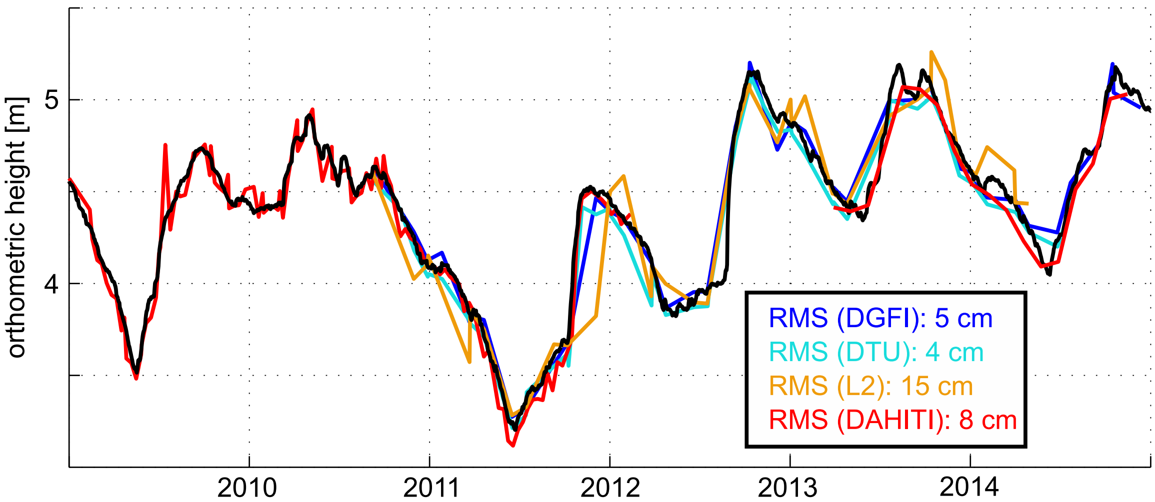

Fig. 2.12: *Five different solutions for the water level of the Lake Okeechobee: CryoSat-2 DGFI-TUM (blue), modeled CryoSat-2 DTU (cyan), ESA CryoSat-2 L2 (orange), Envisat and SARAL/AltiKa DAHITI solution (red), and gauge data (black). RMS values indicate the RMS differences with respect to the gauge data.*

come from the reflection of the inland water body. The waveforms over water are retracked with the Improved Threshold Retracker (ITR; Hwang et al., 2006[3]) with a threshold of 50%. In our implementation of the ITR the leading sub-waveform is located around the maximum peak. Afterwards, the median of the orthometric heights is determined and outliers are rejected before the determination of the water level. In Fig. 2.12, the CryoSat-2 DGFI-TUM water level time series for the Lake Okeechobee is compared with modeled water levels based on CryoSat-2

CryoSat-2 SAR data from primary peak empirical retrackers. Advances in Space Research 55(1), 40-50, doi:10.1016/j.asr.2014.09.006, 2015

[3]Hwang C., Guo J., Deng X., Hsu H.Y., Liu Y.: Coastal gravity anomalies from retracked Geosat/GM altimetry: improvement, limitation and the role of airborne gravity data. Journal of Geodesy 80(4), 204–216, doi:10.1007/s00190-006-0052-x, 2006

SAR data provided by the Technical University of Denmark (DTU; Nielsen et al., 2015[4]), ESA CryoSat-2 L2 products, water level time series from Envisat and SARAL provided by DAHITI (Schwatke et al., 2015), and gauge data from the National Water Information System (waterdata.usgs.gov/nwis). The accuracy of the Cryosat-2 solutions DGFI-TUM and DTU is about 5 and 4 cm, respectively, whereas the accuracy of the Envisat and SARAL/AltiKa solutions is only 8 cm. Thus, the new SAR measurements of CryoSat-2 (and Sentinel-3) improve the accuracy of water level time series of lakes. Furthermore, CryoSat-2 observations can be used to close the gap between the altimeter missions Envisat and SARAL in order to determine long-term water level time series of lakes.

CryoSat-2 SAR data has proven useful not only for lakes, but also for rivers. The smaller footprint size is even more important over rivers as the latter are usually much smaller than lakes. The stack data introduced in Section 2.1 can be used for river water detection. Radar returns collected over the river show up as a peak in the stack data and can be identified accordingly. The extraction of water returns was tested in the southern Mekong basin in South-East Asia. The river is well depicted in the data, but water bodies besides the river are also extracted. To separate returns from the river and other water bodies, probably external information about the river will be required.
The main disadvantage of using CryoSat-2 data over rivers is the orbit with its long repeat cycle of 369 days. Therefore, it is not possible to follow the standard virtual station approach, i.e. to merge the data into a time series at one location. This will be discussed in the following.

Modeling of river systems with multi-mission altimeter data

The combination of different altimetry missions to derive one common time series is well established for lakes and reservoirs in DGFI's inland altimetry database DAHITI (see above). The multi-mission approach leads to a higher temporal resolution of the time series. This is possible due to the homogeneous water level of the lake surface. However, combining measurements of different altimeter missions over rivers is more complicated since the water level changes rapidly with time and space. Detailed information on the river topography has to be known and considered, as well as changes in the seasonal behavior of the water level along the river.

The altimeter missions with short repeat cycles (e.g. Envisat, SARAL, and Jason-2) provide measurements along the river at well-defined locations (crossing points of the satellite's ground track with the river), so-called virtual stations. Especially the Envisat and SARAL missions proved to be useful as they have a denser spatial pattern than Jason-2. The temporal resolution of 35 days is appropriate to detect seasonal and monthly variations.

We developed a new methodology to combine different altimeter missions along a river based on spatio-temporal kriging. Kriging is a geostatistical method used for prediction. The technique is based on spatio-temporal covariances of the input data. The spatio-temporal covariances (illustrated by a so-called variogram) reflect how much influence a certain data point has on any other data point in space and time. With this method it is possible to connect the different measurements and to simulate the river flow.

However, this method cannot close the temporal data gap between Envisat and SARAL. Jason-2 provides data in 2011 and 2012 but only with sparse spatial resolution. Using solely data from classical repeat-cycle missions, only a strong annual signal can be extrapolated to the data gap. CryoSat-2 data (see above) can help to fill the data gap when incorporated into the time series with the kriging method. First tests have been made with simulated CryoSat data. We predicted data at the site of the gauge in Nakhom Phanom in the time frame between 2011–2013 once

[4]Nielsen K., Stenseng L., Andersen O.B., Villadsen H., Knudsen P.: Validation of CryoSat-2 SAR mode based lake levels, Remote Sensing of Environment, 171, 162–170, doi:10.1016/j.rse.2015.10.023, 2015

only with Envisat, SARAL, and Jason-2 data and once with additional simulated CryoSat data (see Fig. 2.13). The signal predicted without CryoSat data is mostly governed by the strong annual signal of the Mekong River. Considering the (simulated) CryoSat data we are able to improve the time series in this time period significantly. The improvement with CryoSat data might be even larger, but the two years considered were standard years without exceptional events. Therefore, the prediction based on data from previous and subsequent years is quite sufficient. The RMS drops from 1.13 m to 0.56 m.

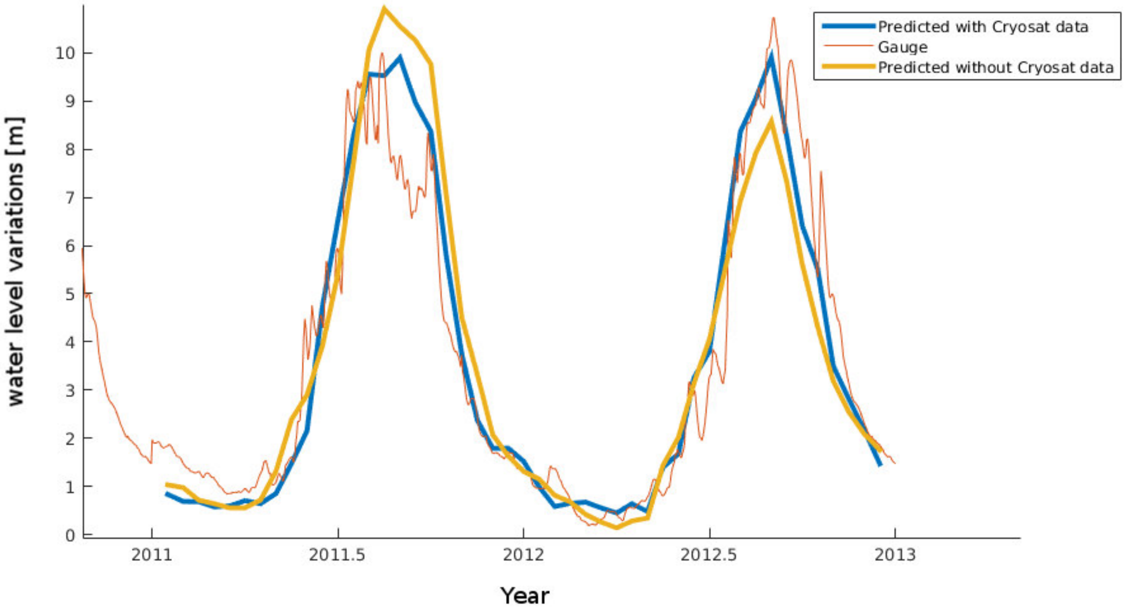

Fig. 2.13: *Predicted water level time series for a Mekong gauging station (no altimeter track crossing). Comparison between the gauge data and two signal predictions: with and without CryoSat data, respectively.*

Related publications

Dettmering D., Schwatke C., Bosch W.: Global calibration of SARAL/AltiKa using multi-mission sea surface height crossovers. Marine Geodesy 38 (supl 1): pp 206–218, doi:10.1080/01490419.2014.988832, 2015

Schwatke C., Dettmering D., Boergens E., Bosch W.: Potential of SARAL/AltiKa for inland water applications. Marine Geodesy 38 (supl 1): 626–643, doi:10.1080/01490419.2015.1008710, 2015

Schwatke C., Dettmering D., Bosch W., Seitz F.: DAHITI – an innovative approach for estimating water level time series over inland waters using multi-mission satellite altimetry. Hydrol. Earth Syst. Sci., 19, 4345–4364, doi:10.5194/hess-19-4345-2015, 2015

3 Cross-Cutting Research Topics

The three overarching research topics Atmosphere, Regional Gravity Field, and Standards and Conventions are highly cross-related to the research areas Reference Systems and Satellite Altimetry for which they provide important foundations.

The atmosphere (Section 3.1) affects all space geodetic measurement techniques. On the one hand, atmospheric effects such as refraction or signal delay are a major error source that needs to be considered. Thus the optimization of respective corrections and models means an important research challenge. On the other hand, the observation data of various geodetic measurement techniques that are influenced by the atmosphere in different ways provide valuable information on state and dynamics of the atmosphere. These are of great interest for other disciplines such as meteorology or navigation. In particular the DGFI-TUM has built up strong experience in the modelling and prediction of global and regional physical structures of the Earth's ionosphere (4D electron content, space weather) from the joint analysis of space geodetic observations.

The precise knowledge of the Earth's gravity field (Section 3.2) is vital for various applications in geodesy, such as the realization and unification of height systems and the determination of highly precise satellite orbits. The latter are a prerequisite for the computation of accurate reference frames or for reliable estimates of water heights from satellite altimetry. Furthermore the geoid provides the reference surface for ocean circulation. Temporal changes of the gravity field contain information about mass transports in the Earth system and are of great interest, for example, for the investigation of dynamic processes in the Earth's interior or within the hydrosphere. The DGFI-TUM primarily focuses on theoretical and practical aspects of regional gravity field determination. The goal is the creation of highly resolved and accurate potential fields for delimited areas through combination of various available data sets, e.g. satellite gravity field information, satellite altimetry, or terrestrial and airborne gravity data.

A fundamental prerequisite for any meaningful combination of different data sets is the definition and application of common standards and conventions (Section 3.3) in order to assure highest consistency of parameters and products. In the frame of the Global Geodetic Observing System (GGOS) the DGFI-TUM manages the GGOS Bureau of Products and Standards (BPS) that is jointly operated with partners of the FGS.

3.1 Atmosphere

As shown in Fig. 3.1, the Earth's atmosphere can be structured into various layers depending on different physical parameters. Following the temperature profile, for instance, the atmosphere can be split into troposphere, stratosphere, mesosphere, thermosphere, and exosphere. Following the degree of ionization, the atmosphere is composed of the neutral atmosphere up to around 50 km altitude, the ionosphere from around 50 km up to 1000 km, and the plasmasphere and magnetosphere.

In modern geodesy, the atmosphere is not only seen as a disturbing quantity but increasingly also as a target quantity since almost all geodetic measurement techniques provide valuable information about the current state of the atmosphere. Thus, atmosphere modeling meets the GGOS goal of providing highly precise and consistent products from the joint evaluation of measurements from heterogeneous space geodetic observation techniques such as terrestrial

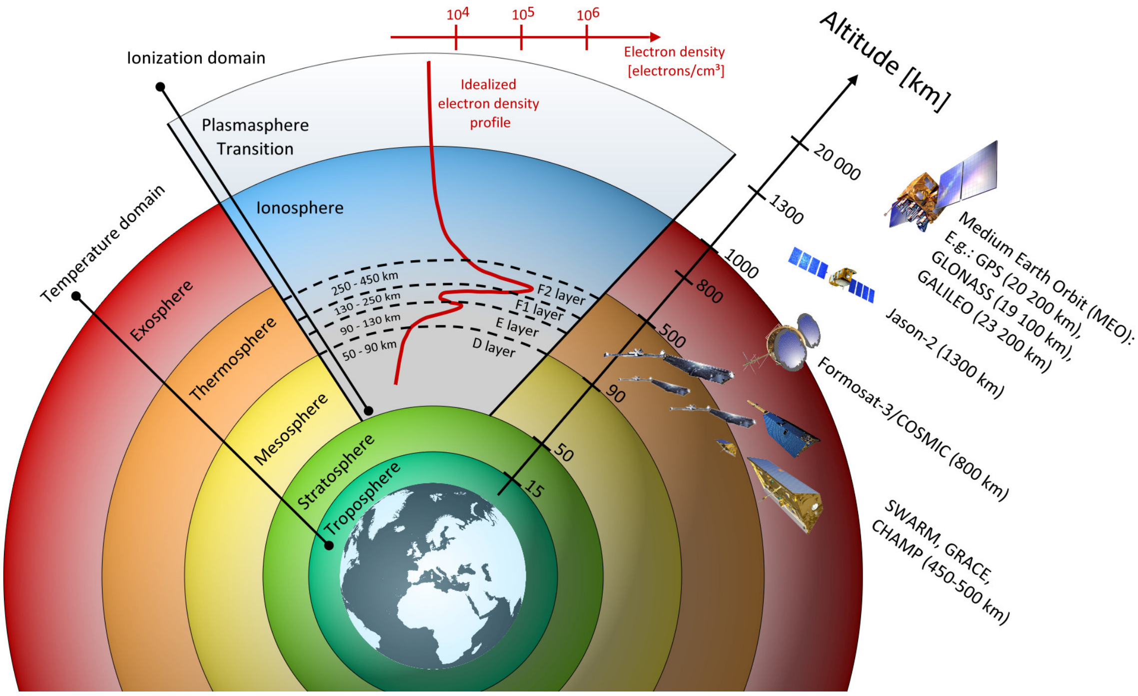

Fig. 3.1: *Layers of the atmosphere depending on the temperature (left) and on the degree of ionization (mid); vertical variation of the electron density within the ionosphere and the plasmasphere; orbit heights of selected satellites and satellite missions (right) (Limberger, 2015).*

GNSS, satellite altimetry, DORIS, and radio occultations with LEO satellites. GGOS also addresses issues relevant to the society such as global change or space weather. Since our modern society is highly dependent on space-borne techniques for, e.g., communication and navigation, space weather and its risks are gaining more and more importance in politics and science. Near real-time or even real-time procedures are currently under development to monitor and analyze the ionosphere state and to predict ionosphere target parameters such as the electron density (ED) or the vertical total electron content (VTEC) for hours or even days under the consideration of space weather events. From the ionosphere-thermosphere coupling, the influence of thermosphere winds on satellites like LEOs and their instrumentation as well as the interrelation of the thermosphere density with climate change can be studied.

In the reporting period, DGFI-TUM was working on three atmosphere projects. The projects OPTIMAP and ADAPIO mainly deal with the ionosphere, the project INSIGHT focusses on the ionosphere-thermosphere coupling.

Operational Tool for Ionospheric Mapping And Prediction - Project OPTIMAP

The project OPTIMAP aims at the computation and prediction of VTEC from various space geodetic observation techniques and is funded by the Bundeswehr Geoinformation Centre (BGIC) located in Euskirchen. Project partners are the German Space Situational Awareness Centre (GSSAC) in Uedem and the Institute of Astrophysics of the University of Göttingen (IAG). Key part of OPTIMAP is the deployment of an operational service for the provision of ionosphere information. Therefore, a software application has to be developed that allows to model VTEC as well as the ED distribution on a global scale with regional densifications.

Satellite observation techniques

In 2015, the OPTIMAP software has been extended for the processing of satellite altimetry, DORIS and radio occultation data. Observation-driven ionosphere models significantly benefit from the large amount of measurements that become available through the increasing number of space missions improving the spatial and temporal data distribution. The temporal distribution refers to the sampling of measurements but also to the latency, i.e. the time gap between the measurement and the provision of the data through online data servers. The latter aspect plays a key role for the challenge of running operational monitoring services to model ionospheric key quantities such as VTEC or ED in space and time as a sequential process. Therefore, the combination of different satellite observation techniques is considered for sounding the ionosphere with different geometries and sensitivities. At DGFI-TUM, the combination of GNSS (GPS and GLONASS), satellite altimetry, DORIS and occultation measurements is performed. In addition, IAG provides Sun observations that will later be incorporated as an additional information about upcoming solar storms that may trigger ionospheric disturbances. The satellite missions basically provide three observation types that are considered for OPTIMAP:

1. slant total electron content (STEC) from GPS, GLONASS and DORIS
2. vertical total electron content (VTEC) from satellite altimetry
3. electron density (ED) derived from radio occultation measurements

The observation techniques together with their observables are depicted in Fig. 3.2. It shall be noted that the ED is retrieved from STEC measurements between GPS and LEOs such as the six satellites of the Formosat-3/COSMIC (F-3/C) mission, i.e., they can be denoted as a second order quantity or Level-2 (L2) product.

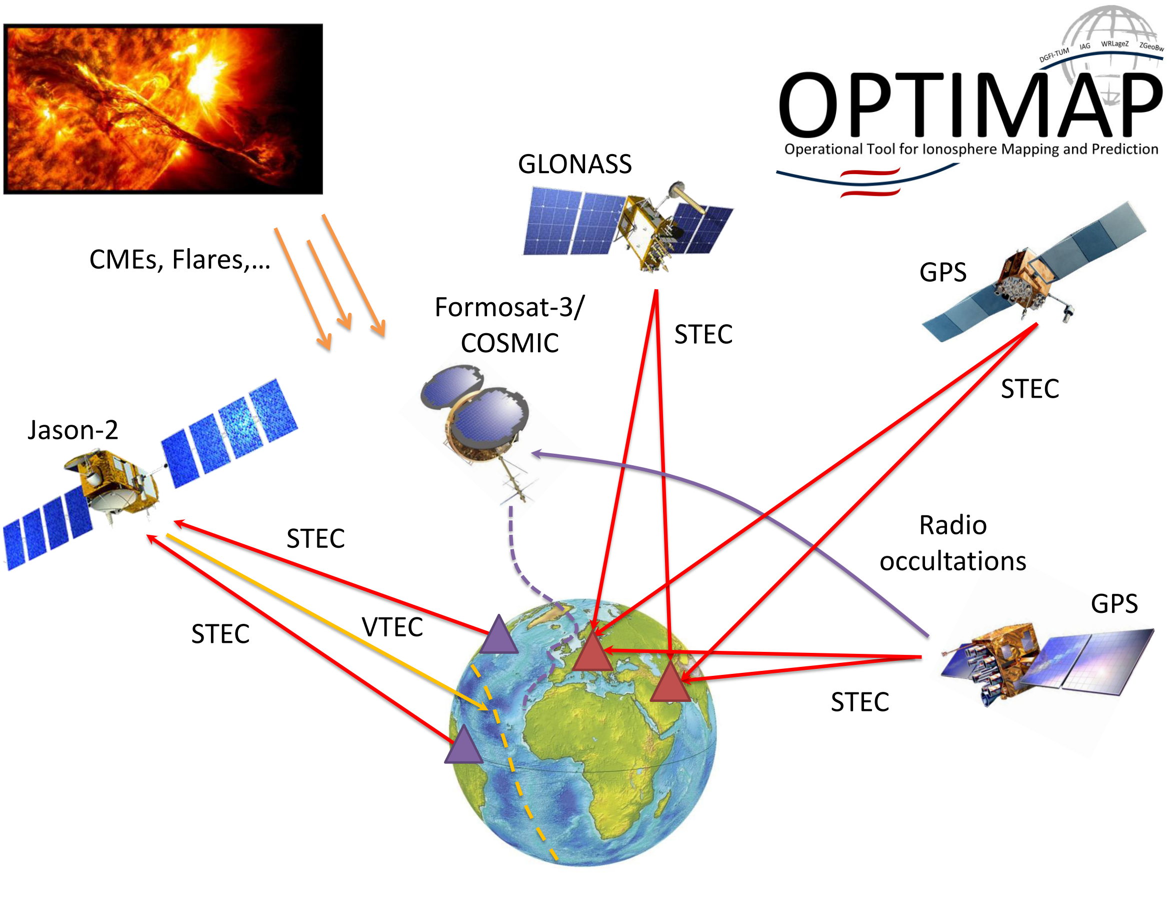

Fig. 3.2: *Overview of the satellite observation techniques implemented in the OPTIMAP processing part.*

The OPTIMAP pre-processor performs a batch processing of raw observations to extract ionospheric information to be saved in a local database. For GNSS and DORIS, the steps include amongst others the calculation of the geometry-free linear combination, the phase leveling and the mapping of STEC into VTEC under the consideration of a single-layer mapping function. From altimetry, e.g., the Jason-2 mission, the VTEC observation is derived from the range measurement in nadir direction. Furthermore, occultation data of the F-3/C mission are taken into account for the retrieval of ED profiles below the LEO orbit based on the Abel inversion (Limberger, 2015; Limberger et al., 2015). The computed ED profile can then be approximated, e.g., by a set of Chapman layer functions accounting for the different layers of the ionosphere. To be more specific, the multi-layer approach

$$N_e(h) = N_e^D(h) + N_e^E(h) + N_e^{F_1}(h) + N_e^{F_2}(h) + N_e^P(h) = \sum_{Q=1}^{4} N_m^Q\, p^Q(h) + N_0^P\, p^P(h) \tag{3.1}$$

was set up where the notations D, E, F_1, F_2 and P refer to the $D-, E-, F_1-$ and F_2-layer of the ionosphere as well as to the plasmasphere (see Fig. 3.4, bottom left). The profile functions $p^Q(h)$ with $Q \in \{D, E, F_1, F_2\}$ represent the electron density distribution related to the layer Q and are, in case of Chapman functions, characterized by the (peak) height h_m^Q of the corresponding maximum density value N_m^Q and the scale height H^Q. The plasmasphere profile function $p^P(h)$ usually is only described by the scale height H^P. From the total number of unknown key parameters various subsets of unknowns have been selected and estimated from F-3/C data. Figure 3.3 shows, as an example, the electron density profile based on five estimated key parameters, namely $N_m^E, N_m^{F_1}, N_m^{F_2}$, $h_m^{F_2}$ and H^{F_2}, derived from F-3/C profile data. The estimated multi-layer profile function (3.1) is finally integrated along the vertical between 100 km

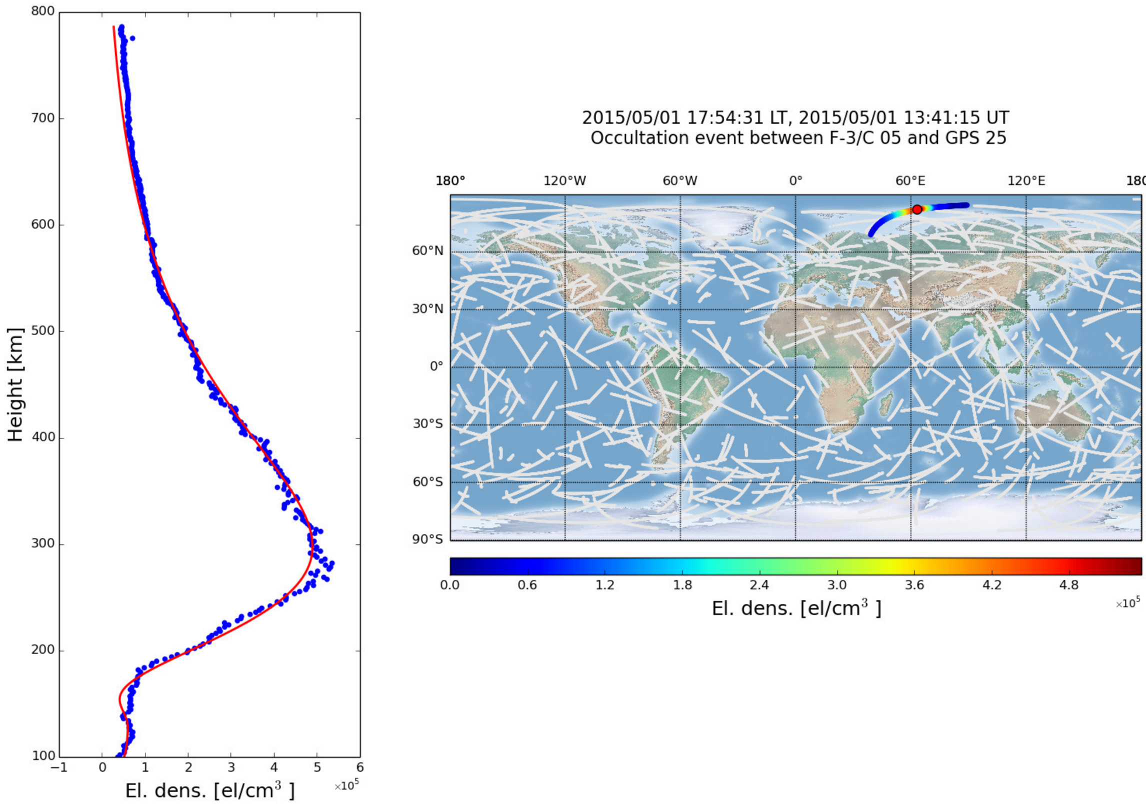

Fig. 3.3: *Left panel: estimated electron density profile (red line) from F-3/C profile data (blue dots). The parameters $N_m^E, N_m^{F_1}, N_m^{F_2}$, $h_m^{F_2}$ and H^{F_2} were estimated by least squares adjustment, the remaining key parameters were fixed (e.g., $h_m^{F_1} = 170$ km). Right panel: global distribution of electron density profiles from the F-3/C satellites on May 1, 2015. The colored arc measured at 13:41 UT provides the electron density values (blue dots) for the left panel.*

and 3000 km to derive VTEC by means of a Gauss-Legendre quadrature. It follows that the current status of OPTIMAP allows for the derivation of VTEC from all four techniques.

The VTEC observables together with relevant meta information are stored in a database based on the Hierarchical Data Format (HDF) that is used as an input data pool for the sequential processing of the measurements. Currently, the model aims at the global monitoring of VTEC, i.e., a 3-D model has been developed. An overview of the main processing steps is shown in Fig. 3.4. Exemplarily, a global VTEC map generated with OPTIMAP is shown on the right. In a later stage of the project, OPTIMAP shall be extended for modeling the 4-D ED distribution.

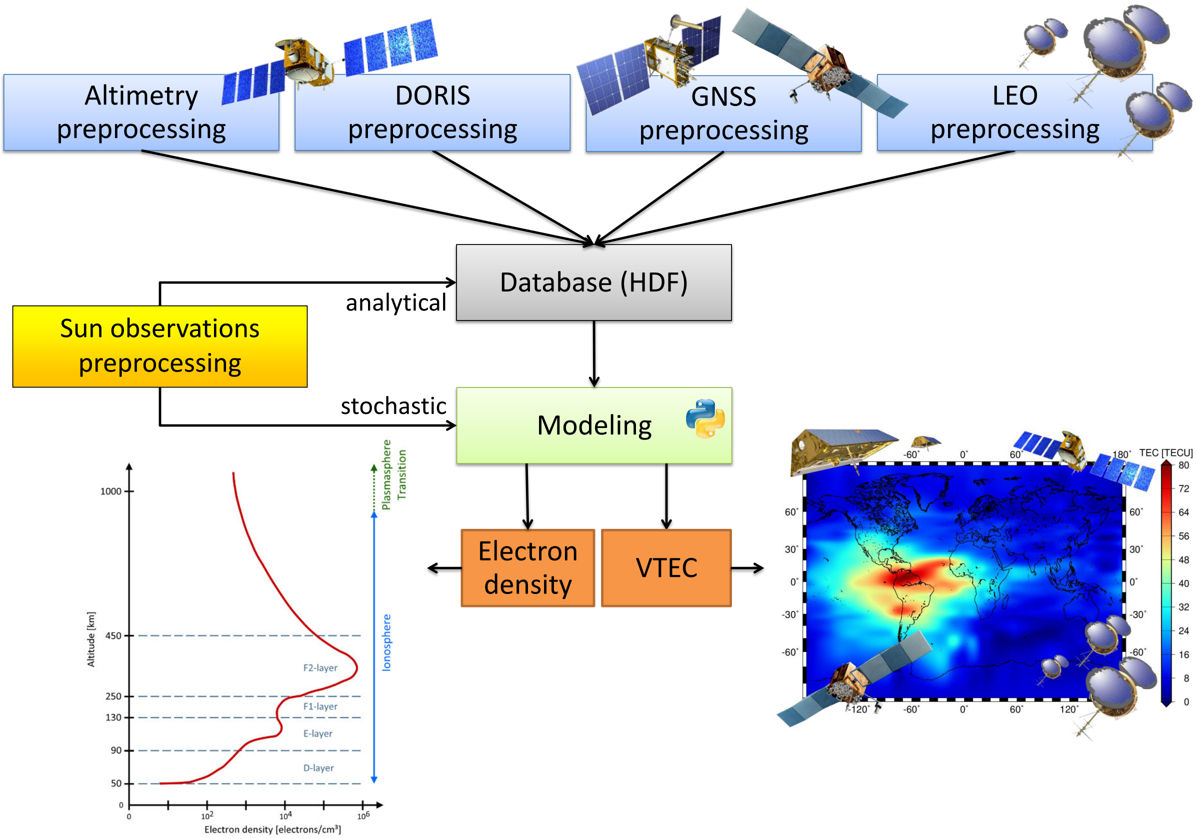

Fig. 3.4: *From observation preprocessing toward ionosphere products – a flowchart of the main OPTIMAP processing steps.*

Recursive filtering

After preprocessing the observations of all four techniques, the observations are forwarded to a Kalman filter (KF) that sequentially processes the data according to the sampling of the observation epochs, e.g., 30 s in case of GNSS. The global representation of the data is realized by localizing B-splines where polynomial B-splines (PBS) and trigonometric B-splines (TBS) are considered for the parameterization w.r.t. latitude and longitude, respectively (see, e.g., Schmidt et al., 2015). VTEC parameters as well as DCBs for satellites and receivers are estimated by the KF approach.

Adaptive global model of the VTEC - Project ADAPIO

The ADAPIO project, funded by the German Aerospace Center (DLR) and finalized at the end of 2015, focused on the development of an adaptive global model of the VTEC in terms of B-spline functions as well as on the realization of a data assimilation framework for the estimation of unknown model parameters in near real-time. As already mentioned above, GNSS data, in particular GPS and GLONASS, provide the fundamental ionosphere information for VTEC estimation procedures. GPS data can be obtained from IGS online servers, with different latencies, e.g., as daily, hourly or real-time products. Since the project aimed at near real-time processing, hourly GPS products were selected and processed automatically. GLONASS data can be acquired with one hour latency, too. Furthermore, satellite altimetry data from the Jason-2 mission have a latency of about 3 hours. Other techniques with a higher latency, such as DORIS with a latency of about 3 to 4 days, have not been used in this project.

Adaptive modeling approach

The primary goal of the project was the development of a model for global VTEC representation taking the inhomogeneous distribution of observation sites into account (Fig. 3.6). The BMARS ('multivariate adaptive regression B-splines') algorithm which utilizes data adaptive basis functions was studied and extended for global VTEC modeling. An example for a uniform and a non-uniform polynomial basis formation of B-spline basis functions is depicted in Fig. 3.5. The BMARS algorithm was applied to hourly GPS data. Although the results show an overall agreement with the corresponding IGS products, artefacts appear in the maps (not presented here), probably due to the lack of the application of necessary constraints to preserve a spherical geometry for global modeling. The classical BMARS algorithm does not allow to take such constraints into account. Besides, the very high workload and processing time of the BMARS approach avoids an efficient and suitable implementation of the algorithm for near real-time applications.

However, a data adaptive basis definition of the BMARS algorithm that leads to a non-uniform adaptive B-spline (NABS) model can be used instead to consider the necessary constraints and

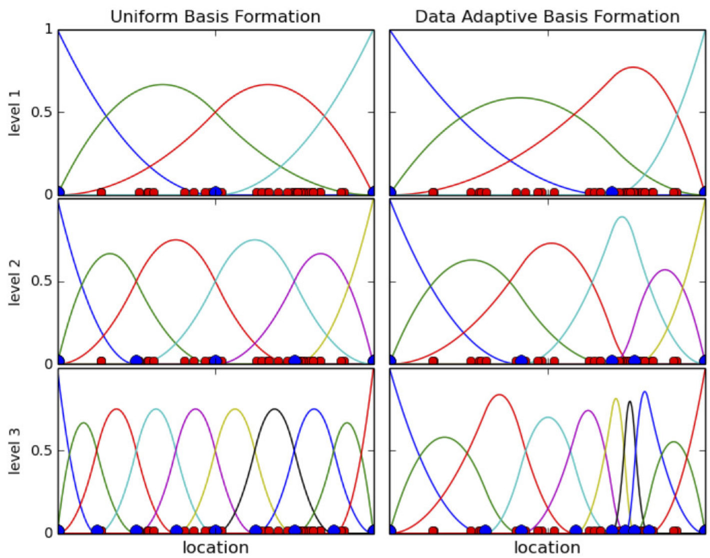

Fig. 3.5: *The data adaptive basis formation of different B-spline levels using NABS (right panels) compared to uniform B-splines (left panels). The red dots indicate the observation locations whereas the blue dots are the knot points used to define the B-spline functions.*

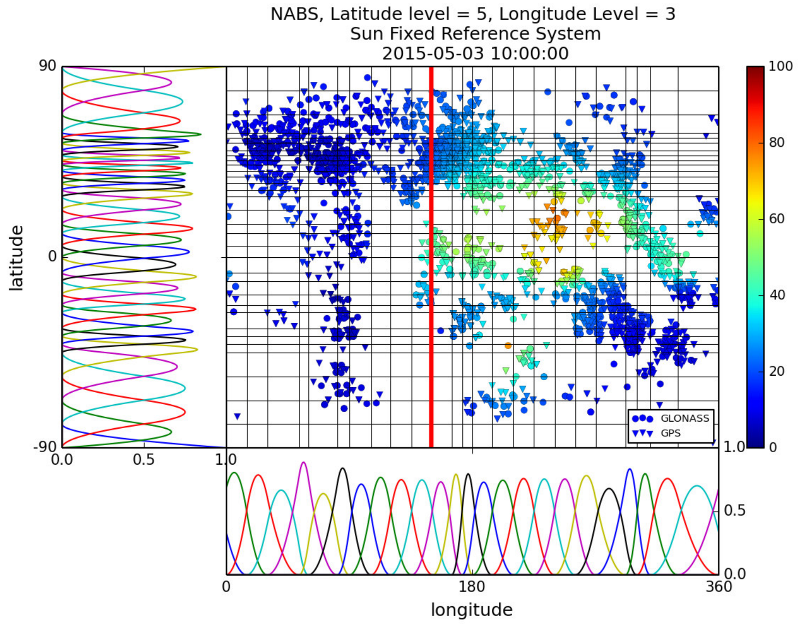

Fig. 3.6: *Global VTEC representation at 10:00 am with NABS using level 5 for polynomial B-splines in latitude direction and level 3 for trigonometric B-splines in longitude direction. The red line shows the prime meridian at Greenwich.*

to decrease the computational load. Therefore, the focus was directed to the use of NABS for global VTEC representation. Figure 3.6 shows an example for the use of non-uniform adaptive B-spline basis functions (level 5 for polynomial B-splines in latitude and level 3 for trigonometric B-splines in longitude) generated from GPS and GLONASS data acquired within a 1 min time span.

The initial ADAPIO framework for global VTEC modeling was based on the BMARS algorithm performed sequentially with hourly time intervals using a background VTEC model provided by a KF. Since the BMARS algorithm can remove or add new basis functions resulting in a changing number of unknown coefficients, it is not an easy task to track the BMARS coefficients from one measurement epoch to the next. In case of the NABS based design, however, the ionosphere data are directly assimilated by a KF in a sequential manner with a temporal sampling of 1 min. As the number of NABS is constant, the coefficients can be easily tracked. Consequently, the NABS framework allows – at least approximately – that the state vector of the KF is composed of the unknown B-spline coefficients.

Recursive filtering methods are considered to achieve a near real-time assimilation of the ionosphere observations. A classical KF which is the most popular method for (near) real-time applications was implemented for global VTEC estimation. In addition, the unscented Kalman filter (UKF) and the ensemble Kalman filter (EnKF) were analyzed. These filters generally provide better results, especially in case of severe non-linearities in the models and errors due to unknown effects or model simplifications. The EnKF was selected and implemented as an additional approach to investigate the potential improvement of global VTEC estimates. The implemented recursive filters require the definition of a measurement model to assimilate the observations and a dynamical model to represent the time variation of the unknown parameters. To model the measurements, the system of equations for both the combination of the observations from GNSS and altimetry and for the necessary constraints were established (see, e.g., Schmidt et al., 2015).

Regularization techniques were studied to obtain a further stabilization of the estimation algorithms. Methods based on L-curve, generalized cross validation (GCV) and variance component estimation (VCE) were implemented and tested separately for performance evaluation. The VCE represents an efficient algorithm for near real-time processing due to its lower computational burden and a similar accuracy compared to other methods. Therefore, the VCE was incorporated into the KF. The incorporation of variance components leads to an adaptive Kalman filtering approach that allows the computation of statistical parameters (standard deviations of the measurement noise and process noise) automatically during run time. In classical KF, these statistical parameters have to be defined manually by the user before running the filter.

All implemented filters are capable of running both in off-line mode (non-operational) to analyze historical data and in on-line mode (operational) for near real-time processing. In both modes, the unknown parameters are estimated sequentially with a resolution of 1 min and the output is stored in a file every 15 min. VTEC maps are generated with a resolution of 15 min using the estimated parameters contained in the output files. At the end of a day, a VTEC product with 1 h sampling is generated. Although the implemented filters are capable of running in (near) real-time, the observations can only be assimilated with a time delay due to their latency. Figure 3.7 shows the time schedule for the filtering process if only hourly GNSS data are used. The data are downloaded and pre-processed at the beginning of every hour. Due to the latency of the data, the filter processes the observations with a 2 h latency.

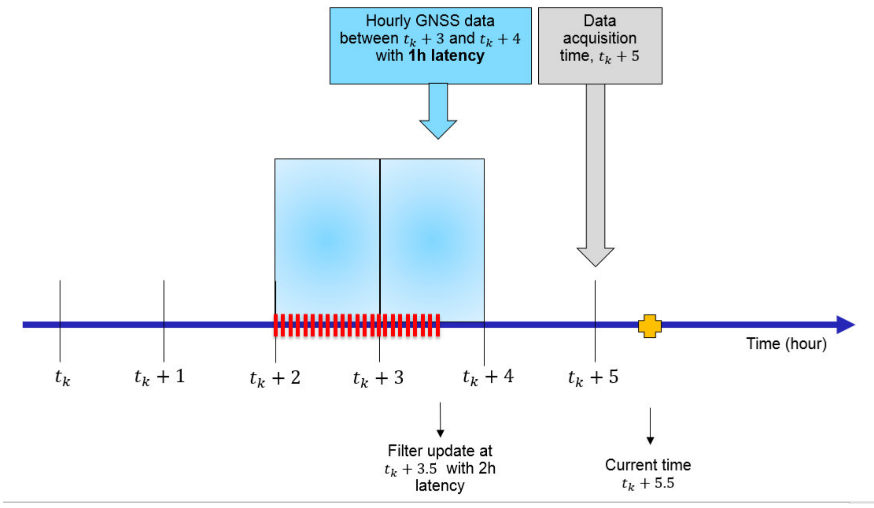

Fig. 3.7: *Flowchart for near real-time recursive filtering with a latency of 2 h using only GNSS data. The yellow mark shows the current moment; the red lines represent the 1 min steps of the recursive filter.*

VTEC forecasts

For VTEC predictions of several days, i.e. forecasts, an algorithm based on a harmonic analysis was developed. The algorithm uses historical VTEC maps to compute the harmonic coefficients representing the main trend. Then, these coefficients are used for the forecast. Figure 3.8 shows the time schedule to generate estimated and forecasted VTEC products.

Validation

To assess the quality of the products, two validation approaches were implemented. One approach checks the general consistency of the computed VTEC products with the solutions of the four IGS analysis centers (JPL, CODE, ESA and UPC) and with the official IGS combined solution. The second approach called the self-consistency check allows to compare the temporal and spatial variation of the product with respect to the highly precise observations generated by differencing slant total electron content (STEC) observations.

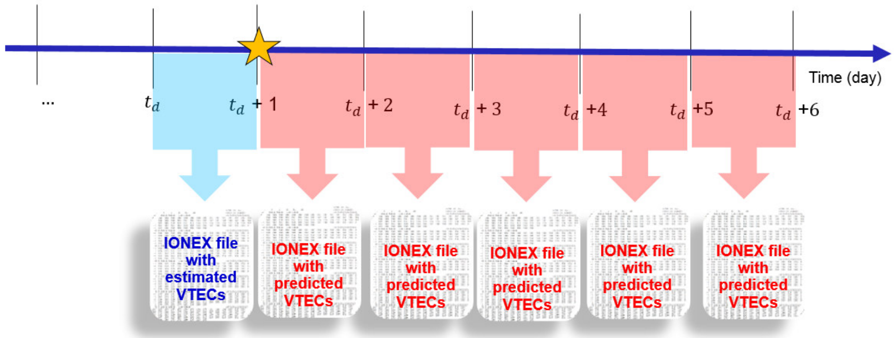

Fig. 3.8: *Flowchart for the IONEX generation process. At the end of each day, a VTEC file in the IONEX format for the current day using the estimated coefficients of the filter and the forecasted maps for the subsequent 5 days are generated.*

Dynamics of thermosphere and ionosphere – Project INSIGHT

This project aims at the investigation of thermospheric and ionospheric dynamics for the purpose of studying the interactions of these layers with geodetic sensors employed by various space missions (Fig. 3.1). It is funded within the special priority programme "Dynamic Earth" of the German Research Foundation (DFG); project partners are the Chair of Astronomical and Physical Geodesy of the TUM (APG), the GFZ German Research Centre for Geosciences Potsdam and the Institute of Geodesy (IfE) of the Leibniz University Hannover.

Estimation of thermospheric neutral densities

The observation equation for SLR measurements contains, besides a large number of correction terms, the distance between the 3-D position vector $\mathbf{r}_{\text{sat}}$ of the satellite and the 3-D position vector $\mathbf{r}_{\text{sta}}$ of the station. The equation of motion of the satellite, i.e. its overall acceleration $\ddot{\mathbf{r}}_{\text{sat}} = \mathbf{a}$ can be expressed as the sum of a direct and an indirect gravitational acceleration as well as non-gravitational accelerations. The latter comprise radiation forces such as direct solar radiation pressure and Earth albedo, drag-like forces and other forces such as relativistic effects. The drag-like forces can be split into atmospheric drag, solar wind and interplanetary dust (for a detailed description of all these relations see Bloßfeld, 2015).

In order to model the thermospheric neutral density distribution at various altitudes from SLR observations to LEO satellites, a careful analysis of the atmospheric drag acting on the satellites must be performed. To be more specific, for LEO satellites the atmospheric drag represents the largest non-gravitational perturbation, always pointing opposite to the velocity vector of the satellite relative to the atmosphere and causing a deceleration of the satellite. Therefore, the atmospheric drag $\mathbf{a}_D$ is a velocity-dependent (non-conservative) perturbation:

$$\mathbf{a}_D = -\frac{1}{2}\frac{A_{\text{ref}}}{m} C_D \rho\, v_{\text{rel}}^2\, \hat{\mathbf{u}}_D \tag{3.2}$$

where C_D is the dimensionless aerodynamic drag coefficient describing the interaction of the atmosphere with the satellite surface, $\hat{\mathbf{u}}_D$ the corresponding drag unit vector, A_{ref} the effective cross-section of the satellite interacting with the atmosphere, m the satellite mass, ρ the atmospheric neutral density and v_{rel} the velocity of the satellite relative to the atmosphere.

As a first approximation, the velocity of the atmosphere can be identified with the Earth's co-rotation velocity. However, in order to obtain a more realistic velocity of the atmosphere, it is important to consider also the wind velocity with respect to a co-rotating atmosphere. The wind velocity is usually specified in local coordinates (East, North, Up), defining the zonal, meridional and vertical winds, respectively. Therefore, the relative velocity of the satellite with respect to the atmosphere is computed as the difference between the orbital satellite velocity and the sum of the co-rotation and the wind velocity.

For satellites with accurately known shape and attitude, the largest error sources in the drag computation are the atmospheric neutral density ρ and the aerodynamic drag coefficient C_D. Since both quantities are multiplied in Eq. (3.2), it is impossible to separate these two components. In order to obtain density measurements, which is our purpose, the aerodynamic drag coefficient has to be computed analytically. Its numerical value is highly sensitive to the chosen gas-surface interaction model which describes how gas particles exchange energy and momentum with the surface of an object. The fundamental parameter of this model is the accommodation coefficient, the average fraction of energy lost by molecules impinging on the satellite surface. In particular, a gas particle colliding with a spacecraft surface can be either adsorbed and re-emitted later on or directly reflected (specularly or diffusely). The fundamental assumption, common to all gas-surface interaction models, is the condition of "free molecular flow" of the atmosphere, stating that at satellite altitude (above about 140 km) the mean free path of the molecules is much greater than the characteristic satellite dimension.

The two most popular gas-surface interaction models are Schamberg's and Sentman's model. Both models provide analytical solutions of the aerodynamic coefficients but cover different orbital regimes.

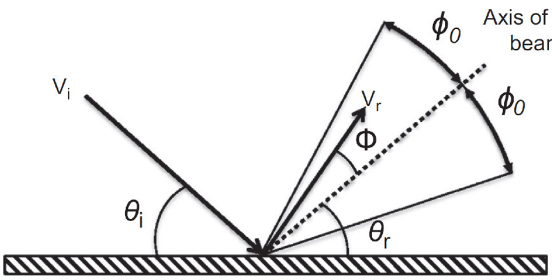

Fig. 3.9: *Quasi-specular reflection (Schamberg's model; Prieto et al., 2014).*

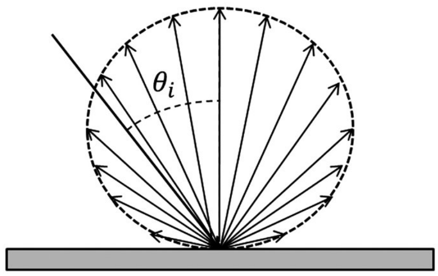

Fig. 3.10: *Completely diffuse reflection (Sentman's model; Mehta et al., 2014).*

The model proposed by Schamberg in 1959 is based on the hyperthermal flow assumption according to which the random thermal component of the gas molecular velocities is negligible compared to the macroscopic (bulk) velocity, so that all the incident neutral particles have the same velocity and direction corresponding approximately to the satellite velocity relative to the neutral atmosphere. This model considers a quasi-specular reflection of molecules within a conical beam, ranging from incomplete to complete accommodation, and a constant velocity of the re-emitted particles (Fig. 3.9[1]).

The model developed by Sentman in 1961 is based on the thermal flow assumption, describing the incident flow at every point on the satellite surface as a superposition of the Maxwell-Boltzmann molecular velocity distribution and the incident velocity vector of the atmosphere relative to the spacecraft. This has significant implications in spacecraft aerodynamics, because particles with high thermal velocities not aligned with the macroscopic velocity of the flow can collide with surfaces that could, at first, appear to be shadowed. This model considers a fully diffuse reflection of molecules with complete accommodation and a Maxwell-Boltzmann velocity of the re-emitted particles (Fig. 3.10[2]). Sentman's closed-form solutions can be modified

[1] Prieto D.M., Graziano B.P., Roberts P.C.E. (2014): Spacecraft drag modelling, Progress in Aerospace Sciences, 64, 56–65, doi:10.1016/j.paerosci.2013.09.001

[2] Mehta P.M., Walker A., McLaughlin C.A., Koller J. (2014): Comparing physical drag coefficients computed using different gas-surface interaction models, Journal of Spacecraft and Rockets, 51(3), 873–883, doi:10.2514/1.A32566

to account for incomplete accommodation and diffuse re-emission. This leads to the so-called DRIA (diffuse reflection with incomplete accommodation) model based on Sentman's solutions.

Both Schamberg's and Sentman's DRIA model have been implemented in DOGS-OC for spherical and non-spherical SLR satellites. They can be selected according to the orbital regime of the processed satellite. Schamberg's model is appropriate for calculating drag coefficients at altitudes above 500 km where the quasi-specular reflection is more significant as the amount of adsorbed atomic oxygen decreases. However, the hyperthermal approximation of Schamberg's model can lead to large errors in the aerodynamic coefficients of satellites with elongated shape and varying attitude like CHAMP, GRACE, GOCE, or SWARM. On the other hand, Sentman's DRIA model is especially accurate at altitudes below 500 km where the satellite surface is covered with a layer of adsorbed atomic oxygen, allowing for diffuse reflection.

In order to investigate the possibility to derive the thermospheric density from SLR observations, a sensitivity study to thermospheric density variations will be performed using DOGS-OC. Different thermospheric models and a horizontal wind model (Table 3.1) will be tested during the processing of some spherical SLR satellites at an altitude below 500 km.

Summarizing the procedure related to Eq. (3.2) the aerodynamic drag coefficient C_D which describes the interaction of the satellite surfaces with the atmosphere is computed analytically according to an appropriate gas-surface interaction model. The velocity v_{rel} is calculated by means of the chosen wind model. Finally, the atmospheric density ρ is approximated by the relation

$$\rho = f_{sc}\,\rho_m \tag{3.3}$$

where the model density ρ_m is computed from the adopted atmospheric density model. Assuming that the errors of all models are negligible, the atmospheric scaling factor f_{sc}, estimated with a selected temporal resolution, directly determines the target quantity ρ according to Eq. (3.3). The implementation of the thermospheric and horizontal wind models has been recently completed.

Table 3.1: *Thermospheric and horizontal wind models.*

Model family	Model name	Reference
Jacchia	JB2008	(Bowman et al., AIAA/AAS Astrodynamics Specialist Conference, 2008)
DTM	DTM	(Barlier et al., Annales Geophysicae, 1978)
MSIS	CIRA-86 NRLMSISE-00	(Hedin et al., JGR, 1988) (Picone et al., JGR, 2002)
HWM	HWM14	(Drob et al., Earth and Space Science, 2015)

Related publications

Bloßfeld M.: The key role of Satellite Laser Ranging towards the integrated estimation of geometry, rotation and gravitational field of the Earth. PhD thesis, German Geodetic Commission, C745, 2015

Limberger M.: Ionosphere modeling from GPS radio occultations and complementary data based on B-splines. PhD thesis, German Geodetic Commission, C755, 2015

Limberger M., Hernandez-Pajares M., Aragon-Angel A., Altadill D., Dettmering D.: Long-term comparison of the ionospheric F2 layer electron density peak derived from ionosonde data and Formosat-3/COSMIC occultations. Journal of Space Weather and Space Climate 5, A21, doi:10.1051/swsc/2015023, 2015

Schmidt M., Dettmering D., Seitz F.: Using B-spline expansions for ionosphere modeling. In: Freeden W., Nashed M.Z., Sonar T. (Eds.) Handbook of Geomathematics (Second Edition), 939–983, Springer, doi:10.1007/978-3-642-54551-1_80, 2015

3.2 Regional Gravity Field

Quasi-geoid heights in Northern Germany

High-resolution gravity data are only available for very few regions. Typically, they stem from terrestrial, ship- or airborne observations and reach a spatial resolution down to a few kilometers. The aim is to extract the optimum gravitational information from a combination of all available data in Northern Germany and to model a high-resolution regional gravity field. The resulting quasi-geoid heights (Lieb et al., 2016), as one out of several gravitational quantities, are validated against the German Combined Quasigeoid 2011 (GCG2011).
A study area was chosen from 6.2° to 14.0° longitude and from 53.5° to 55.0° latitude (cf. Fig. 3.11, green box). It contains both on- and offshore areas with different gravitational structure and, thus, allows the combination of a variety of data sets. Figure 3.11 shows the spatial distribution of the different data sets projected on the Earth's surface. Over the sea, measurements from mid-resolution altimetry missions are available (dark green dots), supplemented by shipborne measurements (red dots) in the Baltic Sea. High-resolution airborne gravimetry observations cover the ocean as well as the land surface (orange lines). The largest data set consists of terrestrial observations (yellow dots) with a very high spectral and spatial resolution due to precise gravity measurement systems and the density of observation sites from 53.5° in the south up to the German coastline in the north. The average spatial resolution of all observations is about 10 km.

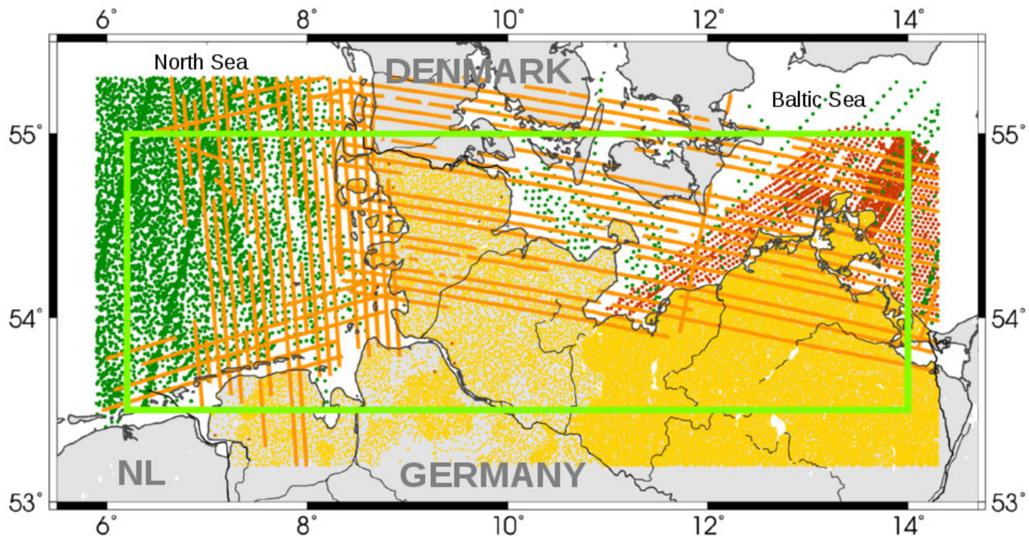

Fig. 3.11: *Distribution of the observations in the test area of Northern Germany (green box): satellite altimetry (dark green), shipborne (red), airborne (orange), and terrestrial data (yellow).*

According to the regional gravity modeling specifications described by Lieb et al. (2016), the series expansion is developed up to a maximum resolution of $L = 2190$ in the analysis with a low-pass filtering Shannon kernel, and smoothed down to degree $l = 2047$ in the synthesis with a Blackman kernel. All observations are reduced by the spherical harmonic (SH) background model GOCO05s up to degree $l = 127$ in order to remove well-modeled long wavelengths from the regional data sets. The estimation model contains the functional relationships for 9 different observation groups: terrestrial, airborne (two campaigns in the North and Baltic Sea), and shipborne gravimetry as well as altimetry (ERS-1e, ERS-1f, Cryosat, Envisat EM, Jason-1 GM). As the single data sets are based on diverse measurement techniques with different spatial and spectral resolutions and accuracies, variance component estimation (VCE) is applied to handle these inhomogeneities properly. GOCO05s up to $l = 127$ is introduced as prior information and assumed to be free of noise. The 9 observation groups are treated as independent data sets.
The quasi-geoid heights ζ (w.r.t. GOCO05s, $l = 127$) in Fig. 3.12a reach minimum values down to -0.48 m in the German lowlands. Maximum values up to 1.06 m appear along the coastline in the North Sea, in the Baltic Sea between 12° and 13° latitude, and at the northern boundary of the target area (at 8°, 9.5°, between 12° and 13° latitude). The corresponding standard deviations (Fig. 3.12b) increase up to a maximum of 0.12 m along the northern borderline and in the south-west corner due to data gaps (cf. Fig. 3.11). The mean value of the standard deviations of only 1 cm (maximum value of 2.2 cm) approves the high internal precision of the modeling approach.

Restoring the previously subtracted background model GOCO05s delivers the full gravity signal $l = 0, \ldots, 2047$ (Fig. 3.13a). The amplitudes vary from 34.40 m to 40.73 m and indicate the total height above the reference ellipsoid GRS80.
In order to validate our regional modeling approach, differences w.r.t. the model GCG2011 are computed. The latter is provided by BKG and IfE (Institut für Erdmessung, Leibniz Universität Hannover) and represents the official German height reference with an offshore pre-

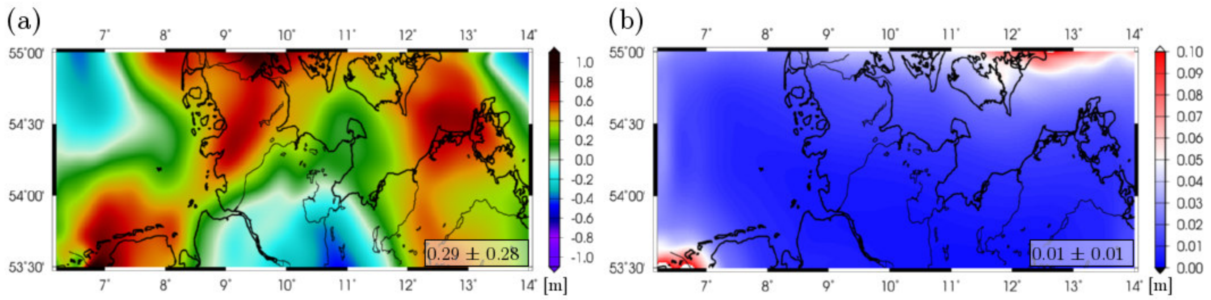

Fig. 3.12: *Quasi-geoid heights ζ (a) up to degree $l = 2047$, w.r.t. GOCO05s up to $l = 127$, and their standard deviations (b). Mean values and their standard deviations are depicted in boxes (values in m).*

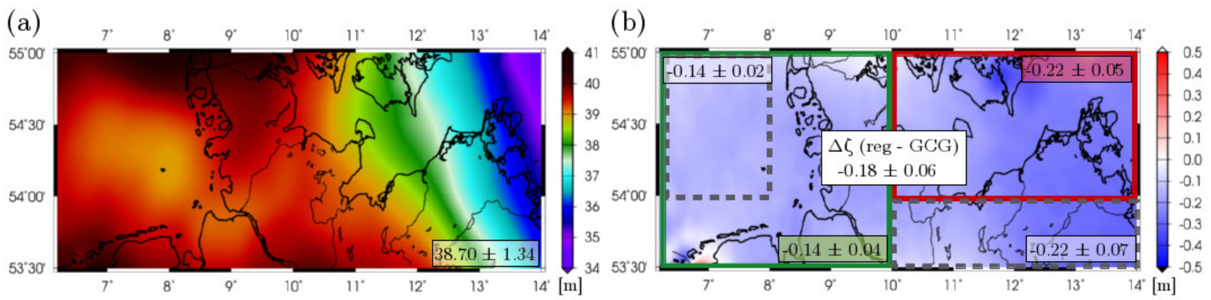

Fig. 3.13: *Quasi-geoid heights ζ (a) up to degree $l = 2047$ (background model GOCO05s restored) and differences $\Delta\zeta$ (b) w.r.t. the regional GCG2011 model. Mean values and their standard deviations (depicted in boxes, values in m) are computed for different areas: the entire area, the altimetry validation area (green box), the shipborne validation area (red box) and a pure off- and onshore area (dashed boxes).*

cision of 4–10 cm and an onshore precision of 1–2 cm in the German lowlands (source: www.geodatenzentrum.de/docpdf/quasigeoid.pdf). Thus, the precision is comparable with the mean standard deviation of 1 cm of our regional model (Fig. 3.12b).

For further comparisons, we computed differences w.r.t. the global model EGM2008 ($l = 2047$, Blackman smoothed) as well. The statistics of all differences are listed in Tab. 3.2. The mean value of the difference $\Delta\zeta$ (reg – GCG) between our regional estimation (reg) and the GCG2011 model (GCG) predominates with -18 cm the small standard deviation of 6 cm. Comparing the global EGM2008 model (EGM) with GCG2011 results in an offset of -28 ± 3 cm. The negative offset seems to originate from the GCG2011 model, as the difference $\Delta\zeta$ (reg – EGM) at exactly the same grid points yields a mean value of $+9 \pm 6$ cm. In contrast to our regional model, the GCG2011 is not a pure gravimetric geoid model, as it is adapted to a number of GNSS leveling points in order to allow transformations to geometric reference frames.

Figure 3.13b shows the differences for certain sub-regions. The offset increases from the west (-14 cm for the green box) to the east (-22 cm). The standard deviations of the differences increase as well, but they also differ between off- and onshore regions. Over the North Sea, mainly observed by altimetry (dashed box), they amount to 2 cm compared to 4 cm for the entire green box, containing both off- and onshore areas. Over the Baltic Sea, they rise up to 5 cm, and we finally obtain 7 cm over the south-eastern pure onshore area (dashed box). Comparing those values with the given precision of the GCG2011 model, the differences $\Delta\zeta$ (reg – GCG) are not significant in offshore areas, but over land. As the GCG2011 is based on the same terrestrial, air- and shipborne input data sets as our regional model, the deviations may result from topographic corrections applied to the GCG2011 model (source: www.geodatenzentrum.de/docpdf/quasigeoid.pdf). However, the two regional models fit very well to each other, and the small deviations confirm the high precision of our modeling result. Further studies in mountainous regions, together with the use of a topographic model as prior information are planned.

Table 3.2: *Differences between quasi-geoid heights obtained with our regional approach (reg), the regional quasi-geoid model GCG2011 (GCG), and the global model EGM2008 (EGM). The values $\Delta\zeta$ are computed at the given 1' $\times$ 1.5' GCG2011 grid.*

difference	range	mean	std. deviation
$\Delta\zeta$ (reg – GCG)	$-0.38 \ldots +0.20$ m	-0.18 m	0.06 m
$\Delta\zeta$ (EGM – GCG)	$-0.38 \ldots -0.15$ m	-0.28 m	0.03 m
$\Delta\zeta$ (reg – EGM)	$-0.08 \ldots +0.38$ m	$+0.09$ m	0.06 m

References

Lieb V., Schmidt M., Dettmering D., Börger K. (2016): Combination of various observation techniques for regional modeling of the gravity field. Journal of Geophysical Research (under review)

Distributed fault slip model for the 2011 Tohoku-Oki earthquake from GNSS and GRACE/GOCE satellite gravimetry[3]

The Gravity Recovery and Climate Experiment (GRACE) mission (launched 2002) and the Gravity Field and Steady-State Ocean Circulation Explorer (GOCE) mission (March 2009 to

[3] Copied and modified from Fuchs et al. (2016)

November 2013) collected spaceborne gravity data for the pre- and post-seismic periods of the 2011 Tohoku-Oki earthquake. In addition, the dense Japan GeoNet GNSS network with approximately 1050 stations measured the co- and post-seismic surface displacements. We combined GNSS, GRACE, and GOCE observations to determine a distributed fault slip model. Our model integrates the co- and post-seismic effects as we include GOCE observations averaged over a 2 year interval, but their inclusion reveals the gravity change with unprecedented spatial accuracy. The gravity gradient grid, evaluated at the GOCE orbit height of 265 km, has an estimated formal error of 0.2 mE ($2 \times 10^{-13}\,s^{-2}$) which provides sensitivity to the mainly co-seismic and integrated post-seismic-induced gravity gradient signal of -1.0 mE. The increased resolution of the gravity change provides valuable information, with GOCE gravity gradient observations sensitive to a more focused slip distribution in contrast to the filtered GRACE equivalent. The 2 year averaging window of the observations makes it important to incorporate estimates of the variance/covariance of unmodeled processes in the inversion. The GNSS and GRACE/GOCE combined model shows a slip pattern with 20 m peak slip at the trench. The total gravity change (approx. 200 μGal) and the spatial mapping accuracy would have been considerably lower by omitting the GOCE-derived fine-scale gravity field information.

Satellite gravity gradient grids for geophysics[4]

GOCE was ESA's first satellite gravity mission that delivered scientific data from November 2009 until October 2013. The aim of the mission was to determine the Earth's mean gravity field with unprecedented accuracy at a spatial resolution of 100 km or better. The main on-board instrument was the gradiometer that provided gravity gradients, i.e., the Cartesian second spatial derivatives of the gravitational potential. In combination with data from the on-board GPS receiver, the gradients have been used to recover global gravity field models in terms of Stokes coefficients. These models also allow computing arbitrary quantities of the gravitational potential everywhere on or above the Earth's surface. Nevertheless, for geophysical users it may be more convenient to use gravity gradients instead of a set of Stokes coefficients, and dedicated regional gravity field solutions may be able to represent the local high-resolution signal more accurately than global models do.

The original GOCE gravity gradients are complicated to use because of their error characteristics and because they are given in a rotating instrument frame indirectly related to the Earth. We therefore combine GOCE with accurate long wavelength information from the GRACE satellite gravity mission and compute gravity gradients in grids at 225 km and 255 km altitude above the reference ellipsoid corresponding to the GOCE nominal and lower orbit phases, respectively. We find that the grids may contain additional high-frequency content compared with GOCE-based global models. A test on the gradient sensitivity for crustal depth slices using a 3D lithospheric model of the North-East Atlantic region shows that the depth sensitivity differs from gradient to gradient. In addition, the relative signal power for the individual gradient component changes comparing the 225 km and 255 km grids, implying that using all components at different heights reduces parameter uncertainties in geophysical modeling. Furthermore, since gravity gradients contain complementary information to gravity, we foresee the use of the grids in a wide range of applications from lithospheric modeling to studies on dynamic topography, and from glacial isostatic adjustment to bedrock geometry determination under ice sheets.

[4] Copied and modified from Bouman et al. (2016)

Related publications

Bouman J., Ebbing J., Meekes S., Abdul Fattah R., Fuchs M., Gradmann S., Haagmans R., Lieb V., Schmidt M., Dettmering D., Bosch W. (2015): GOCE gravity gradient data for lithospheric modeling. International Journal of Applied Earth Observation and Geoinformation, doi:10.1016/j.jag.2013.11.001

Bouman J., Ebbing J., Fuchs M., Sebera J., Lieb V., Haagmans R., Novak P. (2016): Satellite gravity gradient grids for geophysics. Sci. Rep. 6, 21050; doi:10.1038/srep21050

Fuchs M. (Hrsg.): Detection and in-depth assessment of the 2011 Tohoku-Oki earthquake evaluating GOCE gravity gradients. Dissertation, ISBN 978-3-00-051113-4, 2015

Fuchs M.J., Broerse T., Hooper A., Pietrzak J., Bouman J.: GRACE gravity data to enhance the modeling of coseismic slip distribution for the 2011 Tohoku-Oki earthquake. IAG Symposia, doi:10.1007/1345_2015_90, 2015

Fuchs, M.J., A. Hooper, T. Broerse, and J. Bouman (2016): Distributed fault slip model for the 2011 Tohoku-Oki earthquake from GNSS and GRACE/GOCE satellite gravimetry. J. Geophys. Res. Solid Earth, 121, doi:10.1002/2015JB012165.

3.3 Standards and Conventions

In order to fully benefit from the ongoing technological improvements of the geodetic observing systems, it is essential that the analysis of the precise observations is based on the definition and application of common standards and conventions and a consistent representation and parameterization of the relevant quantities. This is of crucial importance for the establishment of highly accurate and consistent geodetic reference frames, as the basis for a reliable monitoring of the time-varying shape, rotation and gravity field of the Earth (see Fig. 3.14).

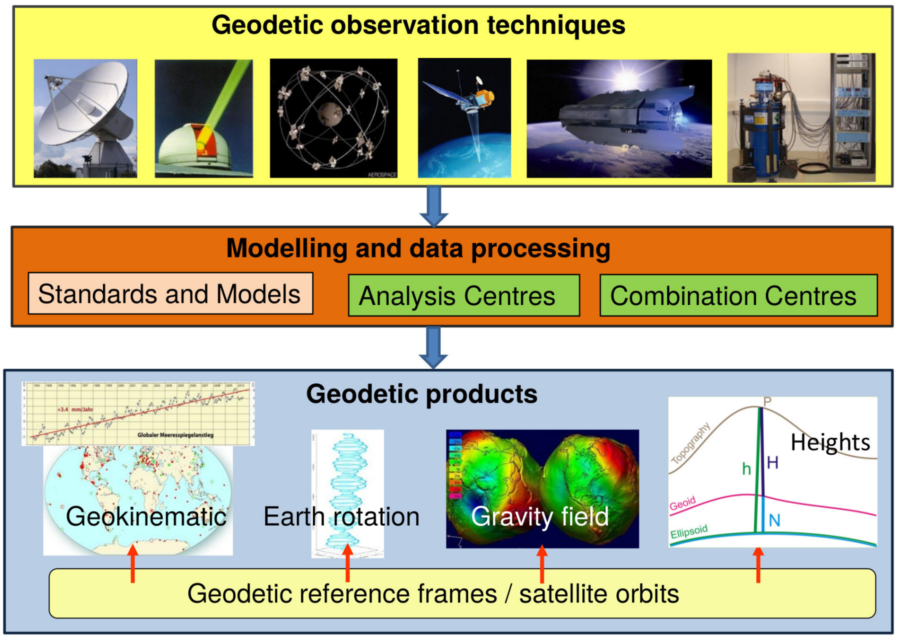

Fig. 3.14: *From geodetic observations to consistent products for a reliable monitoring of the time-varying shape, rotation and gravity field of the Earth.*

GGOS Bureau of Products and Standards

The Bureau of Products and Standards (BPS) is a recent reorganization of the former Bureau of Standards and Conventions (BSC) which was established in 2009 (Angermann et al. 2015a,b). This resulted from a re-alignment of the organization of the Global Geodetic Observing System (GGOS) in 2015. The present organizational structure of GGOS is shown in Fig. 3.15.

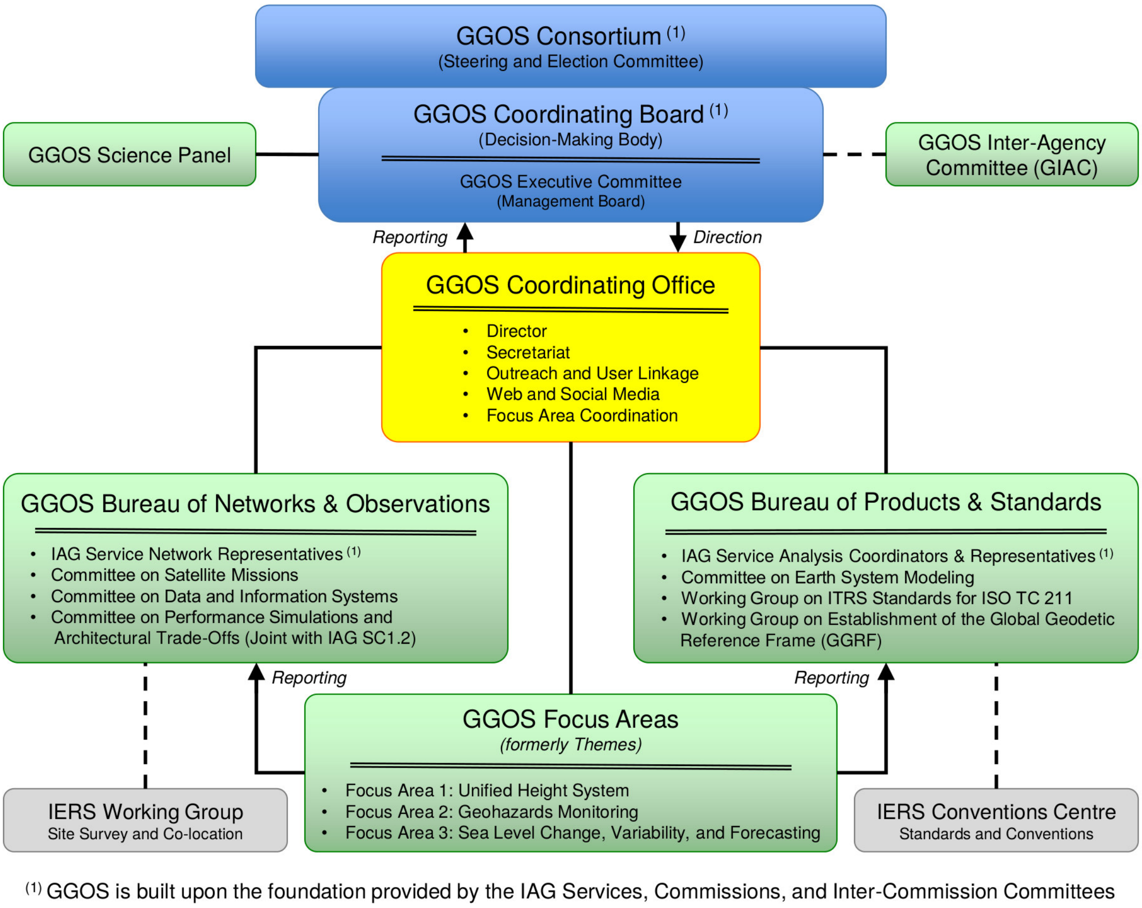

Fig. 3.15: *Organizational structure of IAG's Global Geodetic Observing System (GGOS).*

The BPS is hosted and supported by the DGFI-TUM and the Institute for Astronomical and Physical Geodesy (IAPG) of the Technische Universität München, within the Forschungsgruppe Satellitengeodäsie (FGS).

Purpose and scope

The work of the BPS is primarily focused on the IAG Services and the products they derive on an operational basis for Earth monitoring making use of various space geodetic observation techniques such as VLBI, SLR/LLR, GNSS, DORIS, altimetry, gravity satellite missions, gravimetry, etc. The Bureau builds upon existing observing and processing systems of the IAG and serves as a contact and coordinating point for the IAG analysis and combination services.

The BPS supports the IAG in its goal to obtain products of highest possible accuracy, consistency, and temporal and spatial resolution, which should refer to a consistent reference frame, stable over decades in time. To achieve this important goal, it is a fundamental requirement that common standards and conventions are used by all IAG components for the analysis of the different space geodetic observations. The BPS also concentrates on the integration of geometric and gravimetric parameters and the development of new products required to address important geophysical questions and societal needs.

BPS staff and representation of IAG components and other entities

The present (December 2015) BPS staff:

- Director: D. Angermann
- Deputy director: T. Gruber
- Geodetic fields covered by the BPS team:
  - Geometry, orbits, TRF: D. Angermann, U. Hugentobler, P. Steigenberger (as associated member)
  - Earth orientation, CRF: M. Gerstl, R. Heinkelmann (as IAU representative)
  - Gravity, height systems: T. Gruber, L. Sánchez

Currently, the following GGOS entities are associated with the BPS:

- Committee "Contributions to Earth System Modelling", Chair: M. Thomas (Germany),
- Joint Working Group "Establishment of the Global Geodetic Reference Frame (GGRF)", Chair: U. Marti (Switzerland),
- Working Group "ITRS Standards for ISO TC211", Chair: C. Boucher (France).

The IAG Services and other entities involved in standards and geodetic products have delegated representatives to serve as associated members of the BPS. The Bureau comprises the staff members, the chairs of the associated GGOS components, the committee and the two working groups as listed above, as well as representatives of the IAG Services and other entities. The status of December 2015 is summarized in Table 3.3. As regards the development of standards, there is a link with the IERS Conventions Center, the IAU Working Group "Numerical Standards for Fundamental Astronomy", BIPM, CODATA, NIST and ISO/TC211.

Table 3.3: *Associated members of the BPS representing the IAG Services, IAU and other entities (status: December 2015).*

T. Herring, USA, G. Petit, France	International Earth Rotation and Reference Systems Service (IERS)
U. Hugentobler, Germany	International GNSS Service (IGS)
E. Pavlis, USA	International Laser Ranging Service (ILRS)
J. Gipson, USA	International VLBI Service for Geodesy and Astrometry (IVS)
F. Lemoine, J. Ries, USA	International DORIS Service (IDS)
J.-M. Lemoine, H. Capdeville, France	International DORIS Service (IDS)
R. Barzaghi, Italy	International Gravity Field Service (IGFS)
F. Barthelmes, Germany	International Center for Global Gravity Field Models (ICGEM)
S. Bonvalot, France	Bureau Gravimetrique International (BGI)
R. Heinkelmann, Germany	International Astronomical Union (IAU), Working Group "Numerical Standards for Fundamental Astronomy"
M. Craymer, Canada	Chair of Control Body for ISO Geodetic Registry Network
L. Hothem, USA	Vice-Chair of Control Body for ISO Geodetic Registry Network
J. Ádám, Hungary	Chair of the IAG Communication and Outreach Branch
J. Ihde, Germany	IAG representative to ISO/TC211
J. Kusche, Germany	Representative of gravity community
P. Steigenberger, Germany	Representative of GNSS community

Inventory of standards and conventions

According to its charter, a key activity of the BPS is to assess the standards and conventions currently adopted and used by the IAG and its components for the processing of geometric and gravimetric observations as a basis for the generation of IAG products. A publication entitled "GGOS Bureau of Products and Standards: inventory of standards and conventions used for the generation of IAG products" has been reviewed by an external board, and the revised version has been submitted for the IAG Geodesist's Handbook 2016. The document will also be made available on the GGOS website as a living document.

This inventory gives a brief introduction into GGOS including its mission and objectives and an overview about its structure. It contains some general information on standards and conventions and summarizes the current standards, standardized units, fundamental physical constants, resolutions, and conventions that are relevant for geodesy. Chapter 3 of this document provides the status regarding numerical standards including time and tide systems and the geopotential value W_0. As shown in the inventory, different sources for numerical standards are currently in use, and the fundamental parameters are partly given in different time and tide systems which is a potential source for inconsistencies and even errors in geodetic products. Thus, it is essential that the numerical standards and applied conventions are clearly documented for all geodetic products. The key element is a product-based inventory (Chapter 4) which addresses the following major topics:

- Celestial reference systems and frames
- Terrestrial reference systems and frames
- Earth orientation parameters
- GNSS satellite orbits
- Gravity and geoid
- Height systems and their realizations

As a major outcome, the inventory presents, for each of these products (or topics), the current status regarding standards and conventions, identifies gaps and inconsistencies, and provides recommendations for improvements. These recommendations should be discussed with experts in the field, and future actions and responsibilities should be defined to resolve the remaining issues.

As the list of products addressed in the current version of this inventory is far from complete, additional products that may be specified as IAG products will be included in an updated version.

Implementation of a UN resolution for a Global Geodetic Reference Frame

The United Nations General Assembly adopted the resolution on a Global Geodetic Reference Frame for Sustainable Development (A/RES/69/266) on February 26, 2015. This resolution recognizes the importance of geodesy for many societal and economic benefit areas, including navigation and transport, construction and monitoring of infrastructure, process control, surveying and mapping, and the growing demand to provide the basis for global change research in Earth sciences. The resolution stresses the significance of a global reference frame for accomplishing these tasks, for natural disaster management, and to provide accurate information for decision-makers. The UN Global Geospatial Information Management (UN-GGIM) Working Group on the Global Geodetic Reference Frame (GGRF) has the task to draft a roadmap for the implementation of the GGRF.

Based on its competence in the realization of reference frames, DGFI-TUM is involved in this activity by contributing to a concept paper of the IAG. The main purpose of this paper is to provide a common understanding for the definition of the GGRF and the scientific basis for the preparation of the roadmap to be accomplished by the UN-GGIM Working Group on the GGRF. From the IAG perspective, a broad interpretation of the GGRF should be adopted to support the increasing demand for positioning, navigation, and monitoring of global change phenomena in the Earth system. Thus, the GGRF is intended to include the terrestrial reference frame, the physical height and gravity reference frame as well as the celestial reference frame and the Earth orientation parameters. This concept paper has been submitted to the IAG Executive Committee for a formal approval and further decisions.

Recently, the IAG has established a joint working group (JWG) for the realization of this UN resolution under the umbrella of the BPS (Chair: U. Marti, Switzerland). This JWG works together with representatives of IAG Commissions 1 and 2, the Inter-Commission Committee on Theory (ICCT) and the IERS.

Related publications

Angermann D., Gerstl M., Sánchez L., Gruber T., Hugentobler U., Steigenberger P., Heinkelmann R.: GGOS Bureau of Products and Standards: inventory of standards and conventions for geodesy. IAG Symposia 143, doi:10.1007/1345_2015_165, 2015a

Angermann D.: GGOS Bureau of Products and Standards. In: Drewes H., Hornik H. (Eds.) Travaux de l'AIG 39, IAG Reports 2011–2015, 2015b

4 Information Services and Scientific Transfer

The exchange of observation data, derived scientific data products and research results is a basic requirement to serve the scientific community and the public. DGFI-TUM is strongly cross-linked with other institutions and has continuously been involved in various national and international activities. Intensive collaborations exist in particular in the frame of the international scientific organizations IUGG, IAU and IAG. The international services of the IAG form the backbone for many disciplines of geosciences and the national and international spatial data infrastructure. They were established to continuously collect observations and meta data related to astrometry, geodesy, geophysics and neighboring disciplines.

DGFI-TUM recognizes the outstanding role of the IAG services for science and practice and operates - mostly by long-term commitments - data centers, analysis centers, and research centers (cf. Section 1). In this context the institute operates various internet portals (Section 4.1), and scientists of DGFI-TUM have taken leading positions and supporting functions in IAG's Commissions, Services, Projects, Working and Study Groups, and in the Global Geodetic Observing System (GGOS). A complete list of memberships and functions of DGFI-TUM staff is given in Section 4.2. Publications in peer-reviewed scientific journals are still the most acknowledged way of scientific transfer. Section 4.3 provides a list of articles printed or published online in 2015. It is followed by a list of posters and oral presentations (Section 4.4) that were presented by DGFI-TUM staff at numerous international conferences, symposia and workshops (Section 4.5). DGFI-TUM's strong national and international scientific network is also reflected by various guests that visit DGFI-TUM every year in the frame of research co-operations or for a period of study or research (Section 4.6).

4.1 Internet representation

The Internet has become an indispensable medium for the exchange of data and scientific information. The DGFI-TUM maintains several independent internet sites and wikis to meet growing demands for information about different scientific aspects. Furthermore, mailing lists are maintained by DGFI-TUM to fulfill the requirements for information exchange within the International Laser Ranging Service (ILRS), and the Reference System SIRGAS.

With effect from January 1st 2015 the Deutsches Geodätisches Forschungsinstitut has become an institute of the Technische Universität München (TUM). This also led to a transition of the web-domain from dgfi.badw.de to dgfi.tum.de for all web services maintained by DGFI-TUM. In 2015, the following websites were maintained by DGFI-TUM.

Deutsches Geodätisches Forschungsinstitut der Technischen Universität München (DGFI-TUM)

The website of DGFI-TUM, available at www.dgfi.tum.de, informs about the structure and results of the current research programme, ongoing research topics, the national and international projects DGFI-TUM is involved in and the multiple contributions of DGFI-TUM to international services. The web site (see Fig. 4.1) also provides a complete list of papers and reports published since 1994 by the employees as well as a compilation of all posters and oral presentations. Annual reports and DGFI reports are also available in electronic form.

Fig. 4.1: Web sites of DGFI-TUM (left) and SIRGAS (right)

Geocentric Reference System for the Americas (SIRGAS)

SIRGAS is the Geocentric Reference System for the Americas. The web site is operated by the SIRGAS Vice-President at DGFI-TUM and located at www.sirgas.org.

The SIRGAS web site comprises (see Fig. 4.1)

- a scientific description presenting definition, realization, and kinematics of the SIRGAS reference frame,
- an organizational summary showing the operational structure and functions of the different components of SIRGAS,
- a bibliographic compilation with reports, articles, presentations, and posters related to the SIRGAS activities.

EUROLAS Data Centre (EDC)

The EUROLAS Data Center (EDC) provides access to the database of SLR observations and derived products (see Fig. 4.2). This web site informs about the data flow within the Operation Centre (OC) and the data holding of the Data Centre (DC). This site is available at edc.dgfi.tum.de.

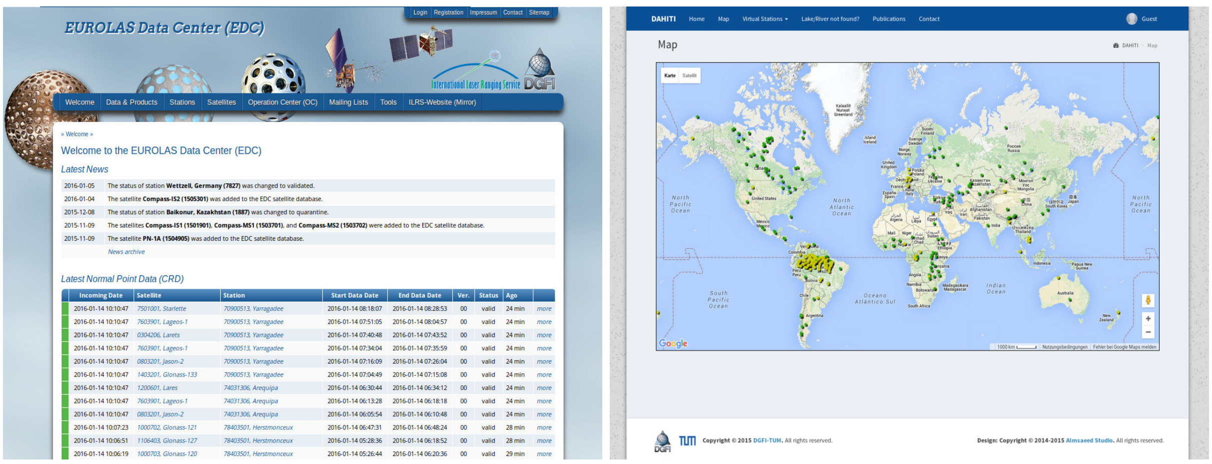

Fig. 4.2: Web sites of EDC (left) and DAHITI (right)

Database for Hydrological Time Series of Inland Waters (DAHITI)

The Database for Hydrological Time Series of Inland Waters (DAHITI) provides about 350 water level time series of lakes, rivers, reservoirs, and wetland derived from multi-mission satellite altimetry. The web site of DAHITI is available at dahiti.dgfi.tum.de (see Fig. 4.2)

Open Altimeter Database (OpenADB)

OpenADB is a database for multi-mission altimeter data and derived high-level products. It is designed for users with little experience in satellite altimetry and scientific users evaluating data and generating new products, models and algorithms. OpenADB allows fast parameter updates and enables database extracts with user-defined formats and parameters. The usage of OpenADB is open after registration to anyone. This site is available at openadb.dgfi.tum.de.

GGOS Bureau of Products and Standards (BPS)

The GGOS Bureau of Products and Standards (BPS) was established as a GGOS component in 2009. The BPS is hosted and supported by DGFI-TUM and the Institut für Astronomische und Physikalische Geodäsie (IAPG) of the Technische Universität München, within the Forschungsgruppe Satellitengeodäsie (FGS). The web site is located at ggos-bps.dgfi.tum.de

Office of the International Association of Geodesy (IAG)

Since the 24th General Assembly of the IUGG (2007) in Perugia, Italy, DGFI has been hosting the IAG Office as the former director of DGFI holds the position of the IAG Secretary General. The web site is available at iag.dgfi.tum.de

Project-Website: Swarm magnetic gradients for lithospheric modelling (SLIM)

The web site of the ESA supported project Swarm magnetic gradients for lithospheric modelling (SLIM) is located at slim.dgfi.tum.de and provides information about the project and related publications. The objective of this project is to study at feasibility level the use of magnetic gradient grids derived from Swarm data for lithospheric modelling.

Project-Website: Wetland Dynamics (WLDYN)

The website of the DFG project WLDYN (Assessing the spatiotemporal dynamics of water volumes in large wetlands and lakes by combining remote sensing with macro-scale hydrological modeling) is available at wldyn.dgfi.tum.de. The project is a joined project with the GFZ Potsdam and Johann Wolfgang Goethe-Universität. The project aims at incorporating altimetry data into the WGHM hydrology model for six global lakes and wetlands. The web page informs about the current status of the research and project related publications and data.

IAG Joint Working Group 0.1.1: Vertical datum standardization (closed 07/2015)

The web site whs.dgfi.tum.de summarizes the main activities developed by the Working Group Vertical Datum Standardisation, which was operative from July 2011 up to July 2015. This working group was an initiative of GGOS Focus Area 1 (former GGOS Theme 1), the IAG Commission 1 (Reference Frames), the IAG Commission 2 (Gravity Field) and the International Gravity Field Service (IGFS). Its main objective was the recommendation on a W_0 value to be introduced as the conventional reference level for the realisation of the International Height Reference System (IHRS), see IAG Resolution No. 1, July 2015.

IAG Joint Working Group 1.3: Strategies for Epoch Reference Frames

The website of the IAG Joint Working Group 1.3 is available at erf.dgfi.tum.de. The aim of this working group is to develop strategies for the computation of epoch reference frames, based on the combination of the space geodetic techniques VLBI, SLR, GNSS and DORIS on normal equation level and to assess their potentials in terms of accuracy, stability and global availability in order to provide recommendations to the IERS.

IAG Joint Study Group 0.3: Methodology of regional gravity field modelling (closed 07/2015)

The web site of the Joint Study Group 0.3 (JSG0.3) is available at jsg03.dgfi.tum.de. The aim of JSG0.3 was to find guidelines on suitable strategies for setting up the parameter estimation of regional gravity field modelling by combining satellite, airborne and terrestrial data. The study group was focused on the methodological foundation of regional gravity field modelling based on series expansions in terms of localizing base functions. Therefore, numerical studies have been concentrated on simulations based on synthetic data.

4.2 Membership in scientific bodies

American Geophysical Union (AGU)

- Journal of Geophysical Research - Solid Earth,
  Associate Editor: Bouman J.

Centre National d'Etudes Spatiales (CNES) / National Aeronautics and Space Administration (NASA)

- Ocean Surface Topography Science Team for Jason-2,
  Member: Bosch W., Dettmering D.

Deutsche Geodätische Kommission der Bayerischen Akademie der Wissenschaften (DGK)

- *Member: Seitz F.*

Deutsche Gesellschaft für Geodäsie, Geoinformation und Landmanagement (DVW)

- Working Group 7: Experimentelle, Angewandte und Theoretische Geodäsie,
  Member: Schmidt M., Seitz F.

European Geosciences Union (EGU)

- Geodesy Division,
  President: Schmidt M.,
  Deputy President (until 2015): Bouman J.

European Space Agency (ESA) / European Organisation for the Exploitation of Meteorological Satellites (EUMETSAT)

- Sentinel-3 Validation Team, Altimetry sub-group,
  Member: Dettmering D.

International Association of Geodesy (IAG)

- Commission 1 Sub-Commission 1.3b: Regional Reference Frame for South and Central America (until 2015),
  Vice-Chair: Sánchez L.
- Commission 1, Sub-Commission 1.4: Interaction of celestial and terrestrial reference frames,
  Member: Seitz M.
- Commission 4, Joint Working Group 4.3.3 "Combination of Observation Techniques for Multi-dimensional Ionosphere Modelling" (since 2015),
  Member: Erdogan E., Schmidt M.
- Commission 4, Study Group 4.3.1: Ionosphere modelling and analysis (until 2015),
  Chair: Schmidt M., Member: Dettmering D., Liang W., Limberger M.
- Commission 4, Sub-Commission 4.3 "Atmosphere Remote Sensing" (since 2015),
  Chair: Schmidt M.
- Commission 4, Working Group "Real Time Ionosphere Monitoring" (since 2015),
  Member: Dettmering D.
- Commission 4, Working Group 4.3.2 "Ionosphere Predictions" (since 2015),
  Member: Erdogan E.

- Commission 4, Working Group 4.3.5 "Ionosphere Scintillations" (since 2015),
  Member: Schmidt M.
- Global Geodetic Observing System (GGOS) Bureau of Products and Standards,
  Director: Angermann D., Member: Sánchez L.
- Global Geodetic Observing System (GGOS) Coordinating Board (since 2015),
  Member: Angermann D., Sánchez L., Schmidt M.
- Global Geodetic Observing System (GGOS) Executive Committee,
  Member: Angermann D.
- Global Geodetic Observing System (GGOS) Focus Area 1 Unified Height System (since 2015),
  Lead: Sánchez L.
- Global Geodetic Observing System (GGOS) Joint Working Group on the Realization of the IHRS (since 2015),
  Chair: Sánchez L.
- Global Geodetic Observing System (GGOS) Working Group on Performance Simulations and Architectural Trade-Offs (PLATO),
  Member: Seitz M.
- ICCT Joint Study Group 0.1: Application of time series analysis in geodesy,
  Member: Schmidt M.
- ICCT Joint Study Group 0.27 "Space weather and ionosphere" (since 2015),
  Member: Erdogan E., Schmidt M.
- ICCT Joint Study Group 0.3: Methodology of regional gravity field modelling (until 2015),
  Chair: Schmidt M., Member: Lieb V.
- ICCT Joint Study Group 0.5: Multi-sensor combination for the separation of integral geodetic signals (until 2015),
  Chair: Seitz F., Member: Schmidt M., Seitz M.
- ICCT Joint Study Group 0.6: Applicability of current GRACE solution strategies to the next generation of inter-satellite range observations (until 2015),
  Member: Bouman J., Haberkorn C., Schmidt M.
- ICCT Study Group 5: Fusion of multi-technique satellite geodesy data (since 2015),
  Member: Bloßfeld M.
- Joint Working Group 0.1.1: Vertical datum standardization (until 2015),
  Chair: Sánchez L.
- Joint Working Group 1.1: Tie vectors and local ties to support integration of techniques,
  Member: Seitz M.
- Joint Working Group 1.3: Strategies for epoch reference frames (until 2015),
  Chair: Seitz M., Member: Bloßfeld M., Sánchez L.
- Joint Working Group JWG2.8 "Modeling and Inversion of Gravity-Solid Earth Coupling",
  Member: Bouman J.
- Symposia Series (since 2015),
  Assistant Editor-in-Chief: Sánchez L.

- Working Group 1.3.1: Integration of dense velocity into the ITRF (until 2015),
  SIRGAS representative: Sánchez L.
- Working Group 1.3.2: Deformation models for reference frames (until 2015),
  Member: Sánchez L.
- Working Group for the establishment of the Global Geodetic Reference Frame (GGRF) (since 2015),
  Member: Sánchez L.

International Astronomical Union (IAU)

- Commission 19, Rotation of the Earth (until 2015),
  Secretary: Seitz F.
- Commission A.2, Rotation of the Earth (since 2015),
  Vice-President: Seitz F.
- Division A Working Group: Third Realisation of International Celestial Reference Frame,
  Member: Seitz M.

International Earth Rotation and Reference Systems Service (IERS)

- ITRS Combination Centre,
  Chair: Seitz M., Member: Bloßfeld M.
- Working Group on Combination at the Observation Level,
  Member: Angermann D., Bloßfeld M., Co-Chair: Seitz M.
- Working Group on SINEX Format,
  Member: Seitz M.
- Working Group on Site Coordinate Time Series Format,
  Member: Seitz M.
- Working Group on Site Survey and Co-location,
  Member: Angermann D., Schmid R., Seitz M.

International GNSS Service (IGS)

- Antenna Working Group,
  Chair: Schmid R.
- Governing Board,
  Member: Schmid R., Network Representative: Sánchez L.
- GPS Tide Gauge Benchmark Monitoring - Working Group,
  Member: Sánchez L.

International Laser Ranging Service (ILRS)

- Analysis Standing Committee,
  Member: Bloßfeld M., Müller H.
- Data Centre (EDC),
  Chair: Schwatke C., Member: Müller H.
- Data Formats and Procedures Standing Committee,
  Chair: Müller H., Member: Schwatke C.

- Governing Board,
  Member: Müller H.
- LARGE (LAser Ranging to GNSS s/c Experiment) Study Group (since 2015),
  Member: Müller H.
- Operations Centre (EDC),
  Chair: Schwatke C.
- Study Group on ILRS Software Library,
  Member: Schwatke C.

International Union of Geodesy and Geophysics

- *Representative to the Panamerican Institute for Geodesy and History (PAIGH): Drewes H., Sánchez L.*

International VLBI Service for Geodesy and Astrometry (IVS)

- Operational Analysis Centre,
  Member: Schmid R., Seitz M.

Sistema de Referencia Geocéntrico para las Américas (SIRGAS)

- *Vicepresident: Sánchez L.*
- Scientific Committee (since 2015),
  Member: Sánchez L.

4.3 Publications

Abelen S., Seitz F., Abarca-del-Rio R., Güntner A.: *Droughts and floods in the La Plata basin in soil moisture data and GRACE*. Remote Sensing 7(6): 7324–7349, doi:10.3390/rs70607324, 2015

Alizadeh M.M., Schuh H., Schmidt M.: *Ray tracing technique for global 3-D modeling of ionospheric electron density using GNSS measurements*. Radio Science 50(6): 539–553, doi:10.1002/2014RS005466, 2015

Angermann D., Gerstl M., Sánchez L., Gruber T., Hugentobler U., Steigenberger P., Heinkelmann R.: *GGOS Bureau of Products and Standards: inventory of standards and conventions for geodesy*. IAG Symposia 143, doi:10.1007/1345_2015_165, 2015

Angermann D.: *GGOS Bureau of Products and Standards*. In: Drewes H., Hornik H. (Eds.) Travaux de l'AIG 39, IAG Reports 2011–2015, 2015

Bachmann S., Messerschmitt L., Schmid R., Bloßfeld M., Thaller D.: *BKG/DGFI Combination Center Annual Report 2014*. In: Baver K.D., Behrend D., Armstrong K.L. (Eds.) International VLBI Service for Geodesy and Astrometry 2014 Annual Report, 204–207, NASA/TP-2015-217532, 2015

Bentel K., Schmidt M.: *Combining different types of gravity observations in regional gravity modeling in spherical radial basis functions*. IAG Symposia, doi:10.1007/1345_2015_2, 2015

Bloßfeld M., Müller H., Gerstl M., Stefka V., Bouman J., Göttl F., Horwath M.: *Second-degree Stokes coefficients from multi-satellite SLR*. Journal of Geodesy 89(9): 857–871, doi:10.1007/s00190-015-0819-z, 2015

Bloßfeld M.: *The key role of Satellite Laser Ranging towards the integrated estimation of geometry, rotation and gravitational field of the Earth*. Dissertation, Technische Universität München und Reihe C der Deutschen Geodätischen Kommission (ISBN: 978-3-7696-5157-7), 2015

Bloßfeld M., Seitz M., Angermann D.: *Epoch reference frames as short-term realizations of the ITRS – datum stability versus sampling*. IAG Symposia 143, doi:10.1007/1345_2015_91, 2015

Bloßfeld M., Seitz M., Angermann D., Moreaux G.: *Quality assessment of IDS contribution to ITRF2014 performed by DGFI-TUM*. Advances in Space Research, doi:10.1016/j.asr.2015.12.016, 2015

Bloßfeld M., Stefka V., Müller H., Gerstl M.: *Satellite laser ranging – a tool to realize GGOS?*. IAG Symposia 143, doi:10.1007/1345_2015_202, 2015

Bouman J., Ebbing J., Meekes S., Fattah R.A., Fuchs M., Gradmann S., Haagmans R., Lieb V., Schmidt M., Dettmering D., Bosch W.: *GOCE gravity gradient data for lithospheric modeling*. International Journal of Applied Earth Observation and Geoinformation 35(A): 16–30, Elsevier, doi:10.1016/j.jag.2013.11.001, 2015

Dettmering D., Schwatke C., Bosch W.: *Global calibration of SARAL/AltiKa using multi-mission sea surface height crossovers*. Marine Geodesy 38 (supplement 1): 206–218, doi:10.1080/01490419.2014.988832, 2015

Fuchs M.: *Detection and in-depth assessment of the 2011 Tohoku-Oki earthquake evaluating GOCE gravity gradients*. Dissertation, ISBN 978-3-00-051113-4, 2015

Fuchs M.J., Broerse T., Hooper A., Pietrzak J., Bouman J.: *GRACE gravity data to enhance the modeling of coseismic slip distribution for the 2011 Tohoku-Oki earthquake*. IAG Symposia, doi:10.1007/1345_2015_90, 2015

Göttl F., Schmidt M., Seitz F., Bloßfeld M.: *Separation of atmospheric, oceanic and hydrological polar motion excitation mechanisms based on a combination of geometric and gravimetric space observations*. Journal of Geodesy 89(4): 377–390, Springer, doi:10.1007/s00190-014-0782-0, 2015

Haberkorn C., Bloßfeld M., Bouman J., Fuchs M., Schmidt M.: *Towards a consistent estimation of the Earth's gravity field by combining normal equation matrices from GRACE and SLR*. IAG Symposia 143, doi:10.1007/1345_2015_76, 2015

Ihde J., Barzaghi R., Marti U., Sánchez L., Sideris M., Drewes H., Foerste C., Gruber T., Liebsch G., Pail R.: *Report of the Ad-hoc Group on an International Height Reference System (IHRS)*. In: Drewes H., Hornik H. (Eds.) Travaux de l'AIG 39, IAG Reports 2011–2015, 2015

Kutterer H., Seitz F., Alkhatib H., Schmidt M. (Hrsg.): *The 1st International Workshop on the Quality of Geodetic Observation and Monitoring Systems (QuGOMS'11)*. IAG Symposia 140, Springer, doi:10.1007/978-3-319-10828-5, 2015

Liang W., Limberger M., Schmidt M., Dettmering D., Hugentobler U.: *Combination of ground- and space-based GPS data for the determination of a multi-scale regional 4-D ionosphere model*. IAG Symposia, doi:10.1007/1345_2015_25, 2015

Liang W., Limberger M., Schmidt M., Dettmering D., Hugentobler U., Bilitza D., Jakowski N., Hoque M.M., Wilken V., Gerzen T.: *Regional modeling of ionospheric peak parameters using GNSS data – an update for IRI*. Advances in Space Research 55(8): 1981–1993, doi:10.1016/j.asr.2014.12.006, 2015

Lieb V., Bouman J., Dettmering D., Fuchs M., Schmidt M.: *Combination of GOCE gravity gradients in regional gravity field modelling using radial basis functions*. IAG Symposia, Springer, doi:10.1007/1345_2015_71, 2015

Limberger M., Hernández-Pajares M., Aragón-Àngel A., Altadill D., Dettmering D.: *Long-term comparison of the ionospheric F2 layer electron density peak derived from ionosonde data and Formosat-3/COSMIC occultations*. Journal of Space Weather and Space Climate 5, A21, doi:10.1051/swsc/2015023, 2015

Limberger M.: *Ionosphere modeling from GPS radio occultations and complementary data based on B-splines*. Dissertation, Technische Universität München und Reihe C der Deutschen Geodätischen Kommission (ISBN: 978-3-7696-5167-6), 2015

Montenbruck O., Schmid R., Mercier F., Steigenberger P., Noll C., Fatkulin R., Kogure S., Ganeshan A.S.: *GNSS satellite geometry and attitude models*. Advances in Space Research 56(6): 1015–1029, Elsevier, doi:10.1016/j.asr.2015.06.019, 2015

Panafidina N., Hugentobler U., Seitz M.: *Interaction between subdaily Earth rotation parameters and GPS orbits*. IAG Symposia, Springer, doi:10.1007/1345_2015_180, 2015

Sánchez L., Dayoub N., Cunderlík R., Minarechová Z., Mikula K., Vatrt V., Vojtísková M., Síma Z.: *Report of Joint Working Group 0.1.1: Vertical Datum Standardization (JWG 0.1.1)*. In: Drewes H., Hornik H. (Eds.) Travaux de l'AIG 39, IAG Reports 2011–2015, 2015

Sánchez L., Drewes H., Brunini C., Mackern M.V., Martínez-Díaz W.: *SIRGAS core network stability*. IAG Symposia 143, doi:10.1007/1345_2015_143, 2015

Sánchez L.: *SIRGAS Regional Network Associate Analysis Center Technical Report 2014*. In: Jean Y., Dach R. (Eds.) International GNSS Service Technical Report 2014, 101–110, IGS Central Bureau, 2015

Schmid R., Dach R., Collilieux X., Jäggi A., Schmitz M., Dilssner F.: *Absolute IGS antenna phase center model igs08.atx: status and potential improvements*. Journal of Geodesy, Springer, doi:10.1007/s00190-015-0876-3, 2015

Schmid R.: *Antenna Working Group Technical Report 2014*. In: Jean Y., Dach R. (Eds.) International GNSS Service Technical Report 2014, 129–132, IGS Central Bureau, 2015

Schmid R., Gerstl M., Seitz M., Angermann D.: *DGFI Analysis Center Annual Report 2014*. In: Baver K.D., Behrend D., Armstrong K.L. (Eds.) International VLBI Service for Geodesy and Astrometry 2014 Annual Report, 210–212, NASA/TP-2015-217532, 2015

Schmidt M., Dettmering D., Seitz F.: *Using B-spline expansions for ionosphere modeling*. In: Freeden W., Nashed M.Z., Sonar T. (Eds.) Handbook of Geomathematics (Second Edition), 939–983, Springer, doi:10.1007/978-3-642-54551-1_80, 2015

Schmidt M., Sebera J., Bouman J., Fabert O.: *Towards ellipsoidal representations of the gravity field*. Leibniz Online, 2015, 19, 2015

Schmidt M., Göttl F., Heinkelmann R.: *Towards the combination of data sets from various observation techniques*. In: Kutterer H., Seitz F., Alkhatib H., Schmidt M. (Eds.) The 1st International Workshop on the Quality of Geodetic Observation and Monitoring Systems (QuGOMS'11), IAG Symposia 140: 35–43, Springer, doi:10.1007/978-3-319-10828-5_6, 2015

Schöne T., Bingley R., Deng Z., Griffiths J., Habrich H., Hunegnaw A., Jia M., King M., Merrifield M., Mitchum G., Neilan R., Noll C., Prouteau E., Sánchez L., Teferle N., Thaller D., Tregoning P., Williams S., Wöppelmann G., Woodworth P.: *Tide Gauge Benchmark Monitoring Working Group Technical Report 2014*. In: Jean Y., Dach R. (Eds.) International GNSS Service Technical Report 2014, 187–202, IGS Central Bureau, 2015

Schwatke C.: *Historical development of the SLR data holding at EDC between 1976 and 2014*. Proceedings of 19th International Laser Ranging Workshop, Annapolis, USA, 2015

Schwatke C., Dettmering D., Boergens E., Bosch W.: *Potential of SARAL/AltiKa for inland water applications*. Marine Geodesy 38(Supplement 1): 626–643, doi:10.1080/01490419.2015.1008710, 2015

Schwatke C., Dettmering D., Bosch W., Seitz F.: *DAHITI – an innovative approach for estimating water level time series over inland waters using multi-mission satellite altimetry*. Hydrology and Earth System Sciences 19(10): 4345–4364, doi:10.5194/hess-19-4345-2015, 2015

Seitz M.: *Comparison of different combination strategies applied for the computation of terrestrial reference frames and geodetic parameter series*. In: Kutterer H., Seitz F., Alkhatib H., Schmidt M. (Eds.) The 1st International Workshop on the Quality of Geodetic Observation and Monitoring Systems (QuGOMS'11), IAG Symposia 140: 57–64, doi:10.1007/978-3-319-10828-5_9, 2015

Seitz M., Angermann D., Gerstl M., Bloßfeld M., Sánchez L., Seitz F.: *Geometrical reference systems*. In: Freeden W., Nashed M.Z., Sonar T. (Eds.) Handbook of Geomathematics (Second Edition), Springer, pp 2995–3034, doi:10.1007/978-3-642-54551-1_79, 2015

Seitz M., Angermann D., Bloßfeld M., Gerstl M., Müller H.: *ITRS Combination Centres: Deutsches Geodätisches Forschungsinstitut (DGFI)*. In: Dick W.R., Thaller D. (Eds.) IERS Annual Report 2014, Verlag des Bundesamts für Kartographie und Geodäsie, pp 120–123, 2015

Singh A., Kumar U., Seitz F.: *Remote sensing of storage fluctuations of poorly gauged reservoirs and state space model (SSM)-based estimation*. Remote Sensing 7(12): 17113–17134, doi:10.3390/rs71215872, 2015

Singh A., Seitz F.: *Updated bathymetric chart of the East Aral Sea*. Deutsches Geodätisches Forschungsinstitut, Munich, doi:10.1594/PANGAEA.855779, 2015

4.4 Posters and oral presentations

Abelen S., Seitz F., Abarca del, Güntner A.: *Signatures of droughts and floods in soil moisture and GRACE data in the La Plata Basin in South America*. 26th IUGG General Assembly 2015, Prague, Czech Republic, 2015-06-27

Angermann D.: *Inventory of IAG products: General issues and discussion*. GGOS Days 21015, Frankfurt/Main, Germany, 2015-10-22

Angermann D., Gruber T., Gerstl M., Hugentobler U., Sánchez L., Heinkelmann R., Steigenberger P.: *GGOS Büro für Produkte und Standards*. Geodätische Woche, Stuttgart, Germany, 2015-15-09

Angermann D.: *GGOS Bureau of Products and Standards*. BPS Meeting, Prague, Czech Republic, 2015-06-27

Angermann D., Gruber T., Gerstl M., Hugentobler U., Sánchez L., Heinkelmamm R., Steigenberger P.: *GGOS Bureau of Products and Standards: Inventory of standards and conventions*. 26th IUGG General Assembly 2015, Prague, Czech Republic, 2015-06-27

Bloßfeld M.: *The contribution of geodesy to Earth system sciences (invited)*. 26th IUGG General Assembly 2015, Prague, Czech Republic, 2015-06-27

Bloßfeld M.: *The key role of Satellite Laser Ranging towards the integrated estimation of geometry, rotation and gravitational field of the Earth*. TU München, Germany, 2015-01-30

Bloßfeld M., Roggenbuck O., Seitz M., Angermann D., Thaller D.: *The impact of non-tidal atmospheric pressure loading on global reference frames*. EGU General Assembly 2015, Vienna, Austria, 2015-04-15

Bloßfeld M., Seitz M., Angermann D.: *DTRF2014: Results of the analysis and impact of the contribution of the International Laser Ranging Service*. ILRS Analysis Working Group Meeting, Vienna, Austria, 2015-04-16

Boergens E., Schwatke C., Dettmering D., Seitz F.: *Using the Hooking Effect in satellite altimetry data for water level time series estimation over smaller rivers in the Mekong basin*. Hydrospace 2015, ESA-ESRIN, Frascati, Italy, 2015-09-15 (Poster)

Boergens E., Schwatke C., Dettmering D., Seitz F.: *Correcting the Hooking Effect in satellite altimetry data for time series estimation over smaller rivers*. EGU General Assembly, Vienna, Austria, 2015-04-16

Boergens E., Dettmering D., Göttl F.,Schwatke, Seitz F.: *Water level variations within the Lower Mekong River network derived by satellite altimetry*. Earth Oberservation for Water Cycle Science 2015, 2015-10-21

Bosch W., Mueller F., Dettmering D.: *Validating geostrophic currents of a dynamic ocean topography estimate with data of ARGO floats and surface drifters*. EGU General Assembly 2015, 2015-04-15 (Poster)

Bothmer V., Hinrichs J., Venzmer M., Schmidt M., Dettmering D., Limberger M., Seitz F., Börger K., Brandert S., Görres B., Kersten W.: *Bestimmung der solaren Weltraumwetter-Impact-Parameter auf die terrestrische Ionosphäre und deren Vorhersage*. Weltraum-Wetterwork-shop am DLR, Neustrelitz, Germany, 2015-05-13

Cipollini P., Calafat F., Passaro M., Cotton D., Benveniste J.: *Global coastal altimetry data enable an improved look at coastal dynamics and sea level*. AGU, San Francisco, USA, 2015-12-14

Dettmering D.: *Inlandaltimetrie*. FGS Begutachtung, Bad Kötzting, Germany, 2015-06-17

Dettmering D., Schwatke C., Braakmann-Folgmann A., Boergens E.: *Monitoring of water level variations of inundation areas within the Pantanal Wetland*. 26th IUGG General Assembly 2015, Prague, Czech Republic, 2015-06-25

Dettmering D., Müller F., Bosch W.: *Validation of altimetry-derived Ocean Dynamic Topography by in-situ measurements of ocean currents*. 26th IUGG General Assembly 2015, Prague, Czech Republic, 2015-06-27 (Poster)

Dettmering D., Schwatke C., Bosch W.: *Latest results of DGFI's multi-mission crossover analysis*. OSTST 2015, Reston, VA, USA, 2015-10-21

Drewes H., Sánchez L.: *Post-seismic crustal deformations after the 2010 earthquakes in the SIRGAS region*. Symposium SIRGAS 2015, Santo Domingo, Dominican Republic, 2015-11-20

Erdogan E., Dettmering D., Limberger M., Schmidt M., Seitz F., Börger K., Brandert S., Görres B., Kersten W., Bothmer V., Hinrichs J., Venzmer M.: *Generation of global VTEC maps from low latency GNSS observations based on B-spline modeling and Kalman filtering*. EGU General Assembly, Vienna, Austria, 2015-04-17 (Poster)

Erdogan E., Durmaz M., Liang W., Kappelsberger M., Dettmering D., Limberger M., Schmidt M., Seitz F., Börger K., Brandert S.: *Development of a novel adaptive model to represent global ionosphere information from combining space geodetic measurement systems*. EGU General Assembly, Vienna, Austria, 2015-04-17 (Poster)

Fuchs M.: *GOCE - Enhanced gravity gradients along the orbit*. EGU 2015, Wien, Österreich, 2015-04-14 (Poster)

Fuchs M.: *GOCE - Enhanced gravity gradients along the orbit*. 26th IUGG General Assembly 2015, Prag, Czech Republic, 2015-06-02

Haberkorn C., Bouman J., McMillan M., Bloßfeld M., Fuchs M.: *Comparison of Antarctic basin scale mass change from GRACE/GOCE and CryoSat-2*. 26th IUGG General Assembly 2015, Prague, Czech Republic, 2015-06-25

Haberkorn C., Bloßfeld M., Bouman J., Fuchs M., McMillan M.: *Evaluation of different C20 coefficients for the determination of ice mass loss in Antarctica and Greenland*. EGU General Assembly 2015, Vienna, Austria, 2015-04-16

Haberkorn C., Fuchs M., Ressler G., Schwatke C.: *Assessing the potential to increase the spatial resolution of water storage variations from a combination of GRACE and GOCE*. EOFWCS 2015, Frascati, Italien, 2015-10-21

Hinrichs J., Bothmer V., Venzmer M., Erdogan E., Dettmering D., Limberger M., Schmidt M., Seitz F., Boerger K., Brandert S., Goerres B., Kersten W., Bernert B., Florczak J.: *Ionosphere Response to EUV Emission from Post-eruptive Arcades*. EGU General Assembly, Vienna, Austria, 2015-04-17 (Poster)

Hugentobler U., Seitz M., Angermann D., Panzetta F., Bloßfeld M., Panafidina N.: *Consistent dynamic satellite reference frames and terrestrial geodetic datum parameters – PN 6*. Projekttreffen der DFG-Forschergruppe FOR1503, Hannover, Germany, 2015-02-06

Hugentobler U., Seitz M., Angermann D.: *Consistent dynamic satellite reference frames and terrestrial geodetic datum parameters – PN6*. Projekttreffen der DFG-Forschergruppe FOR1503, Frankfurt/Main, Germany, 2015-10-13

Ihde J., Sánchez L.: *Physical Height and the GGRF – Earth Gravity Field and the GGRF – GGRF an Integrated Approach*. GGOS Days 2015, Frankfurt a.M., Germany, 2015-10-22

Ihde J., Barzaghi R., Marti U., Sánchez L., Sideris M., Drewes H., Foerste Ch., Gruber Th., Liebsch G., Pail R.: *Definition and Realization of an International Height Reference System*. International Union of Geodesy and Geophysics General Assembly 2015, Prague, Czech Republic, 2015-06-26

Lieb V.: *Erstellung einer Software-Anwendung zur Erzeugung hochgenauer regionaler Geoidmodelle als Höhenbezugsfläche in Einsatzgebieten*. RegGRAV II Abschlusspräsentation, Projektabnahme 3. Meilenstein, Generalmajor-Freiherr-von-Gersdorff-Kaserne, Euskirchen, Germany, 2015-01-14

Lieb V., Seitz F.: *Geodetic Earth Observation from Space*. DAAD Thematic Network Meeting, GIS, Stuttgart, Germany, 2015-11-19

Limberger M., Erdogan E., Schmidt M., Dettmering D., Durmaz M., Karslioglu M.: *Mapping the global TEC by means of an adaptive B-spline parametrization and space-geodetic techniques*. Atlantic Radio-Science Conference 2015, Maspalomas, Gran Canaria, Spain, 2015-05-20

Müller F., Bosch W., Dettmering D.: *Vergleich der aus geodätischen Weltraumverfahren abgeleiteten, zeitvariablen Meerestopographie mit in-situ Beobachtungssystemen der Ozeanographie*. Geodetic Week 2015, Stuttgart, Deutschland, 2015-09-15

Müller F., Dettmering D., Bosch W.: *Pointwise comparison of geostrophic currents of altimetry-derived instantaneous Ocean Dynamic Topography with in-situ measurements*. OSTST 2015, Reston, USA, 2015-10-22 (Poster)

Müller F., Bosch W., Dettmering D.: *Validating geostrophic currents of a dynamic ocean topography with data of ARGO floats and surface drifters*. EGU General Assembly, Vienna, Austria, 2015-04-15 (Poster)

Müller H., Bloßfeld M.: *Impact of range biases on global reference frames*. ILRS technical Workshop, Matera, Italy, 2015-10-29

Panzetta F., Bloßfeld M., Seitz M.: *Jason-2 POD and geodetic parameter estimation from SLR observations with DOGS-OC*. Statusseminar FOR1503, Frankfurt, Germany, 2015-10-12

Panzetta F., Bloßfeld M., Müller H., Gerstl M., Seitz M.: *Geodetic parameter time series from Jason-2 and multi-satellite SLR solutions*. 26th IUGG General Assembly 2015, Prague, Czech Republic, 2015-06-25 (Poster)

Ressler G., Boergens E., Buhl S.: *GRACE and Altimetry Data in the Amazon Basin: Analysis and Geostatistical Homogenisation*. IGSSE Forum 2015, 2015-07-01/03 (Poster)

Ressler G., Eicker A., Lieb V., Schmidt M., Seitz F., Shang K., Shum C.K.: *Water storage variations extracted from GRACE data by combination of multi-resolution representation (MRR) and principal component analysis (PCA)*. EGU General Assembly, Vienna, Austria, 2015-04-16

Ressler G., Schmidt M., Seitz F., Shum C.K., Shang K.: *Water storage variations at different temporal scales derived from GRACE data by wavelet-based multi-resolution representation (MRR) and principal component analysis (PCA)*. Hydrospace 2015, ESA-ESRIN, Frascati, Italy, 2015-09-15

Ressler G., Boergens E., Buhl S.: *Monitoring and Prediction of Regional Water Availability for Agricultural Production under the Influence of Climate Anomalies and Weather Extremes (Status Report)*. IGSSE Water Focus Area 1'st Winter Workshop, 2015-02-09

Rudenko S., Esselborn S., Dettmering D., Schöne T., Neumayer K.-H.: *Impact of improved models for precise orbits of altimetry satellites on the orbit accuracy and regional mean sea level trends*. EGU General Assembly 2015, 2015-04-16 (Poster)

Rudenko S., Neumayer K-H., Dettmering D., Esselborn S., Schöne T: *Improvements in precise orbit determination of altimetry satellites*. OSTST 2015, Reston, VA, USA, 2015-10-21

Rudenko S., Neumayer K.-H., Dettmering D., Esselborn S., Schöne T: *New orbits of ERS-1, ERS-2, TOPEX/Poseidon, Envisat, Jason-1 and Jason-2 for altimetry applications and their validation*. OSTST 2015, Reston, VA, USA, 2015-10-20/23 (Poster)

Sánchez L., Drewes H.: *Post-seismic crustal deformations after the 2010 earthquakes in Latin America*. International Union of Geodesy and Geophysics General Assembly 2015, Prague, Czech Republic, 2015-07-01 (Poster)

Sánchez L., Ihde J., Barzaghi R., Drewes H., Foerste Ch., Liebsch G., Marti U., Sideris M.: *Establishment of an International Height Reference System in the frame of GGOS*. Symposium SIRGAS 2015, Santo Domingo, Dominican Republic, 2015-11-19

Sánchez L.: *Kinematics of the SIRGAS Reference Frame*. Symposium SIRGAS 2015, Santo Domingo, Dominican Republic, 2015-11-20

Sánchez L.: *Realisation of a vertical reference system for South America as a densification of an International Height Reference System*. International Union of Geodesy and Geophysics General Assembly 2015, Prague, Czech Republic, 2015-06-26

Sánchez L.: *Unification of height systems in the frame of GGOS*. EGU2015, Vienna, Austria, 2015-04-17

Sánchez L., Cunderlík R., Mikula K., Minarechová Z., Dayoub N., Síma Z., Vatrt V., Vojtísková M.: *A new best estimate for the conventional value W0 - Final Report of the WG on Vertical Datum Standardization -*. International Union of Geodesy and Geophysics General Assembly 2015, Prague, Czech Republic, 2015-06-27

Sánchez L.: *Recent activities of the IGS Regional Network Associate Analysis Centre for SIRGAS (IGS RNAAC SIRGAS)*. Symposium SIRGAS 2015, Santo Domingo, Dominican Republic, 2015-11-18 (Poster)

Sánchez L., Drewes H., Schmidt M.: *A post-seismic deformation model after the 2010 earthquakes in Latin America*. EGU2015, Vienna, Austria, 2015-04-15 (Poster)

Sánchez L., Drewes H., da Silva, De Almeida, Brunini C., Cioce V., Cisneros D., Gasca L., Guagni H., Mackern V., Moya J., Parada I., Sandoval P., Suárez O.: *SIRGAS: the core geodetic infrastructure in Latin America and the Caribbean*. International Union of Geodesy and Geophysics General Assembly 2015, Prague, Czech Republic, 2015-06-29

Sánchez L.: *SIRGAS regional stations available for the second reprocessing of the SIRGAS reference frame*. Symposium SIRGAS 2015, Santo Domingo, Dominican Republic, 2015-11-18 (Poster)

Sánchez L.: *Lecture on Vertical Reference Systems*. III Workshop of the SIRGAS Working Group III (Vertical Datum), Universidade Federal do Paraná, Curitiba, Brazil, 2015-05-18/20

Schmid R., Bloßfeld M., Angermann D., Gerstl M.: *DGFI part of project PN 5 - status report*. Projekttreffen der DFG-Forschergruppe FOR1503, Hannover, Germany, 2015-02-05

Schmid R., Bloßfeld M., Gerstl M., Angermann D.: *DGFI part of project PN 5 - status report*. Projekttreffen der DFG-Forschergruppe FOR1503, Frankfurt/Main, Germany, 2015-10-12

Schmidt M.: *Inverse Modeling in Ionospheric Research*. 2015 SIAM Conference on Mathematical & Computational Issues, Stanford Univ., Palo Alto, USA, 2015-07-02

Schmidt M., Lieb V., Eicker A., Schall J., Gerlach C.: *Regional gravity field modeling using radial basis functions: comparisons with spherical harmonic solutions within IAG*. EGU General Assembly 2015, Vienna, Austria, 2015-04-13

Schmidt M., Erdogan E., Liang W., Dettmering D., Limberger M., Seitz F., Brandert S., Börger K., Bothmer V., Hinrichs J.: *Mapping the global TEC by means of an adaptive B-spline parametrization and space-geodetic techniques*. SGI Workshop 2015, TUB Berlin, Germany, 2015-07-07/08

Schmidt M., Dettmering D., Limberger M., Seitz F., Börger K., Brandert S., Görres B., Kersten W.F., Bothmer V., Hinrichs J., Venzmer M.: *Globale VTEC-Modellierung auf Grundlage geodätischer Raumverfahren und sonnenbeobachtender Weltraummissionen in Nahe-Echtzeit*. Weltraum-Wetterworkshop am DLR, Neustrelitz, Germany, 2015-05-11/13

Schmidt M., Sebera J., Bouman J., Fabert O.: *Towards ellipsoidal representations of the Earth's gravitational field*. Kolloquium der Leibniz-Sozietät – aus Anlass des 75. Geburtstages von Prof. Erik W. Grafarend, Berlin, Germany, , 2015-02-13

Schmidt M., Erdogan E., Liang W., Dettmering D., Limberger M., Seitz F., Brandert S., Börger K.: *Modelling of the global ionosphere by means of a data adaptive technique using observations acquired from various space geodetic systems* . 26th IUGG General Assembly 2015, Prague, Czech Republic, 2015-06-26

Schmidt M., Dettmering D., Limberger M., Seitz F., Börger K., Brandert S., Görres B., Kersten W.F., Bothmer V., Hinrichs J., Venzmer M.: *Low-latency global TEC modeling from space observations and localizing B-splines*. 26th IUGG General Assembly 2015, Prague, Czech Republic, 2015-06-26

Schwatke C., Dettmering D., Boergens E.: *Database for Hydrological Time Series of Inland Waters (DAHITI)*. Ocean Surface Topography Science Team Meeting, Reston, Virginia, USA, 2015-10-20/23 (Poster)

Schwatke C., Dettmering D., Boergens E.: *Height Estimation and Error Assessment ofcalculated by a Kalman Filter Approach usingInland Water Level Time Series Multi-Mission Satellite Altimetry*. EGU General Assembly, Vienna, Austria, 2015-04-16 (Poster)

Schwatke C., Dettmering D.: *Classification of Altimeter Waveforms for an Improved Estimation of Water Level Time Series over Inland Water*. 9th Coastal Altimetry Workshop, Reston, Virginia, USA, 2015-10-18/19 (Poster)

Schwatke C., Dettmering D., Boergens E.: *Database for Hydrological Time Series of Inland Waters (DAHITI)*. Earth Observation for Water Cycle Science, Frascati, Italy, 2015-10-20/23 (Poster)

Schwatke C., Dettmering D., Göttl F.: *Classification of altimeter waveforms for an improved estimation of water level time series over inland water*. Hydrospace 2015, ESA-ESRIN, Frascati, Italy, 2015-09-15 (Poster)

Schwatke C., Dettmering D., Boergens E.: *Height Estimation and Error Assessment of Inland Water Level Time Series calculated by a Kalman Filter Approach using Multi-Mission Satellite Altimetry*. Mapping Water Bodies from Space 2015, Frascati, Italy, 2015-03-18 (Poster)

Schwatke C., Dettmering D.: *DAHITI - An Innovative Approach for Estimating Water Level Time Series over Inland Water using Multi-Mission Satellite Altimetry*. 9th Coastal Altimetry Workshop, Reston, Virginia, USA, 2015-10-18/19, 2015-10-26

Seitz , F. : *Hochgenaue Vermessung der Erde aus dem Weltraum - Aktuelle Arbeiten am Deutschen Geodätischen Forschungsinstitut*. RegGRAV II final project presentation, Euskirchen, Germany, 2015-01-14

Seitz M., Bloßfeld M., Angermann D.: *Contribution of DGFI-TUM to ITRF2014*. AGU 2015, San Francisco, USA, 2015-12-16

Seitz M., Bloßfeld M., Angermann D.: *Contribution of DGFI-TUM to ITRF2014*. IERS Directing Board Meeting, San Francisco, USA, 2015-12-13

Seitz M., Angermann D., Bloßfeld M., Gerstl M., Schmid R.: *DTRF2014: The 2014 ITRS realization of DGFI-TUM*. 26th IUGG General Assembly, Prague, Czech Republic, 2015-06-28

Seitz M., Angermann D., Bloßfeld M.: *ITRS 2014 Realization of DGFI: DTRF2014*. IERS Directing Board Meeting, Vienna, Austria, 2015-04-12

Seitz M., Angermann D., Bloßfeld M.: *Die aktuelle ITRS Realisierung des DGFI-TUM: DTRF 2014*. Geodätische Woche, Stuttgart, 2015-09-15

Seitz M., Angermann D., Bloßfeld M., Gerstl M., Schmid R.: *2014 ITRS realization of DGFI: DTRF2014*. EGU General Assembly 2015, Vienna, Austria, 2015-04-15

Singh A., Seitz F., Kumar U.: *Estimation and prediction of the ungauged basins using satellite remote sensing and state space model*. 26th IUGG General Assembly 2015, Prague, Czech Republic, 2015-06-23

Zlinszky A., Glira P., Boergens E., Pfeifer N.: *Comparing airborne LIDAR water surface heights with synchronous Envisat altimetry over Lake Balaton, Hungary*. EGU General Assembly, Vienna, Austria, 2015-04-16 (Poster)

4.5 Participation in meetings, symposia, conferences

2015-01-14 : **RegGRAV II final project presentation, Euskirchen, Germany**
Lieb V., Schmidt M., Seitz F.

2015-01-27 : **Program for Arctic Regional Climate Assessment (PARCA) Meeting 2015, NASA Goddard Space Flight Center, MD, USA**
Lieb V.

2015-02-05/06 : **Status seminar, DFG Research Unit FOR1503 Reference Systems, Hannover, Germany**
Angermann D., Schmid R.

2015-02-06/07 : **Retreat of the Faculty of Civil, Geo and Environmental Engineering of the TUM, Wildbad Kreuth, Germany**
Seitz F.

2015-02-09 : **IGSSE Focus Area Water Workshop, Garching, Germany**
Börgens E., Ressler G., Seitz F.

2015-02-13 : **Kolloquium der Leibniz-Sozietät – aus Anlass des 75. Geburtstages von Prof. Erik W. Grafarend, Berlin, Germany**
Schmidt M.

2015-03-18 : **Mapping Water Bodies from Space Conference, Frascati, Italy**
Schwatke C.

2015-03-25 : **Annual meeting of DGK Section Geodesy, Frankfurt, Germany**
Seitz, F.

2015-03-25/26 : **Munich Satellite Navigation Summit 2015, Munich, Germany**
Sánchez L., Schmid R.

2015-04-11 : **GGOS Coordinating Board Meeting, Vienna, Austria**
Angermann D.

2015-04-12 : **IERS Directing Board Meeting, Vienna, Austria**
Angermann D.

2015-04-12/17 : **EGU General Assembly, Vienna, Austria**
Bloßfeld M., Boergens E., Müller F, Schmidt M., Seitz M., Ressler G., Limberger M., Sánchez L.

2015-05-11/13 : **Weltraum-Wetterworkshop, Neustrelitz, Germany**
Schmidt M.

2015-06-15/17 : **FGS Review of the Research and Development Programme 2016–2020, Bad Kötzting, Germany**
Angermann D., Dettmering D., Schmidt M., Seitz F., Seitz M.

2015-06-22/07-02 : **IUGG General Assembly 2015, Prague, Czech Republic**
Angermann D., Bloßfeld M., Bouman J., Dettmering D., Panzetta F., Sanchez L., Schmidt M., Seitz F.

2015-06-26 : **GGOS Coordinating Board Meeting, Prague, Czech Republic**
Angermann D.

2015-06-27 : **GGOS Bureau of Products and Standards Meeting, Prague, Czech Republic**
Angermann D., Sanchez L.

2015-06-29/07-02 : **SIAM Conference on Mathematical and Computational Issues in the Geosciences, Stanford University, Palo Alto, USA**
Schmidt M.

2015-07-01/03 : **IGSSE Forum 2015, Burghausen, Germany**
Boergens E., Ressler G.

2015-07-07/08 : **SGI Workshop 2015, Berlin, Germany**
Schmidt M.

2015-07-15 : **Strategy meeting, DGK Section Geodesy, Frankfurt, Germany**
Seitz, F.

2015-07-16/17 : **Round table discussion, DFG SPP 1889 Sea Level and Society, Hamburg, Germany**
Dettmering D., Seitz F.

2015-07-21 : **Kick-off meeting, DFG SPP 1788 Dynamic Earth, Project INSIGHT, Munich, Germany**
Bloßfeld M., Erdogan E., Panzetta F., Schmidt M., Seitz F.

2015-08-05 : **Kick-off meeting, DAAD Thematic Network: Modern Geodetic Space Techniques for Global Change Monitoring, Stuttgart, Germany**
Seitz, F.

2015-09-06/11 : **26. Internationale Polartagung, München, Deutschland**
Müller F.

2015-09-15/16 : **Geodätische Woche, Stuttgart, Deutschland**
Angermann D., Müller F., Schmidt M.

2015-09-15/17 : **Third Space for Hydrology Workshop: Surface Water Storage and Runoff: Modeling, In-Situ data and Remote Sensing, Frascati, Italy**
Schwatke C.

2015-10-12/13 : **Status seminar, DFG Research Unit FOR1503 Reference Systems, Frankfurt/Main, Germany**
Angermann D., Panafidina N., Panzetta F., Schmid R.

2015-10-18/19 : **9th Coastal Altimetry Workshop, Reston, Virginia, USA**
Dettmering D., Schwatke C.

2015-10-20/23 : **Earth Oberservation for Water Cycle Science 2015, Frascati, Italy**
Boergens E., Fuchs M.

2015-10-20/23 : **Ocean Surface Topography Science Team Meeting (OSTST), Reston, Virginia, USA**
Dettmering D., Schwatke C.

2015-10-21/23 : **GGOS Days 2015, Frankfurt, Germany**
Angermann D., Sánchez L., Schmidt M.

2015-10-24/30 : **ILRS Technical Workshop, Matera, Italy**
Müller H.

2015-11-16/17 : **VII SIRGAS School on Reference Systems, Santo Domingo, Dominican Republic**
Sánchez L.

2015-11-18/20 : **SIRGAS Symposium 2015, Santo Domingo, Dominican Republic**
Sánchez L.

2015-11-19 : **DAAD Thematic Network meeting: Modern Geodetic Space Techniques for Global Change Monitoring, Stuttgart, Germany**
Lieb V.

2015-12-14/18 : **AGU Fall Meeting 2015, San Francisco, USA**
Bloßfeld M.

4.6 Guests

2015-01-19 : Dr. Eicker A., University of Bonn, Germany

2015-05-28 : Idzanovic M. and Ophaug V., Norwegian University of Life Sciences, Aas, Norway

2015-06-09 : Prof. Dr. Reinking J. with a group of students, Jade University, Oldenburg, Germany

2015-09-15/12-15 : Vancraen S., TU Delft, Netherlands

2015-09-17/12-31 : Talpe M., University of Colorado, Boulder, USA

2015-11-06 : Dr. Forootan E., University of Bonn, Germany

2015-12-08 : Dr. Kwak Y., Vienna University of Technology, Austria

5 Projects

A large part of DGFI-TUM's research activities is financed through third-party funds from various sources. Funding of the following projects is gratefully acknowledged (in alphabetic order):

ADAPIO Development of a novel adaptive model to represent global ionosphere information from combining space geodetic measurement systems (DLR)

CLIVAR-Hydro Signals of climate variability in continental hydrology from multi-sensor space and in-situ observations and hydrological modeling (DFG/IGSSE)

DAAD Thematic Network Modern Geodetic Space Techniques for Global Change Monitoring (DAAD)

DIGERATI Direct geocentric realisation of the American reference frame by combination of geodetic observation techniques (DFG)

EXTREMES Signals of weather extremes in soil moisture and continental water storage from multi-sensor Earth observation and hydrological modeling (TUM.Diversity/Laura Bassi-Award)

FOR 584, P6 Integration of Earth rotation, gravity field and geometry using space geodetic observations (DFG)

FOR 1503, PN5-1 Consistent celestial and terrestrial reference frames by improved modeling and combination-1 (DFG)

FOR 1503, PN5-2 Consistent celestial and terrestrial reference frames by improved modeling and combination-2 (DFG)

FOR 1503, PN6-1 Consistent dynamic satellite reference frames and terrestrial geodetic datum parameters-1 (DFG)

FOR 1503, PN6-2 Consistent dynamic satellite reference frames and terrestrial geodetic datum parameters-2 (DFG)

GOCE+ MassBalance GRACE/GOCE mass changes over Antarctica (ESA)

GOCE+ WaterStorage GRACE/GOCE water storage changes over the Amazon region (ESA)

MACOS Mass variations in continental surface water storage due to drought and flooding (TUM.Diversity)

MULTIGRAV Multi-resolution representation for regional gravity field modellig (TUM.Diversity/ Laura Bassi-Award)

NEG-OCEAN Variations in ocean currents, sea ice concentration and sea surface temperature along the North-East coast of Greenland (DFG)

OPTIMAP Operational Tool for Ionospheric Mapping And Prediction (ZGeoBw)

RegGRAV II Software application for high-resolution regional geoid models (ZGeoBw)

REWAP Monitoring and Prediction of Regional Water Availability for Agricultural Production under the Influence of Climate Anomalies and Weather Extremes (DFG/IGSSE)

SPP 1788, INSIGHT Interactions of low-orbiting satellites with the surrounding ionosphere and thermosphere (DFG)

SWARM+Innovations SLIM Swarm Magnetic Gradients for Lithospheric Modelling (ESA)

TIDES Highly resolved global data set of sea surface variations due to ocean tides (Prof. H. Ruder, Tübingen)

UHR-GravDat Consistent estimate of ultra-high resolution Earth surface gravity data (DFG)

WLDYN Assessing the spatiotemporal dynamics of water volumes in large wetlands and lakes by combining remote sensing with macro-scale hydrological modelling (DFG)

6 Personnel

6.1 Lectures at the TUM

Bosch W. Lecture "Oceanography and Satellite Altimetry", TUM, WS 2014/15 and WS 2015/16

Bouman J. Lecture "Gravity and Magnetic Field from Space", TUM, WS 2014/15 and WS 2015/16

Schmidt M. Lecture "Numerical Modelling", TUM, WS 2014/15 and WS 2015/16

Schmidt M. Lecture "Numerische Methoden in der Satellitengeodäsie", TUM, SS 2015

Seitz F. Lecture "Earth System Dynamics", TUM, WS 2014/15 and WS 2015/16

Seitz F. Lecture "Seminar ESPACE", TUM, SS 2015

Seitz F. Doktorandenseminar des Deutschen Geodätischen Forschungsinstituts, TUM, SS 2015 and WS 2015/16

6.2 Lectures at seminars and schools

Sánchez L. Lecture on Regional Reference System SIRGAS and on Vertical Reference Systems. VII SIRGAS School on Reference Systems. Santo Domingo, Dominican Republic, 2015-11-16/17

Sánchez L. Lecture on Vertical Reference Systems. III Workshop of the SIRGAS Working Group III (Vertical Datum). Universidade Federal do Paraná, Curitiba, Brazil, 2015-05-18/20

6.3 Thesis supervision

Master Theses

Bosch W., Dettmering D.
Master Thesis Müller F., TUM: Vergleich der aus geodätischen Weltraumverfahren abgeleiteten, zeitvariablen Meerestopographie mit in-situ Beobachtungsverfahren der Ozeanographie. 2015-02-23

Seitz F., Dettmering D.
Master Thesis Chen H., TUM: Studying water level variations of wetlands from satellite altimetry – case study Sudd Swamp. 2015-05-13

Schmidt M., Seitz F., Lieb V.
Master Thesis Buße K., TUM: Verwendung von Schiffsgravimetermessungen für die verbesserte regionale Schwerefeldmodellierung, 2015-11-03

Doctoral Theses

Seitz F. (co-supervisor) Doctoral Thesis Bloßfeld M., TUM: The key role of Satellite Laser Ranging towards the integrated estimation of geometry, rotation and gravitational field of the Earth. 2015-01-30

Seitz F. (co-supervisor) Doctoral Thesis Fuchs M., TUM: Detection and in-depth assessment of the 2011 Tohoku-Oki earthquake evaluating GOCE gravity gradient data. 2015-09-22

Schmidt M. (co-supervisor) Doctoral Thesis Limberger M., TUM: Ionosphere modeling from GPS radio occultations and complementary data based on B-splines. 2015-10-06

6.4 Conferral of Doctorates

Bloßfeld M.

Title: The key role of Satellite Laser Ranging towards the integrated estimation of geometry, rotation and gravitational field of the Earth

Supervisors: Prof. Dr. U. Hugentobler (TUM), Prof. Dr.-Ing. F. Seitz (TUM), Prof. Dr. M. Rothacher (Eidgenössische Technische Hochschule Zürich, Switzerland)

Day of defense: 2015-01-30

Institution: TUM

Fuchs M.

Title: Detection and in-depth assessment of the 2011 Tohoku-Oki earthquake evaluating GOCE gravity gradient data

Supervisors: Prof. Dr. R. Pail (TUM), Prof. Dr.-Ing. F. Seitz (TUM), Prof. Dr. A. Hooper (University of Leeds, United Kingdom)

Day of defense: 2015-09-22

Institution: TUM

Limberger M.

Title: Ionosphere modeling from GPS radio occultations and complementary data based on B-splines

Supervisors: Prof. Dr. U. Hugentobler (TUM), apl. Prof. Dr.-Ing. M. Schmidt (TUM), Prof. Dr. C. Brunini (Universidad Nacional de La Plata, Argentina)

Day of defense: 2015-10-06

Institution: TUM

Passaro M.

Title: Design, validation and application of a new coastal altimetry strategy

Supervisors: Dr. P. Cipollini (National Oceanography Centre, Southampton, United Kingdom), Dr. G. Quartly (Plymouth Marine Laboratory, United Kingdom), Dr. H. Snaith (National Oceanography Centre, Southampton, United Kingdom)

Day of defense: 2015-11-18

Institution: University of Southampton

6.5 TUM Graduate School

International Research Phase

Lieb V.

Academic Institution: Princeton University, USA.
Duration: 2015-01-19 until 2015-03-13
Supervisor: Prof. Dr. F. Simons

Ressler G.

Academic Institution: ESA/ESTEC, Netherlands.
Duration: 2015-10-01 until 2015-12-31
Supervisor: Dr. R. Haagmans